UNIVERSITÄT
BAYREUTH

Dissipativity-Based Analysis of Multiobjective Optimal and Predictive Control

Von der Universität Bayreuth
zur Erlangung des Grades einer
Doktorin der Naturwissenschaften (Dr.rer.nat)
genehmigte Abhandlung

von

Lisa Krügel

aus Kronach

1. Gutachter: Prof. Dr. L. Grüne
2. Gutachterin: Prof. Dr. K. Flasskamp

Tag der Einreichung: 05.10.2023
Tag des Kolloquiums: 08.02.2024

Acknowledgments

I wish to express my thanks to my Ph.D. supervisor Prof. Dr. Lars Grüne, for giving me the opportunity to pursue this research project, for his excellent supervision and support in academic matters, and for the many opportunities for international scientific exchange. Moreover, I greatly appreciate our enlightening discussions, Prof. Grüne's open-door policy, and the pleasant working conditions.

Additionally, I would like to thank Prof. Dr. Kathrin Flaßkamp for committing their time to referee this thesis. I would also like to thank the other members of the examination board Prof. Thomas Kriecherbauer and Prof. Anton Schiela.

Furthermore, I would like to thank all (former and current) colleagues at the Chair of Applied Mathematics of the University of Bayreuth. Special thanks go to Frederik Köhne, Jonas Schießl, and Mario Sperl for the excellent relationship far beyond the work and so many fruitful discussions. I am very grateful for Sigrid Kinder's and Andrea Groll's fantastic organization, administrative assistance, and always having a smile on their lips.

Outside academia, several people accompanied my Ph.D. journey: Sabrina Franz for being by my side since our first math lecture, Bayreuther Faschingsgesellschaft Schwarz-Weiß for clearing my head of math by surrounding me with dance and creativity, my friends Nina Zöllner, Luisa Ermer, Jonas Röckl for countless memorable evenings, and Melanie Barthelmeß for believing in my sewing skills and causing me to found *Glanzstiche*.

Finally, I would like to thank Mama, Norbert, and Anna.

Abstract

Model predictive control (MPC) is an optimization-based method for the feedback control of nonlinear systems. Since MPC can efficiently solve optimal control problems with constraints on large horizons, it enjoys great popularity in science and industry. In the literature, different aspects, as well as possible extensions, are discussed. Moreover, motivated by many applications, considering multiple cost criteria is a natural idea.

This thesis aims to enhance our understanding of multiobjective model predictive control and to provide valuable control theoretical and algorithmic insights in this field. To address this, we investigate multiobjective optimal control problems and analyze their trajectory behavior. In particular, we examine multiobjective strict dissipativity as one of the key ingredients for analyzing both MPC schemes and performance results.

In multiobjective optimal control problems, multiple equilibria are more likely to coexist. Similarly, this occurs in a discounted setting for which we provide a local strict dissipativity and a local turnpike analysis. Since for solving multiobjective optimal control problems, the weighted sum approach is commonly used, conditions under which the convex combination of strictly dissipative stage cost remains strictly dissipative are derived. To this end, we use nonlinear programming techniques and exploit the relationship between strict dissipativity and optimal steady-state problems. Moreover, we present two multiobjective MPC schemes accompanied by assumptions on the problem data that extend the applicability to a broader class of optimal control problems compared to existing literature. We show both (non-) averaged performance results and the trajectory convergence. Inspired by single-objective MPC results for optimal control problems without terminal conditions, we give performance bounds for all cost criteria. Further, a stability analysis is provided by proving that the objective function with strictly dissipative stage cost is a time-varying Lyapunov function.

To substantiate our theoretical findings, we study several numerical examples in each chapter. This thesis concludes by examining the impact of selection rules on the solution behavior, highlighting an aspect specific to multiobjective model predictive control that introduces an additional degree of freedom.

Kurzzusammenfassung

Modellprädiktive Regelung (*engl.* model predictive control, kurz: MPC) ist ein optimierungsbasiertes Verfahren zur Regelung nichtlinearer Systeme. Da modellprädiktive Regelung effizient optimale Steuerungsproblem auf großen Horizont unter Berücksichtigung von nichtlinearen Beschränkungen lösen kann, erfreut es sich in Wissenschaft und Industrie großer Beliebtheit. Aufgrunddessen wurden in der Literatur bereits verschiedenste Aspekte und mögliche Erweiterungen diskutiert. Angesichts der vielen möglichen Anwendungen, ist es eine natürliche Erweiterung mehrere Kostenkriterien anstelle von nur einer Zielfunktion zu berücksichtigen.

Diese Arbeit zielt darauf ab, das Verständnis der multikriteriellen modellprädiktiven Regelung zu verbessern und wertvolle systemtheoretische und algorithmische Erkenntnisse auf diesem Gebiet zu liefern. Der Schwerpunkt liegt dabei auf der Untersuchung von multikriteriellen optimalen Steuerungsproblemen und der Analyse des zugehörigen Trajektorienverhaltens. Insbesondere präsentieren wir eine Formulierung für multikriterielle strikte Dissipativität, die eines der wichtigsten Konzepte für die Analyse von MPC-Schemata darstellt, sowie auf die Regelgüte. Bei multikriteriellen optimalen Kontrollproblemen ist die Koexistenz mehrerer Gleichgewichte üblich. Ein ähnliches Verhalten ist bei diskontierten Problemen zu beobachten, weshalb wir auch eine lokale strikte Dissipativität und eine lokale Turnpike-Analyse durchführen. Da für die Lösung von multikriteriellen optimalen Kontrollproblemen häufig der Ansatz der gewichteten Summe verwendet wird, entwickeln wir Bedingungen, unter denen die Konvexkombination von strikt dissipativen Stufenkosten strikt dissipativ bleibt. Zu diesem Zweck verwenden wir Techniken der nichtlinearen Programmierung und nutzen den Zusammenhang zwischen strikter Dissipativität und optimalen Gleichgewichtsproblemen.

Darüber hinaus stellen wir zwei multikriterielle MPC-Schemata vor, zusammen mit Annahmen zu den Problemdaten, die die Anwendbarkeit auf eine breitere Problemklasse im Vergleich zur bestehenden Literatur erlauben. Wir zeigen sowohl Resultate für die (gemittelte) Regelgüte als auch für die Trajektorienkonvergenz. Inspiriert von bekannten MPC-Ergebnissen für optimale Steuerungsprobleme ohne Endbedingungen, geben wir auch Performance Schranken für alle Kostenkriterien an. Außerdem wird eine Stabilitätsanalyse durchgeführt, indem wir beweisen, dass die Zielfunktion mit streng dissipativen Stufenkosten eine zeitabhängige Lyapunov-Funktion ist.

Zur Untermauerung unserer theoretischen Erkenntnisse untersuchen wir numerische Beispiele in jedem Kapitel. Abschließend werden die Auswirkungen von Auswahlregeln auf das Lösungsverhalten untersucht, was ein spezifischer Aspekt der multikriteriellen prädiktiven Modellsteuerung ist, der einen zusätzlichen Freiheitsgrad darstellt.

Contents

1 Introduction

1.1 Motivation and Scope of this Thesis

When considering autonomous driving, besides staying on the road, some other goals come to mind, such as obeying traffic rules, ensuring driving comfort, and arriving at the destination within a specified timeframe, to name just a few. Of course, the vehicle's motion following physical laws must be considered. Additionally, the vehicle can be controlled by acceleration and steering. Formulating this problem using the language of optimal control leads to a multiobjective optimal control problem. Hence, in practical applications like chemical process engineering, electrical engineering, aerospace engineering, and automotive engineering (see, for example, [36, 61, 68, 82, 85]), it is desirable to consider not just a single cost criterion, but multiple criteria.

A widely used control approach for solving optimal control problems over large time horizons is model predictive control (MPC). The basic concept behind MPC is to decompose the problem with a large or infinite time horizon into numerically more handleable sub-problems on a finite horizon. Predictions are then made about the future behavior of the controlled system over this finite time horizon, and an optimal control is computed. This control minimizes the objective function while ensuring the satisfaction of given constraints. Using the solutions of the sub-problems allows the construction of a control sequence for the problem on the original horizon.

Furthermore, in economic MPC, it is well-known that strict dissipativity is the key ingredient for asymptotic stability and (approximate) optimality of the closed-loop. In recent years, dissipativity has become a highly useful concept for understanding the qualitative behavior of optimally controlled systems. Roughly speaking, strict dissipativity enables the construction of a Lyapunov function from an optimal value function, even when the stage cost of the considered optimal control problem is not positively definite.

When dealing with optimal control problems involving multiple objectives, it is necessary to establish an appropriate notion of optimality. Using the concept of efficiency (also known as Pareto optimality), a whole set of "optimal" solutions is obtained. The generation of these solutions requires the application of multiobjective optimization algorithms. These algorithms often rely on a scalarization approach such that

the interplay between the objective functions becomes crucial for the analysis. The occurrence of multiple optimal equilibria is more likely, or, in the case of combining the objectives to one function, the optimal equilibrium can even change. However, formulating a suitable notion of multiobjective dissipativity remains a challenge.

Additionally, due to the underlying concept of optimality in the multiobjective setting, the question arises of how to select the solution from a set of optimal solutions. This thesis aims to address this question by investigating if and how this selection impacts the solution behavior. Further, this thesis contributes to providing more insights into the dissipativity theory within the context of multiobjective optimal control problems. The analysis also examines multiobjective MPC schemes, relaxing the assumptions on problem data in contrast to recent literature. Lastly, this thesis includes a numerical investigation of various application examples to enhance the understanding of the discussed concepts further.

1.2 Contribution and Outline

Chapter 2
Fundamentals of Single-Objective and Multiobjective Optimal Control

In the next chapter, we briefly overview the basics of control theory and multiobjective optimization. We introduce optimal control problems and a model predictive control algorithm for solving them. Additionally, we present definitions of strict dissipativity and consider the well-known relation between strict dissipativity and the steady-state problem. To exploit this relation, we use nonlinear programming. Moreover, we recall stability results using Lyapunov functions.

Further, we introduce the multiobjective optimality notion we use in this thesis and provide a possibility to solve multiobjective optimal control problems with the weighted sum approach. Merging optimal control problems and multiobjective optimization concludes this chapter. Most of this introduction is based on the books [11, 23, 46].

Chapter 3
Discounted Optimal Control Problems

Recent results in the literature provide connections between the so-called turnpike property, near optimality of closed-loop solutions, and strict dissipativity. We extend this fact to discounted optimal control problems. While we recall and extend existing results in this field in the first part of the chapter, we investigate the local turnpike property in the second part. In contrast to non-discounted optimal control problems,

several asymptotically stable optimal equilibria are more likely to coexist. This is because, due to the discounting and the transition cost from a local to the global equilibrium, staying in a local equilibrium may be more favorable than moving to the global – cheaper – equilibrium. We propose a local notion of discounted strict dissipativity that depends on the discount factor and a local turnpike property. Using these concepts, we investigate the local behavior of (near-)optimal trajectories and develop conditions on the discount factor to ensure convergence to a local asymptotically stable optimal equilibrium. Several examples accompany the results in this chapter.

Some results for infinite horizon problems in this chapter have been published in [43]. In Section 3.3.3, we present previously unpublished results for the finite horizon.

Chapter 4
Multiobjective Strict Dissipativity via the Weighted Sum Approach

We start our analysis of multiobjective optimal control problems by investigating multiobjective strict dissipativity. Since the design of MPC algorithms for directly solving multiobjective problems is rather complicated, particularly if terminal conditions shall be avoided, we use an indirect approach via a weighted sum formulation for solving multiobjective optimal control problems. Thus, we investigate under which conditions a convex combination of strictly dissipative stage costs yields a stage cost for which the system is again strictly dissipative. We first give conditions for problems with linear dynamics and then move on to consider fully nonlinear optimal control problems. We derive both necessary and sufficient conditions on the individual cost functions and weights to conclude strict dissipativity and illustrate our findings with numerical examples.

This chapter comprises results that were published in [50].

Chapter 5
Analysis of Multiobjective Model Predictive Control Schemes

In this chapter, we consider the multiobjective nonlinear model predictive control scheme including terminal conditions presented in [54, 88] together with a relaxed version of this algorithm. We significantly simplify and relax the assumptions made in these works by assuming strict dissipativity and the existence of a compatible terminal cost for only one of the competing objective functions. We give both averaged and non-averaged performance guarantees associated with the strict dissipative cost function for the resulting MPC closed-loop system. In addition, we impose conditions that ensure the asymptotic stability of the closed-loop system. Moreover, considering

the algorithm in [54] combined with our relaxed assumptions, we obtain performance estimates for *all* cost criteria. Numerical simulations on various instances illustrate our findings.

The majority of the results in this chapter have been published in [26].

Chapter 6
Numerical Simulations – The Impact of Selection Rules on the Solution Behavior

The proposed algorithms in the previous chapter require selecting an efficient solution in each iteration. Thus, in this chapter, we examine several selection rules and their impact on the solution behavior. To achieve this, we introduce different selection rules to choose the efficient solutions. First, we illustrate the impact of these selection rules on the solution behavior of an isothermal reactor with two competing objective functions. In contrast, we then show that for an economic growth example, the degree of freedom in choosing the efficient solutions does not necessarily have an impact.

Moreover, we provide a path-following example and theoretically verify why this problem fits into our setting. Then, we numerically discuss the solution behavior for different cost criteria and selection rules. Here, we also illustrate the case of three objective functions. All our examples were simulated with a program introduced in the last part of this chapter.

Some numerical investigations in this chapter have been published in [26]. In Section 6.3, we present previously unpublished results.

2 Fundamentals of Single-Objective and Multiobjective Optimal Control

This chapter provides a brief overview of and introduction to the fundamentals of optimal control, model predictive control, and multiobjective optimization. In the last part of this section, we combine these concepts to establish the basis upon which the findings of this thesis are derived.

2.1 Single-Objective Optimal Control Problems and Model Predictive Control

We consider nonlinear systems in discrete time of the form

$$x(k+1) = f(x(k), u(k)), \quad x(0) = x_0 \tag{2.1}$$

with $f : \mathbb{R}^n \times \mathbb{R}^m \to \mathbb{R}^n$ continuous. We denote the solution of system (2.1) for a control (or input) sequence $\mathbf{u} = (u(0), \dots, u(N-1)) \in (\mathbb{R}^m)^N$ of length N and initial value $x_0 \in \mathbb{R}^n$ by $x_{\mathbf{u}}(\cdot, x_0)$, or short by $x(\cdot)$ if there is no ambiguity about the respective control sequence and the initial value. Additionally, we impose nonempty state and control constraint sets $\mathbb{X} \subseteq \mathbb{R}^n$ and $\mathbb{U} \subseteq \mathbb{R}^m$, respectively, as well as a nonempty terminal constraint set $\mathbb{X}_0 \subseteq \mathbb{X}$. Further, we denote the set of control sequences of length N by $\mathbb{U}^N$ and the set of admissible control sequences for $x_0 \in \mathbb{X}$ up to time $N \in \mathbb{N}$ by

$$\mathbb{U}^N(x_0) := \{\mathbf{u} \in \mathbb{U}^N \mid x_{\mathbf{u}}(k, x_0) \in \mathbb{X},\ \forall\, k = 1, \dots, N-1,\ \text{and}\ x_{\mathbf{u}}(N, x_0) \in \mathbb{X}_0\}$$

or by

$$\mathbb{U}^N(x_0) := \{\mathbf{u} \in \mathbb{U}^N \mid x_{\mathbf{u}}(k, x_0) \in \mathbb{X},\ \forall\, k = 1, \dots, N\}$$

if there are no terminal conditions.

The terminal constraint $x_{\mathbf{u}}(N, x_0) \in \mathbb{X}_0$ can usually not be satisfied for all initial values $x_0 \in \mathbb{X}$, such that we define the feasible set

$$\mathbb{X}_N := \{x_0 \in \mathbb{X} \mid \exists\, \mathbf{u} \in \mathbb{U}^N : x_{\mathbf{u}}(k, x_0) \in \mathbb{X},\ \forall\, k = 1, \dots, N-1,\ \text{and}\ x_{\mathbf{u}}(N, x_0) \in \mathbb{X}_0\}, \tag{2.2}$$

noting that $\mathbb{U}^N(x_0) \neq \emptyset$ if and only if $x_0 \in \mathbb{X}_N$. Besides, $\mathbb{X}_N = \mathbb{X}$ holds if $\mathbb{X} = \mathbb{X}_0$, i.e., if no additional terminal constraints are imposed.

For a given stage cost function $\ell : \mathbb{X} \times \mathbb{U} \to \mathbb{R}$ and a horizon $N \in \mathbb{N}$ we define the *cost functional* $J^N : \mathbb{X} \times \mathbb{U}^N \to \mathbb{R}$ by

$$J^N(x_0, \mathbf{u}) = \sum_{k=0}^{N-1} \ell(x_{\mathbf{u}}(k, x_0), u(k)).$$

If there is a continuous terminal cost $F : \mathbb{X}_0 \to \mathbb{R}_{\geq 0}$ the cost functional J^N is given by

$$J^N(x_0, \mathbf{u}) = \sum_{k=0}^{N-1} \ell(x_{\mathbf{u}}(k, x_0), u(k)) + F(x_{\mathbf{u}}(N, x_0)).$$

With this functional, following the standard notation, see [46], we can formulate an optimal control problem *without* terminal conditions

$$\begin{aligned} \min_{\mathbf{u} \in \mathbb{U}^N(x_0)} \; & J^N(x_0, \mathbf{u}) = \sum_{k=0}^{N-1} \ell(x_{\mathbf{u}}(k, x_0), u(k)) \\ \text{s.t.} \quad & x_{\mathbf{u}}(k+1, x_0) = f(x_{\mathbf{u}}(k, x_0), u(k)), \quad k = 0, \ldots, N-1, \\ & x_{\mathbf{u}}(0, x_0) = x_0 \end{aligned} \tag{OCP$_N$}$$

and an optimal control problem *with* terminal conditions

$$\begin{aligned} \min_{\mathbf{u} \in \mathbb{U}^N(x_0)} \; & J^N(x_0, \mathbf{u}) = \sum_{k=0}^{N-1} \ell(x_{\mathbf{u}}(k, x_0), u(k)) + F(x_{\mathbf{u}}(N, x_0)) \\ \text{s.t.} \quad & x_{\mathbf{u}}(k+1, x_0) = f(x_{\mathbf{u}}(k, x_0), u(k)), \quad k = 0, \ldots, N-1, \\ & x_{\mathbf{u}}(0, x_0) = x_0 \\ & x_{\mathbf{u}}(N, x_0) \in \mathbb{X}_0. \end{aligned} \tag{OCPt}$$

In both cases, we minimize the cost functional over all admissible trajectories of the system starting at the initial value x_0.

Remark

The optimal control problem (OCP$_N$) *can also be defined on the infinite horizon, i.e., for* $N = \infty$. *We denote this problem by (OCP*$_\infty$*). In this case, we optimize over the set of admissible control sequences* $\mathbb{U}^\infty(x_0)$. *We refer to [46, Section 4] for a detailed discussion.*

We sometimes abbreviate $\mathbb{Y} = \mathbb{X} \times \mathbb{U}$ as combined state and input constraint set. For some results, we need $\mathbb{Y}$ to be of the more general form

$$\mathbb{Y} = \{(x, u) \in \mathbb{R}^n \times \mathbb{R}^m \,|\, g(x, u) \leq 0\} \tag{2.3}$$

for a function $g : \mathbb{R}^n \times \mathbb{R}^m \to \mathbb{R}^p$, where "$\leq$" in $\mathbb{R}^p$ is understood componentwise.

The optimal control problems above can be approximately solved using a model predictive control algorithm. In the literature exists a large amount of work on analyzing model predictive control schemes, cf. [3,70,80]. There is also great interest in MPC in various contexts: robustness [72,97], distributed systems [15,55,74], data-driven approaches [9,69], uncertainties [13,76], and various applications [56,61,90]. The basic model predictive control algorithm introduced below can be found, for instance, in [46,81].

Algorithm 1 Basic MPC algorithm

Input: MPC Horizon N, initial value $x(0) \in \mathbb{X}_N$.

for $j = 0, 1, 2, \ldots$:

(1) Measure the state of the system $x(j) \in \mathbb{X}$.

(2) Set $x_0 := x(j)$ and solve the optimal control problem (OCP_N) or (OCPt). We denote the obtained optimal control sequence by $\mathbf{u}^\star(\cdot) \in \mathbb{U}^N(x_0)$.

(3) Define the MPC-feedback value $\mu^N(x(j)) := u^\star(0) \in \mathbb{U}$ and apply the feedback to the system, i.e., evaluate $x(j+1) = f(x(j), \mu^N(x(j)))$.

Output: MPC closed-loop trajectory $x_\mu(j, x_0) := x(j)$, $j \in \mathbb{N}_0$.

Observe that in this algorithm, we assume that an optimal control sequence $\mathbf{u}^\star$ exists. In general, this is not the case, but under continuity and compactness conditions, the existence of $\mathbf{u}^\star$ can be shown, see, for instance, [20,62].

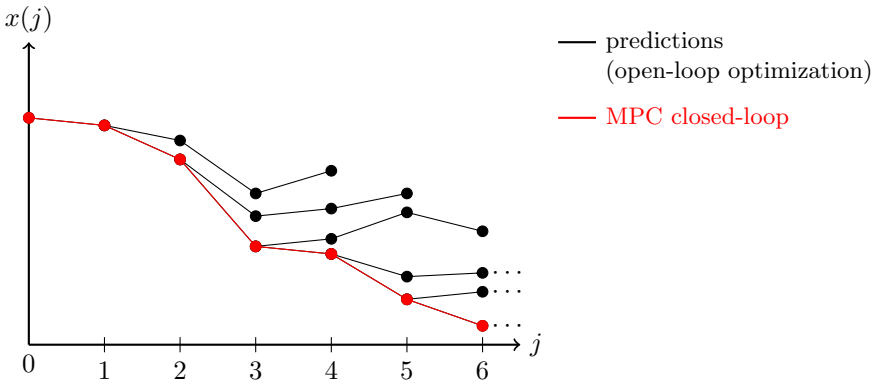

Figure 2.1: Illustration of the conceptual idea of MPC

Figure 2.1 illustrates the concept of model predictive control graphically and the

construction of the closed-loop trajectory. The black lines are the open-loop trajectories with shifted initial values, while the red line concatenates the first steps of the open-loop solution to obtain the closed-loop solution.

In [84], we have published an implementation of the MPC algorithm in Python, including several extensions, which can be used as a template to solve optimal control problems with model predictive control.

The following theorem ensures that the resulting MPC closed-loop system

$$x^+ = f(x, \mu^N(x)) \tag{2.4}$$

is admissible and, thus, satisfies the desired constraints.

Theorem 2.1 ([46, Theorem 3.5])
Consider the MPC Algorithm 1 and the optimal control problem (OCP_N) *or* (OCPt) *with constraint sets* $\mathbb{X}$, $\mathbb{U}$, *and* $\mathbb{X}_0$. *Assume,*

- *in the case* without *terminal condition, that for each* $x \in \mathbb{X}$ *there exists* $u \in \mathbb{U}(x)$ *such that* $f(x,u) \in \mathbb{X}$ *holds (the so-called* viability*). Consider the nominal closed-loop system* (2.4) *and suppose that* $x_\mu(0, x_0) = x_0 \in \mathbb{X}$.

- *in the case* with *terminal condition, that for each* $x \in \mathbb{X}_0$ *there exists* $u \in \mathbb{U}(x)$ *such that* $f(x,u) \in \mathbb{X}_0$ *holds. Consider the nominal closed-loop system* (2.4) *and suppose that* $x_\mu(0, x_0) = x_0 \in \mathbb{X}_N$.

Then,

(i) the constraints are satisfied along the solution of the system, i.e.,

$$(x_\mu(k, x_0), \mu^N(x_\mu(k, x_0))) \in \mathbb{Y} \quad \text{for all } k \in \mathbb{N}.$$

Thus, the MPC-feedback μ^N *is admissible.*

(ii) if a state x *is feasible, then its closed-loop successor state* $f(x, \mu^N(x))$ *is again feasible. We refer to this property as the recursive feasibility of* $\mathbb{X}$ *or* $\mathbb{X}_N$ *(in the presence of terminal constraints).*

In particular, part (i) of Theorem 2.1 implies part (ii) of this theorem. For a detailed discussion see, for instance, [46, 81].

2.1.1 Dynamic Programming

This section provides one of the classical tools in optimal control: the *dynamic programming principle*. We will first formulate the principle for the open-loop sequences of the optimal control problem with terminal conditions (OCPt) on a finite horizon N since the problem without terminal conditions can be obtained as a special case of (OCPt). Further, we also consider the dynamic programming principle for optimal control problems (OCP_N) on the infinite horizon and recall an immediate consequence, which we will also need in the multiobjective setting. We follow Sections 3.4 and 4.2 from [46] and begin by defining the optimal value function.

Definition 2.2 (Optimal value function [46, Definition 3.14, Definition 4.1])
Consider the optimal control problem (OCPt) *with initial value* $x_0 \in \mathbb{X}_N$ *and* $N \in \mathbb{N}$ *and the optimal control problem* (OCP_N) *with initial value* $x_0 \in \mathbb{X}$ *and* $N = \infty$.

In both cases, the function

$$V^N(x_0) := \inf_{\boldsymbol{u} \in \mathbb{U}^N(x_0)} J^N(x_0, \boldsymbol{u})$$

is called optimal value function. *A control sequence* $\boldsymbol{u}^\star \in \mathbb{U}^N(x_0)$ *satisfying*

$$V^N(x_0) = J^N(x_0, \boldsymbol{u}^\star)$$

is called optimal control sequence for x_0 *and the corresponding trajectory* $x_{\boldsymbol{u}^\star}(\cdot, x_0)$ *is called* optimal trajectory.

We assume the optimal value function is finite, i.e., $V^N(x_0) \neq \pm\infty$ for all $x_0 \in \mathbb{X}_N$ or $x_0 \in \mathbb{X}$, respectively. The subsequent theorem is combined from [46, Theorem 3.15] and [46, Theorem 4.4].

Theorem 2.3 (Dynamic programming principle)

(i) Consider the optimal control problem (OCPt) *on a finite horizon* $N \in \mathbb{N}$ *with* $x_0 \in \mathbb{X}_N$.

Then, for all $N \in \mathbb{N}$ *and all* $K = 1, \ldots, N$ *the equation*

$$V^N(x_0) = \inf_{\boldsymbol{u} \in \mathbb{U}^K(x_0)} \left\{ J^{K-1}(x_0, \boldsymbol{u}) + V^{N-K}(x_{\boldsymbol{u}}(K, x_0)) \right\}$$

holds. If an optimal control sequence $\boldsymbol{u}^\star \in \mathbb{U}^N(x_0)$ *exists for* x_0, *then the infimum is attained at the minimizer* $\boldsymbol{u}^\star$, *i.e.,*

$$V^N(x_0) = J^{K-1}(x_0, \boldsymbol{u}^\star) + V^{N-K}(x_{\boldsymbol{u}^\star}(K, x_0)).$$

(ii) Consider the optimal control problem (OCP_N) *on the infinite horizon with* $x_0 \in \mathbb{X}$.

Then, for all $K \in \mathbb{N}$, *the equation*

$$V^\infty(x_0) = \inf_{\boldsymbol{u} \in \mathbb{U}^K(x_0)} \left\{ J^{K-1}(x_0, \boldsymbol{u}) + V^\infty(x_{\boldsymbol{u}}(K, x_0)) \right\}$$

holds. If an optimal control sequence $\boldsymbol{u}^\star \in \mathbb{U}^\infty(x_0)$ *exists for* x_0, *then the infimum is attained at the minimizer* $\boldsymbol{u}^\star$, *i.e.,*

$$V^\infty(x_0) = J^{K-1}(x_0, \boldsymbol{u}^\star) + V^\infty(x_{\boldsymbol{u}^\star}(K, x_0)).$$

We note that the existence of an optimal control sequence $\mathbf{u}^\star$ is not necessary for the dynamic programming principle. An immediate consequence of dynamic programming is that tails of optimal control sequences are again optimal control sequences, cf. [46, Corollary 3.16] and [46, Corollary 4.5].

Corollary 2.4 (Tails of optimal solutions are optimal solutions)

(i) Provided $\boldsymbol{u}^\star$ *is an optimal control sequence for initial value* $x_0 \in \mathbb{X}_N$ *and* $N \in \mathbb{N}_{\geq 2}$, *then for each* $K = 1, \ldots, N-1$ *the sequence* $\boldsymbol{u}^{\star,K} = \boldsymbol{u}^\star(\cdot + K)$, *i.e.,*

$$u_K^\star(k) = u^\star(K + k), \quad k = 0, \ldots, N - K - 1$$

is an optimal control sequence for initial value $x_{\boldsymbol{u}^\star}(K, x_0)$ *and horizon* $N - K$.

(ii) If $\boldsymbol{u}^\star$ *is an optimal control sequence for initial value* $x_0 \in \mathbb{X}$ *and infinite horizon, then for each* $K \in \mathbb{N}$ *the sequence* $\boldsymbol{u}^{\star,K} = \boldsymbol{u}^\star(\cdot + K)$, *i.e.,*

$$u_K^\star(k) = u^\star(K + k), \quad k = 0, 1, \ldots$$

is an optimal control sequence for initial value $x_{\boldsymbol{u}^\star}(K, x_0)$.

2.1.2 Dissipativity and Nonlinear Programming

In recent years, dissipativity, as introduced into systems theory by Willems [93, 94], has become a highly useful concept for understanding the qualitative behavior of optimally controlled systems. Apart from the importance in model predictive control [7, 19, 72, 73], dissipativity leads to a characterization of the turnpike property [51]. The turnpike property describes the phenomenon that a near-optimal trajectory of an optimal control problem stays close to an optimal equilibrium most of the time. Hence, this behavior is a way to generalize asymptotic stability properties of optimal

equilibria to finite and infinite horizon optimal control problems. We will also use this notion here and follow [46, Section 8.2]. To this end, we give a brief overview of dissipativity theory for single-objective optimal control problems and some main results that we will need in the remainder of this thesis. To render the presentation concisely, we consider problems without terminal conditions. However, the theory also applies to problems with terminal conditions since dissipativity refers to the interplay between the system and the stage cost.

Definition 2.5 ((Optimal) equilibrium)
An admissible pair $(x^e, u^e) \in \mathbb{Y}$ *is called an* equilibrium or a steady-state *if*

$$x^e = f(x^e, u^e)$$

holds. We say that an equilibrium (x^e, u^e) *is a* strictly globally optimal equilibrium *if*

$$\ell(x^e, u^e) < \ell(x, u)$$

holds for all equilibria $(x, u) \in \mathbb{Y}$ *with* $x \neq x^e$.

Note that all equilibria we consider are assumed to be admissible, i.e., to lie in $\mathbb{Y}$. Furthermore, we will make use of comparison functions, cf. [63].

Definition 2.6 (Comparison functions)

$$\begin{aligned}
\mathcal{K} &:= \{\alpha : \mathbb{R}_{\geq 0} \to \mathbb{R}_{\geq 0} \mid \alpha \text{ is continuous and strictly increasing with } \alpha(0) = 0\} \\
\mathcal{K}_\infty &:= \{\alpha : \mathbb{R}_{\geq 0} \to \mathbb{R}_{\geq 0} \mid \alpha \in \mathcal{K},\ \alpha \text{ is unbounded}\} \\
\mathcal{L} &:= \{\delta : \mathbb{R}_{\geq 0} \to \mathbb{R}_{\geq 0} \mid \delta \text{ is continuous and} \\
&\qquad \text{strictly decreasing with } \lim_{t\to\infty} \delta(t) = 0\} \\
\mathcal{KL} &:= \{\beta : \mathbb{R}_{\geq 0} \times \mathbb{R}_{\geq 0} \to \mathbb{R}_{\geq 0} \mid \beta \text{ is continuous, } \beta(\cdot, t) \in \mathcal{K}\ \forall t \in \mathbb{R}_{\geq 0}, \\
&\qquad \beta(r, \cdot) \in \mathcal{L}\ \forall r \in \mathbb{R}_{>0}\}.
\end{aligned}$$

Moreover, $\mathcal{B}_\varepsilon(x_0) \subseteq \mathbb{R}^n$ denotes the open ball with radius $\varepsilon > 0$ around $x_0 \in \mathbb{R}^n$. With $\operatorname{int} \mathbb{Y}$ and $\operatorname{cl} \mathbb{Y}$, we denote the interior and the closure of a set $\mathbb{Y} \subset \mathbb{R}^n$, respectively. Further, $\|\cdot\|$ is an arbitrary norm in $\mathbb{R}^n$. We denote the concatenation of two vectors by $(\cdot, \cdot)$, and the corresponding norm by $\|(\cdot, \cdot)\|$.

We recall the definition of strict dissipativity, see for instance [46]. In addition, we use the notion of strict pre-dissipativity, see [41], and of strict (x, u)-dissipativity.

Definition 2.7 (Strict (pre-)dissipativity)

(i) A system (2.1) *is called* strictly pre-dissipative for the supply rate $s(x,u)$ at an equilibrium (x^e,u^e) *if there exists a storage function* $\lambda : \mathbb{X} \to \mathbb{R}$*, bounded on bounded subsets of* $\mathbb{X}$*, and a function* $\alpha \in \mathcal{K}_\infty$*, such that for all* $(x,u) \in \mathbb{Y}$ *with* $f(x,u) \in \mathbb{X}$ *the inequality*

$$s(x,u) + \lambda(x) - \lambda(f(x,u)) \geq \alpha(\|x - x^e\|) \tag{2.5}$$

holds.

(ii) The system (2.1) *is called* strictly dissipative *if it is strictly pre-dissipative and the storage function* $\lambda : \mathbb{X} \to \mathbb{R}$ *is bounded from below on* $\mathbb{X}$*.*

(iii) The system (2.1) *is called* strictly (x,u)-(pre-)dissipative *if (i) or (ii) hold with the inequality*

$$s(x,u) + \lambda(x) - \lambda(f(x,u)) \geq \alpha(\|(x - x^e, u - u^e)\|).$$

(iv) The system (2.1) *is called* locally strictly (pre/(x,u))-dissipative*, if there exists a neighborhood* $\mathcal{N}$ *of* x^e *such that (i), (ii), or (iii), respectively, hold for all* $(x,u) \in \mathrm{cl}\mathcal{N} \times \mathbb{U}$ *with* $f(x,u) \in \mathbb{X}$*.*

(v) If the supply rate is of the form $s(x,u) = \ell(x,u) - \ell(x^e,u^e)$*, with stage cost* ℓ *from the optimal control problem* (OCP_N)*, then we say that the system* (2.1) *is* strictly dissipative (pre-dissipative,...) for the stage cost ℓ at an equilibrium (x^e,u^e) *and call*

$$\widetilde{\ell}(x,u) := \ell(x,u) - \ell(x^e,u^e) + \lambda(x) - \lambda(f(x,u)) \tag{2.6}$$

rotated stage costs*.*

Remark

(i) For simplification, we sometimes assume $\lambda(x^e) = 0$*. This can be made without loss of generality because adding a constant to* λ *does not invalidate inequality* (2.5)*.*

(ii) The notion of strict pre-dissipativity we used above is quite similar to the notion of cyclo-dissipativity, see for instance [58, 92]. However, there are also certain differences. For example, cyclo-dissipativity allows the storage function to be unbounded on bounded sets. Further, cyclo-dissipativity requires controllability and detectability to ensure the existence of a storage function in each x*. Since*

we assume such a storage function exists in the following, pre-dissipativity is the more suitable property for us to work with, especially in Chapter 4 of this thesis.

We exploit the connection between the strict dissipativity and convex functions.

Definition 2.8 (Convex set and function)

(i) A set $D \subset \mathbb{R}^n$ is called convex*, if for all $x_1, x_2 \in D$ and $w \in [0,1]$ the relation $wx_1 + (1-w)x_2 \in D$ holds.*

(ii) Let $D \subset \mathbb{R}^n$ be convex. A scalar-valued function $l : D \to \mathbb{R}$ is called convex *if*

$$l(wx_1 + (1-w)x_2) \leq wl(x_1) + (1-w)l(x_2)$$

holds for all $x_1, x_2 \in D$ with $x_1 \neq x_2$ and all $w \in [0,1]$ and is called strictly convex *if this inequality is strict for all $w \in (0,1)$.*

We now provide a couple of preliminary results on strict (pre-)dissipativity. From the definition of strict (pre-)dissipativity, it is immediate that (x^e, u^e) is a globally optimal equilibrium according to Definition 2.5 since $\lambda(f(x^e, u^e)) = \lambda(x^e)$, i.e., it satisfies $\ell(x^e, u^e) \leq \ell(\hat{x}, \hat{u})$ for all other equilibria $(\hat{x}, \hat{u})$. This means that (x^e, u^e) is a minimizer of the so-called steady-state problem

$$\begin{aligned} &\min_{(x,u)\in\mathbb{Y}} \ell(x,u) \\ &\text{s.t. } \; x - f(x,u) = 0. \end{aligned} \tag{SSP}$$

If the minimizer (x^e, u^e) lies in $\operatorname{int}\mathbb{Y}$, then it is also a local minimum of the steady-state problem without state and control constraints

$$\begin{aligned} &\min_{(x,u)\in\mathbb{R}^n\times\mathbb{R}^m} \ell(x,u) \\ &\text{s.t. } \; x - f(x,u) = 0. \end{aligned} \tag{2.7}$$

We observe further that if the system (2.1) is strictly (x,u)-dissipative for the stage cost ℓ at some equilibrium (x^e, u^e), then this equilibrium is the unique minimizer of the constrained optimization problem (SSP) and the unique minimizer of the rotated cost $\widetilde{\ell}$. This is because, from the strict (x,u)-dissipativity, we can conclude that the rotated stage cost is bounded from below by $\widetilde{\ell}(x,u) \geq \alpha(\|(x - x^e, u - u^e)\|)$ for all $(x,u) \in \mathbb{Y}$ and, thus,

$$0 = \widetilde{\ell}(x^e, u^e) = \min_{(x,u)\in\mathbb{Y}} \widetilde{\ell}(x,u) < \widetilde{\ell}(x,u)$$

for all $(x,u) \in \mathbb{Y}$ with $(x,u) \neq (x^e,u^e)$.

We briefly recall some definitions from nonlinear programming, see, for instance, [11, Chapter 3]. Namely, we use the Karush-Kuhn-Tucker (KKT) optimality conditions, cf. [11, 65], to solve the steady-state problems (SSP) and (2.7). To this end, we consider the more general optimization problem

$$\begin{aligned} &\min_{(x,u)\in\mathbb{Y}} \ell(x,u) \\ &\text{s.t. } h(x,u) = 0 \end{aligned} \tag{2.8}$$

with $h : \mathbb{R}^n \times \mathbb{R}^m \to \mathbb{R}^p$ describing the equality constraints and the inequality constraints defined via the set $\mathbb{Y}$ from (2.3) with function $g : \mathbb{R}^n \times \mathbb{R}^m \to \mathbb{R}^q$.

The following are definitions from nonlinear programming and can be found in [11, Chapter 3] for instance.

Definition 2.9 (Active constraint set, regular point)
Consider the optimization problem (2.8) *with constraints of the form* (2.3) *and assume that the functions ℓ, h, g are continuously differentiable.*

(i) For any feasible point (x,u), the set of active inequality constraints *is denoted by*

$$\mathcal{A}(x,u) = \{j \in \{1,\dots,q\} \mid g_j(x,u) = 0\}.$$

If $j \notin \mathcal{A}(x,u)$, we say that the j-th inequality constraint is inactive *at (x,u).*

(ii) The pair (x,u) is called regular *if the vectors in*

$$\{\nabla h_i(x,u) \mid i = 1,\dots,p\} \cup \{\nabla g_j(x,u) \mid j \in \mathcal{A}(x,u)\}$$

are linearly independent.

Theorem 2.10 (KKT necessary conditions, [11, Proposition 3.3.1])
Let ℓ, h, g from problem (2.8) *be continuously differentiable and assume that (x^e,u^e) is regular and a local minimizer of the problem.*

Then, there exist unique Lagrange multiplier vectors $\nu^e \in \mathbb{R}^p$ and $\eta^e \in \mathbb{R}^q$ such that the necessary optimality or KKT conditions

$$\begin{aligned} \nabla_{(x,u,\nu,\eta)} L(x^e,u^e,\nu^e,\eta^e) &= 0, \\ \eta_j^e &\geq 0, \quad j = 1,\dots,q, \\ \eta_j^e &= 0 \quad \forall j \notin \mathcal{A}(x^\star,u^\star) \end{aligned} \tag{2.9}$$

for the Lagrange function

$$L(x,u,\nu,\eta) = \ell(x,u) + \nu^T h(x,u) + \eta^T g(x,u) \tag{2.10}$$

hold.

Remark 2.11
In the case of the steady-state problem (2.7)*, the KKT conditions simplify to*

$$\frac{\partial L}{\partial x}(x^e, u^e, \nu^e) = 0, \quad \frac{\partial L}{\partial u}(x^e, u^e, \nu^e) = 0, \quad \frac{\partial L}{\partial \nu}(x^e, u^e, \nu^e) = 0. \tag{2.11}$$

The necessary KKT conditions are generally not sufficient, which is why we introduce the second order sufficiency conditions.

Proposition 2.12 (Second order sufficiency conditions [11, Proposition 3.3.2])
Consider the problem (2.8) *with $f, h,$ and g twice continuously differentiable functions, let (x^e, u^e) be a feasible point, and assume that $(x^e, u^e, \nu^e, \eta^e)$ satisfies the KKT conditions* (2.9) *and*

$$y^T \nabla_x^2 L(x^e, u^e, \nu^e, \eta^e) y \geq 0,$$

for all $y \in \mathbb{R}^n$ such that

$$\begin{aligned} \nabla h_i(x^e, u^e)^T y = 0 \quad & \forall\, i = 1, \dots, p, \\ \nabla g_j(x^e, u^e)^T y = 0 \quad & \forall\, j \in \mathcal{A}(x^e, u^e). \end{aligned}$$

Assume further that

$$\eta_j^e > 0, \quad \forall\, j \in \mathcal{A}(x^e, u^e).$$

Then, (x^e, u^e) is a local minimum of the problem (2.8).

The next two results apply to optimal control problems with linear dynamics

$$x^+ = Ax + Bu \tag{2.12}$$

with $A \in \mathbb{R}^{n \times n}$ and $B \in \mathbb{R}^{n \times m}$ and show how strict dissipativity can be verified.

Proposition 2.13
Consider the optimal control problem (OCP_N) *with linear dynamics* (2.12)*, strictly convex stage cost ℓ, and constraint set $\mathbb{Y}$ defined via* (2.3) *with a convex function g. Assume that problem* (SSP) *has a global minimum (x^e, u^e) and satisfies the following Slater condition: There exists a pair $(\hat{x}, \hat{u}) \in \mathbb{R}^n \times \mathbb{R}^m$ with*

$$g(\hat{x}, \hat{u}) < 0 \quad \textit{and} \quad \hat{x} - A\hat{x} - B\hat{u} = 0.$$

Then, there exists a vector $\nu \in \mathbb{R}^n$ such that the system is strictly pre-dissipative for the stage cost ℓ and $\lambda(x) = \nu^T x$.

For a proof of this proposition, see [16, Proposition 4.3]. Note that the Slater condition is satisfied with $(\hat{x}, \hat{u}) = (x^e, u^e)$ for an equilibrium (x^e, u^e) satisfying $(x^e, u^e) \in \operatorname{int} \mathbb{Y}$.

The second result shows that strict dissipativity also holds if the stage cost is not itself convex but can be appropriately bounded by a convex function.

Proposition 2.14
Consider the optimal control problem (OCP_N) *with linear dynamics* (2.12) *and constraint set* $\mathbb{Y}$ *defined via* (2.3) *with a convex function* g*. Assume there is a strictly convex function* $\hat{\ell}$ *with* $\hat{\ell} \leq \ell$ *and* $\hat{\ell}(x^e, u^e) = \ell(x^e, u^e)$ *for the strictly globally optimal equilibrium* $(x^e, u^e) \in \mathbb{Y}$ *of* $\hat{\ell}$*, and that the Slater condition from Proposition 2.13 holds.*

Then, the system (2.1) *is strictly pre-dissipative for the stage cost* ℓ *with linear storage function.*

Proof. From Proposition 2.13, it follows that there exists a linear, hence continuous storage function λ for the stage cost $\hat{\ell}$. For this storage function, we thus obtain

$$\begin{aligned} \lambda(f(x,u)) &\leq \lambda(x) + \hat{\ell}(x,u) - \hat{\ell}(x^e,u^e) - \alpha(\|x - x^e\|) \\ &\leq \lambda(x) + \ell(x,u) - \ell(x^e,u^e) - \alpha(\|x - x^e\|) \end{aligned}$$

for all $(x, u) \in \mathbb{Y}$. This proves strict pre-dissipativity for the stage cost ℓ. □

We note that both Proposition 2.13 and Proposition 2.14 yield strict dissipativity if $\mathbb{Y}$ (in the form of (2.3)) is compact, since then $\mathbb{X}$ is compact, too, and the linear storage function is bounded from below on $\mathbb{X}$.

The next result shows that if $(x^e, u^e) \in \operatorname{int} \mathbb{Y}$, then the linear part of the storage function always coincides with the Lagrange multiplier ν from the necessary optimality conditions (2.11). Here, no linearity assumption on f is needed. This result has first been used in the proof of [72, Theorem 5] and has also been proven in [35, Theorem 3].

Proposition 2.15
Consider the optimal control problem (OCP_N) *and assume that the system is strictly dissipative for the stage cost at an equilibrium* $(x^e, u^e) \in \operatorname{int} \mathbb{Y}$*. Assume that* f*,* ℓ *and* λ *are continuously differentiable.*

Then, there exists a Lagrange multiplier ν^e *satisfying* (2.11) *such that the identity*

$$\nabla_x \lambda(x^e) = \nu^e$$

holds.

Proof. Strict dissipativity implies that x^e is a strict minimizer of the map $x \mapsto \tilde{\ell}(x, u^e)$, with $\tilde{\ell}$ from (2.5). This implies that

$$\begin{aligned} 0 = \frac{\partial \tilde{\ell}}{\partial x}(x^e, u^e) &= \frac{\partial \ell}{\partial x}(x^e, u^e) + \underbrace{\frac{\partial \lambda}{\partial x}(x^e)}_{=\nabla_x \lambda(x^e)^T} \left(I - \frac{\partial f}{\partial x}(x^e, u^e) \right) \\ &= L(x^e, u^e, \nu^e), \end{aligned}$$

which shows the first equation in (2.11). With an analogous computation, the fact that u^e is a (possibly non-strict) minimizer of the map $u \mapsto \tilde{\ell}(x^e, u)$ implies the second equation in (2.11). Finally, the third equation in (2.11) follows since (x^e, u^e) is an equilibrium of f. □

2.1.3 The Turnpike Property

In contrast to the previous section, where we derived conditions for strict dissipativity to hold, we now focus on a property that can be concluded from dissipativity. The so-called *turnpike property* is an important ingredient for understanding the behavior of MPC schemes, c.f. [6, 7, 40, 48]. The turnpike property describes the phenomenon that optimal trajectories stay close to an optimal equilibrium "most of the time". It was already observed and studied in [22, 75], and since then used in various contexts and notions [16, 30, 32, 33, 40, 91].

Proposition 2.16 ([46, Proposition 8.15])
Assume system (2.1) *is strictly dissipative for the stage cost ℓ at an equilibrium (x^e, u^e) with bounded storage function λ.*

Then, for each $\delta > 0$ there exists $\sigma_\delta \in \mathcal{L}$ such that for all $N, P \in \mathbb{N}$, $x_0 \in \mathbb{X}$ and $\boldsymbol{u} \in \mathbb{U}^N(x_0)$ with $J^N(x_0, \boldsymbol{u}) \leq N\ell(x^e, u^e) + \delta$, the set

$$\mathcal{Q}(x_0, \boldsymbol{u}, P, N) := \{k \in \{0, \dots, N-1\} \mid \|x_{\boldsymbol{u}}(k, x_0) - x^e\| \geq \sigma_\delta(P)\}$$

has at most P elements.

In the context of model predictive control, the turnpike property is the basis to show averaged and non-averaged performance estimates in various contexts, see [40, 46, 52, 54, 80]. In classical model predictive control, perhaps the most well-known result is that stability of the MPC closed-loop trajectories can be expected, provided the optimization horizon is sufficiently large and strict dissipativity holds. More precisely, the turnpike behavior can be used to show that the MPC closed-loop feedback μ^N is approximately optimal on the infinite horizon, see [40].

2.1.4 Stability using Lyapunov Functions

Besides the performance results based on the dissipativity theory in the analysis of model predictive control schemes, stability results are of great interest. Establishing convergence of the MPC closed-loop trajectory $x_\mu(\cdot, x_0)$ to an equilibrium relies on the fact that the optimal value function V^N is a Lyapunov function, which then implies stability. We refer to [63, 87] for an introduction to Lyapunov theory in the context of optimal control. For completeness, we first define asymptotic stability [46, Definition 2.14] and practical asymptotic stability [48, Definition 2.2]. Since we consider these properties for analyzing model predictive control schemes, we directly formulate the definitions for the MPC closed-loop system (2.4).

Definition 2.17 ((Practical) asymptotic stability)
Let $x^e \in \mathbb{X}$ be an equilibrium for the closed-loop system (2.4)*, i.e., $x^e = f(x^e, \mu^N(x^e))$.*

(i) The equilibrium is locally asymptotically stable *if there exist $\eta > 0$ and a function $\beta \in \mathcal{KL}$ such that the inequality*

$$\|x(k, x_0) - x^e\| \leq \beta(||x_0 - x^e\|, k)$$

holds for all $x_0 \in \mathcal{B}_\eta(x_0)$ and all $k \in \mathbb{N}_0$.

(ii) The equilibrium is called practically asymptotically stable for $\varepsilon \geq 0$ on a set $S \subseteq \mathbb{X}$ with $x^e \in S$ if there exists $\beta \in \mathcal{KL}$ such that

$$\|x(k, x_0) - x^e\| \leq \max\{\beta(\|x - x^e\|, k), \varepsilon\} \tag{2.13}$$

holds for all $x \in S$ and all $k \in \mathbb{N}$. The equilibrium is globally practically asymptotically stable for $\varepsilon \geq 0$ if inequality (2.13) *holds on $S = \mathbb{X}$.*

Next, we introduce Lyapunov functions [46, Definition 2.18] and practical Lyapunov functions [48, Definition 2.3].

Definition 2.18 ((Practical) Lyapunov function)
Consider the closed-loop system (2.4)*, a point $x^e \in \mathbb{X}$, and let $S \subseteq \mathbb{X}$ be a subset of the state space.*

(i) A function $V : S \to \mathbb{R}_{\geq 0}$ is called a Lyapunov function *on S if there exist functions $\alpha_1, \alpha_2 \in \mathcal{K}_\infty$ and $\alpha_3 \in \mathcal{K}$ such that*

$$\alpha_1(\|x - x^e\|) \leq V(x) \leq \alpha_2(\|x - x^e\|) \tag{2.14}$$

holds for all $x \in S$ and

$$V(f(x, \mu^N(x))) \leq V(x) - \alpha_3(\|x - x^e\|) \tag{2.15}$$

holds for all $x \in S$ with $f(x, \mu^N(x)) \in S$.

(ii) A function $V : S \to \mathbb{R}_{\geq 0}$ *is a* practical Lyapunov function *on* S *for* $\delta > 0$*, if there are* $\alpha_1, \alpha_2 \in \mathcal{K}_\infty$ *and* $\alpha_3 \in \mathcal{K}$ *such that inequality* (2.14) *holds and*

$$V(f(x, \mu(x))) \leq V(x) - \alpha_3(\|x - x^e\|) + \delta \tag{2.16}$$

hold for all $x \in S$*.*

We now provide the well-known results that the existence of Lyapunov functions implies stability. As above, we distinguish practical asymptotic stability and asymptotic stability.

Theorem 2.19 ([48, Theorem 2.4])
Let V *be a practical Lyapunov function for some* $\delta > 0$ *on a set* $S \subseteq \mathbb{X}$*. Assume that either* $S = \mathbb{X}$ *or* $S = V^{-1}([0, L]) := \{x \in \mathbb{X} \mid V(x) \leq L\}$ *for some* $L > \alpha_2(\alpha_3^{-1}(\delta)) + \delta$*.*
Then, x^e *is practically asymptotically stable on* S *for* $\varepsilon = \alpha_1^{-1}(\alpha_2(\alpha_3^{-1}(\delta)) + \delta)$*.*

Remark
The proof of Theorem 2.19 relies on the fact that the set S *is forward invariant, i.e.,* $f(x(k, x_0), \mu^N(x(k, x_0))) \in S$ *for all* $x(k, x_0) \in S$*,* $k \in \mathbb{N}$*. Actually, the theorem still holds true if the relation* $f(x(k, x_0), \mu^N(x(k, x_0))) \in S$ *holds for* $x(k, x_0) \in S$ *with* $k \in \{0, \ldots, M\}$*,* $M \in \mathbb{N}$*.*

Theorem 2.20 ([46, Theorem 2.19])
Let x^e *be an equilibrium of system* (2.1) *and assume that there exists a Lyapunov function* V *on* $S \subset \mathbb{X}$*.*

(i) If S *contains a ball* $\mathcal{B}_\varepsilon(x^e)$ *with* $f(x, \mu^N(x)) \in S$ *for all* $x \in \mathcal{B}_\varepsilon(x^e)$*, then* x^e *is locally asymptotically stable with* $\eta = \alpha_2^{-1} \circ \alpha_1(\varepsilon)$*.*

(ii) If $S = Y$ *holds for some forward invariant set* $Y \subseteq \mathbb{X}$ *containing* x^e*, then* x^e *is asymptotically stable on* Y*.*

(iii) If $S = \mathbb{X}$ *holds, then* x^e *is globally asymptotically stable.*

Additionally, we recall the definition of a uniform time-varying Lyapunov function, which can be found in [46, Definition 2.21]. We will need this time-varying concept to show the stability of our proposed multiobjective model predictive control scheme in Chapter 5. We consider a general time-varying discrete time dynamical system given by

$$x^+ = f(x, \mu^N(k, x)), \tag{2.17}$$

where the feedback $\mu^N(k, x)$ also depends on a time instant $k \in \mathbb{N}$.

Definition 2.21 (Uniform time-varying Lyapunov function)
Consider system (2.17)*, an equilibrium* $x^e \in \mathbb{X}$*, i.e.,* $x^e = f(x^e, \mu^N(k, x^e))$ *for all* $k \in \mathbb{N}_0$*, subsets of the state space* $S(k) \subseteq \mathbb{X}$*,* $k \in \mathbb{N}_0$*, and define*

$$\mathcal{S} := \{(k, x) \mid k \in \mathbb{N}_0,\, x \in S(k)\}.$$

A function $V : \mathcal{S} \to \mathbb{R}_{\geq 0}$ *is called* uniform time-varying Lyapunov function *on* $\mathcal{S}$ *if there exist functions* $\alpha_1, \alpha_2 \in \mathcal{K}_\infty$ *and* $\alpha_3 \in \mathcal{K}$ *such that*

$$\alpha_1(\|x - x^e\|) \leq V(k, x) \leq \alpha_2(\|x - x^e\|)$$

holds for all $(k, x) \in \mathcal{S}$ *and*

$$V(k+1, f(x, \mu^N(k, x))) \leq V(k, x) - \alpha_V(\|x - x^e\|)$$

holds for all $k \in \mathbb{N}_0$ *and* $x \in S(k)$ *with* $f(x, \mu^N(k, x)) \in S(k+1)$*.*

The following theorem shows that the existence of such a Lyapunov function ensures asymptotic stability. For a proof, we refer to [46, Theorem 2.22].

Theorem 2.22
Let x^e *be an equilibrium of system* (2.17)*, i.e.,* $x^e = f(x^e, \mu^N(k, x^e))$ *for all* $k \in \mathbb{N}_0$*, and assume there exists a uniform time-varying Lyapunov function* V *on a set* $\mathcal{S} \subset \mathbb{N}_0 \times \mathbb{R}^n$ *as defined in Definition 2.21.*

(i) If each $S(k)$ *contains a ball* $\mathcal{B}_\nu(x^e)$ *with radius* $\nu > 0$ *with* $f(x, \mu^N(k, x)) \in S(k+1)$ *for all* $x \in \mathcal{B}_\nu(x^e)$*, then* x^e *is locally asymptotically stable with* $\eta = \alpha_2^{-1} \circ \alpha_1(\nu)$*.*

(ii) If the family of sets $S(k)$ *is forward invariant (i.e., if* $f(x, \mu^N(k, x)) \in S(k+1)$ *for all* $(k, x) \in \mathcal{S}$*) then* x^e *is asymptotically stable on* $S(k)$*.*

(iii) If $S(k) = \mathbb{R}^n$ *holds for all* $k \in \mathbb{N}_0$ *then* x^e *is globally asymptotically stable.*

2.2 Multiobjective Optimal Control

In many practical model predictive control applications, as in [61,68,85], it is a natural idea to consider not only one but multiple cost criteria. These criteria might be conflicting, so the resulting optimization problem is a multicriterion or multiobjective optimization problem. In the MPC framework, multiobjective optimization has been investigated in different contexts, e.g., in [36, 54, 88, 95, 96]. Before investigating multiobjective optimal control problems, we present some definitions and results from multiobjective optimization.

2.2.1 Multiobjective Optimization

Multiobjective optimization is an indispensable tool for decision-makers if the benefit of a decision does not depend on one objective only but if several competing objectives are aspired simultaneously. In this section, we consider the multiobjective optimization problem

$$\begin{aligned} &\min_{x\in X}(l_1(x),\dots,l_s(x)) \\ &\text{s.t. } h(x)=0, \\ &\quad g(x)\leq 0 \end{aligned} \tag{2.18}$$

with given functions $l:\mathbb{R}^n\to\mathbb{R}^s$, $s\geq 2$, $h:\mathbb{R}^n\to\mathbb{R}^p$, $g:\mathbb{R}^n\to\mathbb{R}^q$, and $X\subset\mathbb{R}^n$ an admissible constraint set.

Whenever multiple objective functions, i.e., cost criteria, are considered, one has to agree on an optimality notion used for such problems. In general, there will not be one optimal solution for minimizing all cost functionals simultaneously. The formalization we will use here is based on the componentwise ordering in the image space $\mathbb{R}^s$ and is summarized in the following definition. For this definition and for an introduction to multiobjective optimization, we refer, for instance, to [23] or the recent survey [25].

Definition 2.23 (Efficient solutions and nondominated points)

(i) A point $x^\star\in X$ is called an efficient (or Pareto minimal) solution for the multiobjective optimization problem (2.18) *if there exists no other point $x\in X$ such that*

$$\begin{aligned} &l_i(x)\leq l_i(x^\star), \quad \textit{for all } i\in\{1,\dots,s\}, \\ &l_j(x)<l_j(x^\star), \quad \textit{for at least one } j\in\{1,\dots,s\}. \end{aligned}$$

We denote the set of all efficient solutions by $\mathcal{E}\subseteq X$.

(ii) A point $x^\star\in\mathcal{E}$ is called a weakly efficient solution for (2.18) *if there exist no other point $x\in X$ such that*

$$l_i(x)<l_i(x^\star) \quad \textit{for all } i\in\{1,\dots,s\}.$$

(iii) If $x^\star\in\mathcal{E}$ is efficient, then $l(x^\star)$ is called nondominated point.

(iv) The set of all nondominated points $l(\mathcal{E})=\{l(x^\star)\mid x^\star\in\mathcal{E}\}$ is called the nondominated set (Pareto front).

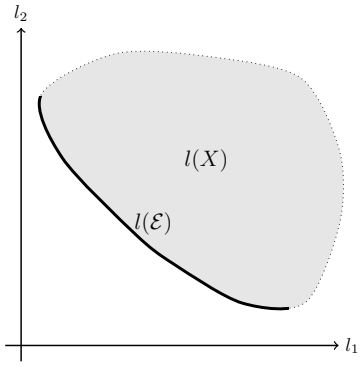

Figure 2.2: Illustration of $l(X)$ and $l(\mathcal{E})$

The nondominated set $l(\mathcal{E})$ is a part of the boundary of the set $l(X) := \{l(x) \in \mathbb{R}^s \mid x \in X\}$. Figure 2.2 illustrates this relation in the case of two objective functions. Further, we note that every efficient solution $x^\star \in \mathcal{E}$ is also weakly efficient. If all objectives l_i, $i = 1, \ldots, s$, are strictly convex and the set X is convex, then every weakly efficient solution $x^\star \in X$ is also an efficient solution.

The Weighted Sum Approach

A common way to solve multiobjective optimization problems (2.18) is to use a weighted sum approach, see, for instance, [23]. This means we consider the sum

$$\sum_{i=1}^{s} w_i l_i(x),$$

where $w \in \mathbb{R}^s$ denotes a weight vector with weights $w_i \in \mathbb{R}_{\geq 0}$, $i = 1, \ldots, s$, $s \geq 2$, and $\sum_{i=1}^{s} w_i = 1$. By solving the single-objective problem

$$\begin{aligned} \min_{x \in X} l_w(x) &:= \sum_{i=1}^{s} w_i l_i(x) \\ \text{s.t. } h(x) &= 0, \\ g(x) &\leq 0, \end{aligned} \tag{SOP$_w$}$$

for each weight w, we can parametrize the efficient solutions of the multiobjective optimization problem (2.18). While the weighted sum approach does not parametrize all efficient solutions, it parametrizes many of them and yields a particularly simple approach to multiobjective optimization, cf. [23, Chapter 3]. We use the following definitions in the remainder of this thesis.

Definition 2.24

(i) A vector-valued function $l = (l_1, \dots, l_s)^T : D \to \mathbb{R}^s$ is called (strictly) convex if all its component functions $l_i : D \to \mathbb{R}$, $i = 1, \dots, s$, are (strictly) convex.

(ii) For functions $l_i : D \to \mathbb{R}$, $i = 1, \dots, s$, we call

$$\sum_{i=1}^{s} w_i l_i \quad \text{for } w_i \in [0,1],\ \sum_{i=1}^{s} w_i = 1$$

a convex combination. *For two functions $l_1, l_2 : D \to \mathbb{R}$, this simplifies to*

$$w l_1 + (1-w) l_2 \quad \text{for } w \in [0,1].$$

(iii) A multiobjective optimization problem (2.18) *is called* (strictly) convex *if all objective functions l_i, $i = 1, \dots, s$, are (strictly) convex.*

In the case of a convex multiobjective optimization problem, the weighted sum approach parametrizes all the efficient solutions. For the justification of doing so, we follow [23, 88].

Lemma 2.25 ([23, Proposition 3.9, Theorem 3.11])
Consider weights $w_i \in \mathbb{R}_{\geq 0}$, $i = 1, \dots, s$, with $\sum_{i=1}^{s} w_i = 1$ and let $x^\star$ be a solution of the single-objective problem (SOP_w).

(i) If $w_i > 0$ for all $i = 1, \dots, s$, then $x^\star$ is an efficient solution for the multiobjective optimization problem (2.18).

(ii) If $x^\star$ is a unique solution of the single-objective problem (SOP_w), *then it is an efficient solution for the multiobjective optimization problem* (2.18), *i.e., $x^\star \in \mathcal{E}$.*

Lemma 2.26 ([88, Lemma 3.9])
Let the multiobjective optimization problem (2.18) *be convex with efficient solution $x^\star \in \mathcal{E}$.*

Then, there exists a weight vector $w = (w_1, \dots, w_s)^T$ with $w_i \in \mathbb{R}_{\geq 0}$ and $\sum_i w_i = 1$ such that $x^\star$ is a solution to the corresponding single-objective problem (SOP_w).

Corollary 2.27 ([23, Theorem 3.15])
Let the multiobjective optimization problem (2.18) *be strictly convex.*

Then, $x^\star \in \mathcal{E}$ is an efficient solution if and only if there exists $w = (w_1, \dots, w_s)^T$ with $w_i \in \mathbb{R}_{\geq 0}$ and $\sum_i w_i = 1$ such that $x^\star$ is a solution to the single-objective problem (SOP_w).

From the results above, we can conclude that the nondominated set (Pareto front) can be completely characterized via a weighted sum approach if the multiobjective optimization problem (2.18) is strictly convex. The following theorem combines the notion of efficiency with the KKT conditions from Section 2.1.2 and is Theorem 4.1 in [59], based on the work [65].

Theorem 2.28 ([59, Theorem 4.1])
Consider a multiobjective optimization problem (2.18) *and a regular point* $x^\star \in X$.

If $x^\star$ *is efficient, then there exist* $w \in \mathbb{R}^s$ *with* $w_i \in \mathbb{R}_{\geq 0}$ *and* $\sum_{i=1}^s w_i = 1$ *and* $\lambda \in \mathbb{R}^p$, $\nu \in \mathbb{R}^q$ *such that*

$$\begin{aligned} \sum_{i=1}^{s} w_i \nabla l_i(x^\star) + \sum_{j=1}^{q} \nu_j \nabla h_j(x^\star) + \sum_{k=1}^{p} \lambda_k \nabla g_k(x^\star) = 0 & \\ h_j(x^\star) = 0, \quad j = 1, \dots, q & \\ \lambda_k \geq 0,\, g_k(x^\star) \leq 0,\, \lambda_k g_k(x^\star) = 0, \quad k = 1, \dots, p & \end{aligned}$$

hold.

We note that $\sum_{i=1}^s w_i \nabla l_i(x) = \nabla l_w(x)$. In particular, the conditions in Theorem 2.28 are equivalent to the claim that $x^\star$ is a KKT point of the corresponding scalar-valued optimization problem with the objective function l_w.

Remark 2.29
In a certain way, the weighted sum approach is based on the result above. However, the approach above does not generally yield the complete nondominated set because the second-order conditions necessary for a point $x^\star$ *to be a local minimizer of the scalar-valued function* l_w *are not necessary for* $x^\star$ *to be efficient.*

2.2.2 Properties of Multiobjective Optimal Control Problems

This thesis is built on the findings from [54, 88], in which a multiobjective MPC algorithm is presented and analyzed. We impose the setting and give an overview of important properties of multiobjective optimal control problems, which we will use in the remainder.

As in the single-objective case, we impose nonempty state and control sets $\mathbb{X}$ and $\mathbb{U}$ and denote by

$$\mathbb{U}^N(x_0) := \{\mathbf{u} \in \mathbb{U}^N \mid x_{\mathbf{u}}(k, x_0) \in \mathbb{X} \; \forall \; k = 1, \dots, N\}$$

the set of admissible control sequences for $x_0 \in \mathbb{X}$ up to time N. Since we aim to minimize all cost functionals $J_1^N, \dots, J_s^N$ simultaneously for a given initial value x_0

with respect to $\mathbf{u}$ and along a solution of system (2.1), this leads to the formulation of a multiobjective optimal control problem

$$\begin{aligned} \min_{\mathbf{u}\in\mathbb{U}^N(x_0)} \; & J^N(x_0,\mathbf{u}) := \big(J_1^N(x_0,\mathbf{u}),\dots,J_s^N(x_0,\mathbf{u})\big) \\ \text{s.t.} \quad & x_{\mathbf{u}}(k+1,x_0) = f(x_{\mathbf{u}}(k,x_0),u(k)), \quad k=0,\dots,N-1 \\ & x_{\mathbf{u}}(0,x_0) = x_0, \\ & x_{\mathbf{u}}(N,x_0) \in \mathbb{X}_0. \end{aligned} \tag{2.19}$$

Regarding the multiobjective optimal control problems, the notion of efficient solutions reads as follows: A sequence $\mathbf{u}^\star \in \mathbb{U}^N(x_0)$ is called efficient for (2.19) with $x_0 \in \mathbb{X}$ if there is no $\mathbf{u} \in \mathbb{U}^N(x_0)$ such that

$$\begin{aligned} & \forall\, i \in \{1,\dots,s\}:\ J_i^N(x_0,\mathbf{u}) \le J_i^N(x_0,\mathbf{u}^\star) \\ \text{and} \quad & \exists\, i \in \{1,\dots,s\}:\ J_i^N(x_0,\mathbf{u}) < J_i^N(x_0,\mathbf{u}^\star). \end{aligned}$$

As in Definition 2.23, the objective $J^N(x_0,\mathbf{u}^\star) = (J_1^N(x_0,\mathbf{u}^\star),\dots,J_s^N(x_0,\mathbf{u}^\star))$ is called nondominated. The set of all efficient solutions of length N for initial value $x_0 \in \mathbb{X}$ is denoted by $\mathbb{U}_{\mathcal{E}}^N(x_0)$, and we define the set of attainable values by

$$\mathcal{J}^N(x_0) := \{J^N(x_0,\mathbf{u}) = (J_1^N(x_0,\mathbf{u}),\dots,J_s^N(x_0,\mathbf{u})) \mid \mathbf{u} \in \mathbb{U}^N(x_0)\},$$

and the nondominated set by

$$\mathcal{J}_{\mathcal{E}}^N(x_0) := \{J^N(x_0,\mathbf{u}) \mid \mathbf{u} \in \mathbb{U}_{\mathcal{E}}^N(x_0)\}.$$

In this case, the min-operator is defined as

$$\min_{\mathbf{u}\in\mathbb{U}^N(x_0)} J^N(x_0,\mathbf{u}) = \mathcal{J}_{\mathcal{E}}^N(x_0)$$

and, accordingly

$$\arg\min_{\mathbf{u}\in\mathbb{U}^N(x_0)} J^N(x_0,\mathbf{u}) = \mathbb{U}_{\mathcal{E}}^N(x_0).$$

We now provide basic definitions and results from the multiobjective optimization theory, adapted from [23, 83] to our setting.

Definition 2.30 (External stability)
The set $\mathcal{J}_{\mathcal{E}}^N(x_0)$ is called externally stable for $\mathcal{J}^N(x_0)$ if for all $y \in \mathcal{J}^N(x_0)$ there is $y_{\mathcal{E}} \in \mathcal{J}_{\mathcal{E}}^N(x_0)$ such that $y \ge y_{\mathcal{E}}$ holds componentwise.

Definition 2.31 (Cone-Compactness)
The set $\mathcal{J}^N(x_0)$ is called $\mathbb{R}^s_{\ge 0}$-compact if for all $y \in \mathcal{J}^N(x_0)$ the set $(y-\mathbb{R}^s_{\ge 0})\cap\mathcal{J}^N(x_0)$ is compact.

Here, we write $z - \mathbb{R}^s_{\geq 0}$ for the difference of the sets $\{z\}$ and $\mathbb{R}^s_{\geq 0} := \{y \in \mathbb{R}^s \mid y_i \geq 0 \ \forall i = 1, \ldots, s\}$ in the Minkowski sense. The next theorem states a condition for external stability of the set $\mathcal{J}^N_{\mathcal{E}}(x_0)$, and a proof can be found in [23, 83].

Theorem 2.32
Given a horizon $N \in \mathbb{N}$ and an initial value $x_0 \in \mathbb{X}$, and if $\mathcal{J}^N(x_0) \neq \emptyset$ and $\mathcal{J}^N(x_0)$ is $\mathbb{R}^s_{\geq 0}$-compact, then the set $\mathcal{J}^N_{\mathcal{E}}(x_0)$ is externally stable for $\mathcal{J}^N(x_0)$.

Since the assumptions of Theorem 2.32 are difficult to verify in practice, the next lemma provides easily checkable conditions for external stability, which we will need for feasibility in Chapter 5. For a proof we refer to Lemma 2.5 in [54] or Lemma 4.8 in [88].

Lemma 2.33
Let $\mathbb{U}$ be compact, $\mathbb{X}$ and $\mathbb{X}_0$ be closed and let $x_0 \in \mathbb{X}$ and $N \in \mathbb{N}$.
Then, the set $\mathcal{J}^N_{\mathcal{E}}(x_0)$ is externally stable for $\mathcal{J}^N(x_0)$.

In the single-objective case, an immediate consequence of the dynamic programming principle (DPP) is that tails of optimal control sequences are again optimal control sequences (see Corollary 2.4). The same result holds for efficient solutions and can be found in [88, Lemma 4.1].

Lemma 2.34 (Tails of efficient solutions are efficient solutions)
Let $K < N$. If $\boldsymbol{u}^{\star,N} \in \mathbb{U}^N_{\mathcal{E}}(x_0)$, then $\boldsymbol{u}^{\star,K} \in \mathbb{U}^{N-K}_{\mathcal{E}}(x_{\boldsymbol{u}^{\star,N}}(K, x_0))$ with

$$\boldsymbol{u}^{\star,K} := \boldsymbol{u}^{\star,N}(\cdot + K)$$

for all $K < N$, where

$$\boldsymbol{u}^{\star,N}(\cdot + K) := (u^{\star,N}(K), u^{\star,N}(K+1), \ldots, u^{\star,N}(N-1)).$$

3 Discounted Optimal Control Problems

In multiobjective optimal control problems, it is much more likely that several asymptotically stable optimal equilibria coexist in contrast to single-objective problems. Since coexisting multiple optimal equilibria are also typical for discounted optimal control problems, we use them to study the behavior of trajectories in the presence of several asymptotically stable optimal equilibria.

Moreover, discounted problems are very popular in many areas, such as reinforcement learning [10, 89], economics [2, 14, 79], and planning algorithms for optimal control [66], which is an additional motivation to concentrate on discounted optimal control problems in this section. The characteristic of this important class of problems is that the cost function incorporates a multiplicative term β^k at each time step $k \in \mathbb{N}_0$, where $\beta \in (0, 1]$ denotes the discount factor. Hence, the higher the time step k, the less important the related costs. For optimal control problems on the infinite horizon, discounting is a way to circumvent the infinite dimensionality. Several works, for instance, [37, 39, 77, 78], have already discussed the stability and the behavior of trajectories of discounted optimal control problems.

Due to the discounting, it may not be possible to compensate for the transition cost from one equilibrium to the other with the lower cost of staying in the cheaper equilibrium. Therefore, locally asymptotically stable equilibria with different costs may coexist even for infinite horizon problems in the discounted case. Indeed, assuming complete controllability, in non-discounted optimal control, multiple optimal equilibria can only coexist for arbitrary long (or infinite) horizons if they yield exactly the same optimal cost. Otherwise, for a sufficiently long time, it will always be beneficial to steer the system from the more expensive equilibrium to the cheaper one. In mathematical economy, where discounted optimal control problems are an important modeling tool, this trajectory behavior is a well-known fact, at least since the pioneering work of Skiba [86] and Dechert and Nishimura [18]. Since then, this behavior has been observed in many other papers, see, e.g., [56] and the references therein.

In addition to discounted strict dissipativity and the discounted turnpike property for a globally optimal equilibrium, we also study the strict dissipativity and the convergence behavior at a locally optimal equilibrium in this chapter. More precisely, we show that in the presence of local strict dissipativity and appropriate growth

conditions on the optimal value functions, there exist bounds on the discount factor β such that convergence of optimal trajectories to the locally optimal equilibrium occurs locally.

3.1 Problem Statement

In this part of the thesis, we concentrate on infinite horizon discounted optimal control problems, i.e., problems of the type

$$\begin{aligned} \min_{\mathbf{u}\in\mathbb{U}^\infty(x_0)} J_\beta^\infty(x_0,\mathbf{u}) &= \sum_{k=0}^{\infty} \beta^k \ell(x_{\mathbf{u}}(k,x_0),u(k)) \\ \text{s.t.} \quad x_{\mathbf{u}}(k+1,x_0) &= f(x_{\mathbf{u}}(k,x_0),u(k)), \quad k\in\mathbb{N}, \\ x_{\mathbf{u}}(0,x_0) &= x_0, \end{aligned} \tag{OCP(β)}$$

where the number $\beta \in (0,1)$ is called the discount factor. We deliberately exclude $\beta = 1$ as this case results in the optimal control problem (OCP_N). For the derivation of our technical results, we make frequent use of the discounted dynamic programming principle [5]

$$V_\beta^\infty(x_0) = \inf_{u\in\mathbb{U}^1(x_0)} \{\ell(x_0,u) + \beta V_\beta^\infty(f(x_0,u))\},$$

where

$$V_\beta^\infty(x_0) := \min_{\mathbf{u}\in\mathbb{U}^\infty(x_0)} J_\beta^\infty(x_0,\mathbf{u})$$

denotes the optimal value function of problem (OCP(β)), see Section 2.1.1. If $\mathbf{u}^\star \in \mathbb{U}^\infty(x_0)$ is an optimal control sequence for an initial value $x_0 \in \mathbb{X}$, i.e. if

$$J_\beta^\infty(x_0,\mathbf{u}^\star) = V_\beta^\infty(x_0)$$

holds, then the identity

$$V_\beta^\infty(x_0) = \ell(x_0,u^\star(0)) + \beta V_\beta^\infty(f(x_0,u^\star(0)))$$

holds. Proofs for these statements can be found, for example, in [46, Section 4.2].

We denote – as usual – the optimal trajectories by $x_{\mathbf{u}^\star}(k,x_0)$ with $x_0 \in \mathbb{X}$, $k \in \mathbb{N}$. Further, in the discounted case, an equilibrium is optimal if

$$V_\beta^\infty(x^\beta) = \frac{\ell(x^\beta,u^\beta)}{(1-\beta)}$$

holds, [45, Definition 5.1], and we denote an equilibrium of system (2.1) by (x^β,u^β) since the equilibria are dependent on the discount factor $\beta \in (0,1)$. For more details, we refer to [45] and the discussion and references therein.

As shown in [37], for discounted optimal control problems, all optimal trajectories converge to a neighborhood of x^β for sufficiently large $\beta \in (0,1)$ provided strict dissipativity at an optimal equilibrium x^β holds. The optimal trajectories converge even to the optimal equilibrium x^β itself and not only to a neighborhood either assuming slightly stronger conditions on the problem data, cf. [37, Section 6] or considering $\beta \to 1$, cf. [37, Theorem 4.4]. We will express this result in the language of turnpike theory in Theorem 3.4 below. While this global turnpike result follows from a relatively straightforward modification of the arguments in [37], the main question that we want to address in this chapter is more complex: Assume that strict dissipativity does not hold globally but only in a neighborhood of a locally optimal equilibrium x_l^β. Can we still expect to observe a turnpike property of trajectories starting close to x_l^β?

3.2 The Global Discounted Turnpike Property

We begin our investigation by assuming *global* strict dissipativity, i.e., the discounted strict dissipativity inequality at the equilibrium (x^β, u^β) defined below holds for all pairs $(x,u) \in \mathbb{X}$. Then, we can conclude a global turnpike result for near-optimal trajectories using similar technical assumptions and a similar proof technique as in [37]. Therefore, we first formalize discounted strict dissipativity, from which we conclude the turnpike property.

3.2.1 Global Discounted Strict Dissipativity

We give in the following a definition of discounted strict dissipativity, which is the strict dissipativity Definition 2.7 adapted to the discounted case and is given in [38, 42, 44] for instance.

Definition 3.1 (Discounted Strict Dissipativity)
Given a discount factor $\beta \in (0,1)$, the system (2.1) *is* discounted strictly dissipative for the supply rate $s : \mathbb{Y} \to \mathbb{R}$ at an equilibrium (x^β, u^β) *if there exists a storage function $\lambda : \mathbb{X} \to \mathbb{R}$ bounded from below with $\lambda(x^\beta) = 0$ and $\alpha \in \mathcal{K}_\infty$ such that the inequality*

$$s(x,u) + \lambda(x) - \beta\lambda(f(x,u)) \geq \alpha(\|x - x^\beta\|) \tag{3.1}$$

holds for all $(x,u) \in \mathbb{Y}$ with $f(x,u) \in \mathbb{X}$.

If the supply rate s is given as $\ell(x,u) - \ell(x^\beta, u^\beta)$, then we denote by

$$\widetilde{\ell}_\beta(x,u) := \ell(x,u) - \ell(x^\beta, u^\beta) + \lambda(x) - \beta\lambda(f(x,u))$$

the *rotated* – or *modified* – stage cost.

The following lemma is Proposition 3.2 from [45]. It shows the advantage of considering the infinite horizon in the discounted case. Namely, replacing the stage cost ℓ in (OCP(β)) by the *rotated* stage cost $\widetilde{\ell}_\beta$ that is positive definite does not affect the optimal solutions and optimal trajectories. For this reason, we consider the modified discounted optimal control problem

$$\begin{aligned} \min_{\mathbf{u}\in\mathbb{U}^\infty(x_0)} \widetilde{J}_\beta^\infty(x_0,\mathbf{u}) &:= \sum_{k=0}^{\infty} \beta^k \widetilde{\ell}_\beta(x_{\mathbf{u}}(k,x_0),u(k)) \\ \text{s.t.} \quad x_{\mathbf{u}}(k+1,x_0) &= f(x_{\mathbf{u}}(k,x_0),u(k)), \quad k\in\mathbb{N}, \\ x_{\mathbf{u}}(0,x_0) &= x_0. \end{aligned} \tag{3.2}$$

Lemma 3.2
Consider the discounted optimal control problem (OCP(β)) *with discount factor* $\beta \in (0,1)$ *and assume system* (2.1) *is discounted strictly dissipative for the supply rate* $s(x,u) = \ell(x,u) - \ell(x^\beta,u^\beta)$ *at an equilibrium* (x^β,u^β) *with bounded storage function* λ.

Then, the optimal trajectories of (OCP(β)) *coincide with those of the problem* (3.2) *with rotated stage cost* $\widetilde{\ell}_\beta$, *which is positive definite in* x^β *at* (x^β,u^β), *i.e., it satisfies* $\widetilde{\ell}_\beta(x^\beta,u^\beta)=0$ *and the inequality* $\widetilde{\ell}_\beta(x,u) \geq \alpha(\|x-x^\beta\|)$ *with* $\alpha\in\mathcal{K}_\infty$ *from* (3.1) *for all* $(x,u)\in\mathbb{Y}$.

Proof. We follow the proof of [45, Proposition 3.2]. Rearranging

$$\begin{aligned} \widetilde{J}_\beta^\infty(x_0,\mathbf{u}) &= \sum_{k=0}^{\infty} \beta^k \widetilde{\ell}_\beta(x_{\mathbf{u}}(k,x_0),u(k)) \\ &= \sum_{k=0}^{\infty} \beta^k \Big(\ell(x_{\mathbf{u}}(k,x_0),u(k)) - \ell(x^\beta,u^\beta) + \lambda(x_{\mathbf{u}}(k,x_0)) - \beta\lambda(x_{\mathbf{u}}(k+1,x_0)) \Big) \end{aligned}$$

and a straightforward calculation shows that

$$\widetilde{J}_\beta^\infty(x_0,\mathbf{u}) = J_\beta^\infty(x_0,\mathbf{u}) - \frac{\ell(x^\beta,u^\beta)}{1-\beta} + \lambda(x_0) - \lim_{k\to\infty} \beta^k \lambda(x_{\mathbf{u}}(k,x_0)). \tag{3.3}$$

Since λ is bounded and $\beta\in(0,1)$, the last limit exists and equals 0. Hence, the objectives J_β^∞ and $\widetilde{J}_\beta^\infty$ differ only by expressions that are independent of $\mathbf{u}$, from which the identity of the optimal trajectories immediately follows. The positive definiteness of $\widetilde{\ell}_\beta$ follows from its definition, using strict dissipativity and the fact that $\lambda(x^\beta)=0$ implies $\widetilde{\ell}_\beta(x^\beta,u^\beta)=0$. □

Remark 3.3
The requirement that $\widetilde{\ell}(x^\beta, u^\beta) = 0$ is the reason for imposing $\lambda(x^\beta) = 0$ as a condition in Definition 3.1. As already discussed, in the undiscounted case, cf. Remark 2.1.2, $\lambda(x^\beta) = 0$ can be assumed without loss of generality since if λ is a storage function, then $\lambda + c$ is a storage function for all $c \in \mathbb{R}$. In the discounted case, this invariance with respect to the addition of constants does not hold anymore.

3.2.2 The Global Turnpike Property

We have already discussed in Section 2.1.2 that strict dissipativity (together with suitable regularity assumptions on the problem data) implies that optimal and near-optimal trajectories exhibit the turnpike property in the non-discounted setting. Indeed, the following theorem shows that this implication also holds in the discounted case. However, we need an appropriate formalization of the discounted turnpike property. To this end, we exploit Definition 4.2 from [49], which incorporates that for merely near-optimal trajectories, the turnpike property can only be guaranteed on a finite discrete interval $\{0, \dots, M\}$. Below, we measure the deviation from optimality by δ. Then, M and δ depend on each other, see the discussion in [49, Section 4]: The smaller we choose δ, the larger M becomes and, conversely, the larger we want M to be, the smaller we need to choose δ. Below, we fix M, choose δ accordingly, and extend the statement in [37] from optimal to near-optimal trajectories. The corresponding proof is a variation of Theorem 3.1 and Corollary 4.3 in [37].

Theorem 3.4
Consider the infinite horizon discounted optimal control problem (OCP(β)) *with discount factor $\beta \in (0,1)$ and assume the system* (2.1) *is discounted strictly dissipative for the supply rate $s(x,u) = \ell(x,u) - \ell(x^\beta, u^\beta)$ at an equilibrium (x^β, u^β). Assume that the optimal value function $\widetilde{V}_\beta^\infty$ of the modified problem* (3.2) *satisfies $\widetilde{V}_\beta^\infty(x) \leq \alpha_V(\|x - x^\beta\|)$ and*

$$\widetilde{V}_\beta^\infty(x) \leq C \inf_{u \in \mathbb{U}} \widetilde{\ell}_\beta(x,u) \tag{3.4}$$

for all $x \in \mathbb{X}$, a function $\alpha_V \in \mathcal{K}_\infty$, and a constant $C \geq 1$ satisfying

$$C < 1/(1-\beta). \tag{3.5}$$

Then, the discounted optimal control problem has the following turnpike property (cf. [49, Definition 4.2]):

For each $\varepsilon > 0$ and each bounded set $\mathbb{X}_b \subset \mathbb{X}$ there exist a constant $P > 0$ such that for each $M \in \mathbb{N}$ there is a $\delta > 0$ such that for all $x_0 \in \mathbb{X}_b$ and $\boldsymbol{u} \in \mathbb{U}^\infty(x_0)$ with

$J_\beta^\infty(x_0, \boldsymbol{u}) \leq V_\beta^\infty(x_0) + \delta$, *the set*

$$\mathcal{Q}(x_0, \boldsymbol{u}, \varepsilon, M, \beta) := \{k \in \{0, \dots, M\} \mid \|x_{\boldsymbol{u}}(k, x_0) - x^\beta\| \geq \varepsilon\}$$

has at most P elements.

Proof. We first show that $\widetilde{V}_\beta^\infty$ is a practical Lyapunov function according to Definition 2.18. It follows from the proof of Lemma 3.2 that the inequality $J_\beta^\infty(x_0, \mathbf{u}) \leq V_\beta^\infty(x_0) + \delta$ implies $\widetilde{J}_\beta^\infty(x_0, \mathbf{u}) \leq \widetilde{V}_\beta^\infty(x_0) + \delta$. Together with a shifting argument and the discounted dynamic programming principle for $\widetilde{V}_\beta^\infty$, we obtain

$$\begin{aligned}
\delta &\geq \widetilde{J}_\beta^\infty(x_0, \mathbf{u}) - \widetilde{V}_\beta^\infty(x_0) \\
&= \widetilde{\ell}_\beta(x_0, u(0)) + \beta \widetilde{J}_\beta^\infty(x_{\mathbf{u}}(1, x_0), \mathbf{u}(\cdot + 1)) - \inf_{u \in \mathbb{U}} \left\{ \widetilde{\ell}_\beta(x_0, u) + \beta \widetilde{V}_\beta^\infty(f(x_0, u)) \right\} \\
&\geq \widetilde{\ell}_\beta(x_0, u(0)) + \beta \widetilde{J}_\beta^\infty(x_{\mathbf{u}}(1, x_0), \mathbf{u}(\cdot + 1)) - \left(\widetilde{\ell}_\beta(x_0, u(0)) + \beta \widetilde{V}_\beta^\infty(f(x_0, u(0))) \right) \\
&= \beta(\widetilde{J}_\beta^\infty(x_{\mathbf{u}}(1, x_0), \mathbf{u}(\cdot + 1)) - \widetilde{V}_\beta^\infty(f(x_0, u(0)))).
\end{aligned}$$

This implies $\widetilde{J}_\beta^\infty(x_{\mathbf{u}}(1, x_0), \mathbf{u}(\cdot + 1)) \leq \widetilde{V}_\beta^\infty(x_{\mathbf{u}}(1, x_0)) + \delta/\beta$, and proceeding inductively results in

$$\widetilde{J}_\beta^\infty(x_{\mathbf{u}}(k, x_0), \mathbf{u}(\cdot + k)) \leq \widetilde{V}_\beta^\infty(x_{\mathbf{u}}(k, x_0)) + \frac{\delta}{\beta^k}$$

for all $k \in \mathbb{N}$. From this, we can conclude the descent condition

$$\begin{aligned}
&\widetilde{V}_\beta^\infty(x_{\mathbf{u}}(k+1, x_0)) - \widetilde{V}_\beta^\infty(x_{\mathbf{u}}(k, x_0)) \\
&\quad = \frac{1}{\beta} \left(\beta \widetilde{V}_\beta^\infty(x_{\mathbf{u}}(k+1, x_0)) - \beta \widetilde{V}_\beta^\infty(x_{\mathbf{u}}(k, x_0)) \right) \\
&\quad = \frac{1}{\beta} \left(\beta \widetilde{V}_\beta^\infty(x_{\mathbf{u}}(k+1, x_0)) - \widetilde{V}_\beta^\infty(x_{\mathbf{u}}(k, x_0)) + (1-\beta) \widetilde{V}_\beta^\infty(x_{\mathbf{u}}(k, x_0)) \right) \\
&\quad \leq \frac{1}{\beta} \Big(\beta \widetilde{J}_\beta^\infty(x_{\mathbf{u}}(k+1, x_0), \mathbf{u}(\cdot + k + 1)) - \widetilde{J}_\beta^\infty(x_{\mathbf{u}}(k, x_0), \mathbf{u}(\cdot + k)) + \frac{\delta}{\beta^k} \\
&\qquad\qquad + (1-\beta) \widetilde{V}_\beta^\infty(x_{\mathbf{u}}(k, x_0)) \Big) \\
&\quad = \frac{1}{\beta} \Big(\beta \widetilde{J}_\beta^\infty(x_{\mathbf{u}}(k+1, x_0), \mathbf{u}(\cdot + k + 1)) - \widetilde{J}_\beta^\infty(x_{\mathbf{u}}(k, x_0), \mathbf{u}(\cdot + k)) \\
&\qquad\qquad + (1-\beta) \widetilde{V}_\beta^\infty(x_{\mathbf{u}}(k, x_0)) \Big) + \frac{\delta}{\beta^{k+1}} \\
&\quad = \frac{1}{\beta} \Big(- \tilde{\ell}(x_{\mathbf{u}}(k, x_0), u(k)) + (1-\beta) \widetilde{V}_\beta^\infty(x_{\mathbf{u}}(k, x_0)) \Big) + \frac{\delta}{\beta^{k+1}}.
\end{aligned}$$

Further, using condition (3.4) and $\kappa = (1-\beta) - 1/C < 0$ because of condition (3.5) leads to

$$\begin{aligned}
&\widetilde{V}_\beta^\infty(x_{\mathbf{u}}(k+1,x_0)) - \widetilde{V}_\beta^\infty(x_{\mathbf{u}}(k,x_0)) \\
&\quad\leq \frac{1}{\beta}\Big(-\tilde{\ell}(x_{\mathbf{u}}(k,x_0),u(k)) + (1-\beta)\widetilde{V}_\beta^\infty(x_{\mathbf{u}}(k,x_0))\Big) + \frac{\delta}{\beta^{k+1}} \\
&\quad\leq \frac{1}{\beta}\Big(-\frac{1}{C}\widetilde{V}_\beta^\infty(x_{\mathbf{u}}(k,x_0)) + (1-\beta)\widetilde{V}_\beta^\infty(x_{\mathbf{u}}(k,x_0))\Big) + \frac{\delta}{\beta^{k+1}} \\
&\quad= \frac{\kappa}{\beta}\widetilde{V}_\beta^\infty(x_{\mathbf{u}}(k,x_0)) + \frac{\delta}{\beta^{k+1}}. \qquad (3.6)
\end{aligned}$$

Moreover, strict discounted dissipativity implies $\widetilde{V}_\beta^\infty(x) \geq \tilde{\ell}(x,u) \geq \alpha(\|x - x^\beta\|)$. Together with the upper bound $\widetilde{V}_\beta^\infty(x) \leq \alpha_V(\|x - x^\beta\|)$ from the assumption this yields that for fixed $M \in \mathbb{N}$ and $k \in \{0,\dots,M\}$ the function $\widetilde{V}_\beta^\infty$ is a practical Lyapunov function. Using Theorem 2.19 restricted to $\{0,\dots,M\}$ and the fact that $\mathbb{X}_b$ is bounded we can conclude that there is a sequence $\eta_k \to 0$ (depending on $\mathbb{X}_b$) and a function $\gamma \in \mathcal{K}_\infty$ with

$$\|x_{\mathbf{u}}(k,x_0) - x^\beta\| \leq \eta_k + \gamma(\delta/\beta^{k+1}) \leq \eta_k + \gamma(\delta/\beta^M)$$

for all $k \in \{0,\dots,M\}$. This implies the desired claim by choosing $P \in \mathbb{N}$ (depending on ε and η_k, hence on $\mathbb{X}_b$) such that $\eta_k < \varepsilon/2$ for all $k \geq P$ and $\delta > 0$ (depending on β, ε and M) such that $\gamma(\delta/\beta^M) < \varepsilon/2$. □

We refer to Figure 3.1 for an illustration of the described turnpike property. This formulation of the discounted turnpike property implies the convergence

$$x_{\mathbf{u}}(k,x_0) \to x^e \quad \text{as} \quad k \to \infty,$$

because otherwise $\mathcal{Q}(x_0,\mathbf{u},\varepsilon,M,\beta)$ would contain infinitely many elements for sufficiently large $P \in \mathbb{N}$, cf. [46, Chapter 8]. We note again that the level δ, which measures the deviation from optimality of the trajectory $x_{\mathbf{u}}(\cdot,x_0)$, depends on M. For guaranteeing the turnpike property on $\{0,\dots,M\}$, $\delta \to 0$ may be required if $M \to \infty$, cf. also Remark 3.5 (iv).

The following remark discusses aspects of the assumptions of Theorem 3.4. The system must be steerable to x^β, at least asymptotically, as discussed in part (i) of the remark. Part (ii) shows that if the state can be steered to x^β fast enough, then a constant C satisfying (3.4) for all $\beta \in (0,1)$ holds. Finally, part (iii) of the remark discusses how inequality (3.4) can be relaxed if such a constant C cannot be found.

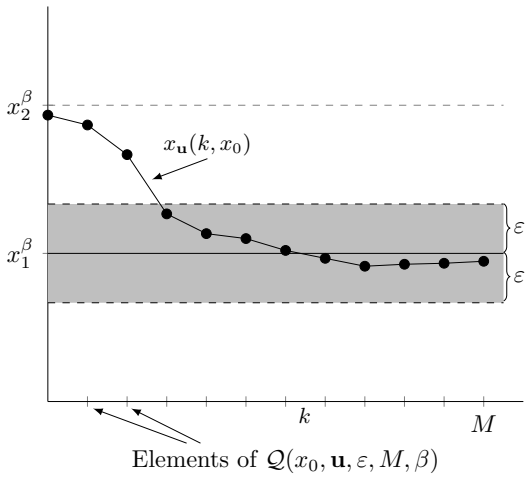

Figure 3.1: Illustration of the set $\mathcal{Q}(x_0, \mathbf{u}, \varepsilon, M, \beta)$

Remark 3.5

(i) A necessary condition for the turnpike property to hold is that the trajectory is steerable to a neighborhood of the equilibrium within at least P steps. More precisely, for each $\varepsilon > 0$, each bounded subset $\mathbb{X}_b \subseteq \mathbb{X}$ and each $x_0 \in \mathbb{X}_b$ there exists a control sequence $\boldsymbol{u} \in \mathbb{U}^{P+1}(x_0)$ with $x_{\boldsymbol{u}}(k, x_0) \in \mathcal{B}_\varepsilon(x^\beta)$ for some $k \leq P+1$, where P is the constant from the turnpike property in Theorem 3.4. This is immediately clear because if such a control does not exist, then the number of points with $x_{\boldsymbol{u}}(k, x_0) \notin \mathcal{Q}(x_0, \boldsymbol{u}, \varepsilon, M, \beta)$ is larger than P for all $\boldsymbol{u}$.

(ii) If a constant C satisfying inequality (3.4) for all $\beta \in (0,1)$ exists, then inequality (3.5) will hold for all sufficiently large $\beta \in (0,1)$. A sufficient condition for the existence of such a constant C is the following exponential stabilizability assumption of the cost at the equilibrium (x^β, u^β): There are constants $\sigma, \theta > 0$ such that for each $x_0 \in \mathbb{X}$ there is $\boldsymbol{u} \in \mathbb{U}^\infty(x_0)$ with

$$\widetilde{\ell}_\beta(x_{\boldsymbol{u}}(k, x_0), u(k)) \leq \sigma e^{-\theta k} \inf_{\hat{u} \in \mathbb{U}} \widetilde{\ell}_\beta(x_0, \hat{u}). \tag{3.7}$$

Then, since $\widetilde{\ell}_\beta \geq 0$ we obtain

$$\begin{aligned} \widetilde{V}_\beta^\infty(x_0) &\leq \sum_{k=0}^{\infty} \beta^k \widetilde{\ell}_\beta(x_{\boldsymbol{u}}(k, x_0), u(k)) \leq \sum_{k=0}^{\infty} \widetilde{\ell}_\beta(x_{\boldsymbol{u}}(k, x_0), u(k)) \\ &\leq \sum_{k=0}^{\infty} \sigma e^{-\theta k} \inf_{\hat{u} \in \mathbb{U}} \widetilde{\ell}_\beta(x_0, \hat{u}) = \frac{\sigma}{1 - e^{-\theta}} \inf_{\hat{u} \in \mathbb{U}} \widetilde{\ell}_\beta(x_0, \hat{u}), \end{aligned}$$

implying inequality (3.4) *with* $C = \sigma/(1 - e^{-\theta})$. *We note that inequality* (3.7) *holds in particular if the system itself is exponentially stabilizable to* x^β *with exponentially bounded controls and* $\widetilde{\ell}_\beta$ *is a polynomial*[1]. *In turn, the exponential stabilizability of the system follows locally around* x^β *from the stabilizability of its linearization in* x^β. *If, in addition, the necessary condition from part (i) of this remark holds, then local exponential stabilizability implies exponential stabilizability for bounded* $\mathbb{X}$. *We refer to [37, Section 6] for a more detailed discussion on these conditions. Note that if* $\widetilde{\ell}_\beta$ *is continuous, then* $\inf_{u\in\mathbb{U}} \widetilde{\ell}_\beta(x,u) \leq \alpha_\ell(\|x - x^\beta\|)$ *holds for an appropriate* $\alpha_\ell \in \mathcal{K}_\infty$. *In this case, inequality* (3.4) *implies the assumed upper bound* α_V *on* $\widetilde{V}_\beta^\infty$.

(iii) If a constant C *meeting the conditions* (3.5) *and* (3.4) *for all* $x \in \mathbb{X}$ *does not exist, then we may still be able to find a constant* C *satisfying* (3.5) *and* (3.4) *for all* $x \in \mathbb{X}$ *with* $\vartheta \leq \|x - x^\beta\| \leq \Theta$, *for parameters* $0 \leq \vartheta < \Theta$. *In this case we can follow the reasoning in the proof of [37, Corollary 4.3] to conclude that we still obtain a turnpike property for* $\varepsilon > \varepsilon_0$ *and* $\mathbb{X}_b = \mathcal{B}_\Delta(x^\beta) \cap \mathbb{X}$, *with* $\varepsilon_0 \to 0$ *as* $\vartheta \to 0$ *and* $\Delta \to \infty$ *as* $\Theta \to \infty$.

(iv) Optimal trajectories, i.e., trajectories for which $J_\beta^\infty(x_0, \boldsymbol{u}) = V_\beta^\infty(x_0)$ *holds, satisfy the assumptions of Theorem 3.4 for each* $\delta > 0$. *Hence, the assertion of the theorem holds for each* $\varepsilon > 0$ *and each* $M \in \mathbb{N}$, *implying that* $x_{\boldsymbol{u}}(k, x_0)$ *converges to* x^β *as* $k \to \infty$. *Thus,* x^β *behaves similarly to an asymptotically stable equilibrium. However, whenever* $\delta > 0$, *the trajectory will typically move away from* x^β *for large times. This is more similar to the classical turnpike phenomenon in optimal control than to asymptotic stability, which is why we prefer this term over asymptotic stability or practical asymptotic stability.*

3.3 The Local Discounted Turnpike Property

In the previous section, we have shown that an equilibrium at which the system is globally discounted strictly dissipative has the discounted turnpike property. Now, we move on to addressing the central question in this chapter. We consider an equilibrium (x_l^β, u_l^β) at which discounted strict dissipativity holds only locally. Because of the local property, we study the trajectory behavior locally and examine under which conditions the trajectory exhibits a turnpike property at the equilibrium (x_l^β, u_l^β). For this purpose, we assume invariance in the neighborhood where the local dissipativity holds and then analyze how to choose the discount factor β to enforce the local

[1] We could further relax this assumption to $\widetilde{\ell}_\beta$ being bounded by $C_1 P$ and $C_2 P$ from below and above, respectively, for constants $C_1 > C_2 > 0$ and a polynomial P.

turnpike behavior.

3.3.1 The Local Turnpike Property Assuming Invariance

We begin our considerations with an equilibrium denoted by (x_l^β, u_l^β) at which discounted strict dissipativity holds only locally, i.e., for all x in a neighborhood $\mathbb{X}_\mathcal{N}$ of x_l^β, in the following sense.

Definition 3.6 (Local Discounted Strict Dissipativity)
Given a discount factor $\beta \in (0,1)$, we say that the system (2.1) *is* locally discounted strictly dissipative for the supply rate $s : \mathbb{Y} \to \mathbb{R}$ at an equilibrium (x_l^β, u_l^β) *if there exists a storage function $\lambda : \mathbb{X} \to \mathbb{R}$ bounded from below with $\lambda(x_l^\beta) = 0$ and $\alpha_\beta \in \mathcal{K}_\infty$ such that the inequality*

$$s(x,u) + \lambda(x) - \beta\lambda(f(x,u)) \geq \alpha_\beta(\|x - x^\beta\|) \tag{3.8}$$

holds for all $(x,u) \in \mathbb{X}_\mathcal{N} \times \mathbb{U}$ with $f(x,u) \in \mathbb{X}$.

Further, we say that system (2.1) *is locally discounted strictly (x,u)-dissipative at the equilibrium (x_l^β, u_l^β) with supply rate $s : \mathbb{X} \times \mathbb{U} \to \mathbb{R}$ if the same holds with the inequality*

$$s(x,u) + \lambda(x) - \beta\lambda(f(x,u)) \geq \alpha_\beta(\|(x - x_l^\beta, u - u_l^\beta)\|). \tag{3.9}$$

As in the global case, we define the rotated stage cost as

$$\widetilde{\ell}_\beta(x,u) := \ell(x,u) - \ell(x_l^\beta, u_l^\beta) + \lambda(x) - \beta\lambda(f(x,u)). \tag{3.10}$$

This definition is local as we only require the dissipation inequalities (3.8) and (3.9) to hold for $x \in \mathbb{X}_\mathcal{N}$. However, the locality refers to the state since we also allow for control values that drive the state out of the neighborhood $\mathbb{X}_\mathcal{N}$ of the equilibrium x_l^β. This property will be important in the proof of Lemma 3.11 below.

Lemma 3.2 remains valid within this definition. Moreover, for $x \in \mathbb{X}_\mathcal{N}$, the modified stage cost $\widetilde{\ell}_\beta$ satisfies the same properties as in the globally dissipative case. Exploiting these properties will enable us to derive a local turnpike property, provided the neighborhood $\mathbb{X}_\mathcal{N}$ contains an invariant set $\mathbb{X}_{\text{inv}} \subset \mathbb{X}_\mathcal{N}$ for the optimally controlled system. Recall that a set $\mathbb{X}_{\text{inv}} \subset \mathbb{X}$ is forward invariant for the optimally controlled system if for each $x_0 \in \mathbb{X}_{\text{inv}}$ it follows that $x_{\mathbf{u}^\star}(k, x_0) \in \mathbb{X}_{\text{inv}}$ for all $k \geq 0$ and all optimal trajectories starting in x_0. The following lemma gives a consequence of this assumption for the modified optimal value function, which will be essential for concluding the local turnpike property.

Lemma 3.7
Consider the discounted optimal control problem (OCP(β)) *with given discount factor* $\beta \in (0,1)$ *and assume that the system* (2.1) *is locally strictly dissipative at* $(x_l^\beta, u_l^\beta) \in \mathbb{X}_\mathcal{N} \subset \mathbb{X}$. *Consider a subset* $\mathbb{X}_{inv} \subset \mathbb{X}_\mathcal{N}$ *such that all optimal solutions* $x_{\boldsymbol{u}^\star}(k, x_0)$ *with* $x_0 \in \mathbb{X}_{inv}$ *satisfy* $x_{\boldsymbol{u}^\star}(k, x_0) \in \mathbb{X}_{inv}$ *for all* $k \geq 0$.

Then, the modified optimal value function $\widetilde{V}_\beta^\infty$ *satisfies*

$$\widetilde{V}_\beta^\infty(x) \geq \alpha_\beta(\|x - x_l^\beta\|) \tag{3.11}$$

for all $x \in \mathbb{X}_{inv}$.

Proof. For all $x \in \mathbb{X}_\mathcal{N}$ and $u \in \mathbb{U}$ the modified cost satisfies

$$\widetilde{\ell}_\beta(x,u) \geq \alpha_\beta(\|x - x_l^\beta\|) \geq 0.$$

This implies

$$\widetilde{V}_\beta^\infty(x_0) = \sum_{k=0}^{\infty} \beta^k \widetilde{\ell}_\beta(x_{\mathbf{u}^\star}(k,x_0), u^\star(k)) \geq \sum_{k=0}^{\infty} \beta^k \alpha_\beta(\|x_{\mathbf{u}^\star}(k,x_0) - x_l^\beta\|) \geq \alpha_\beta(\|x_0 - x_l^\beta\|),$$

which shows the claim. □

The following theorem gives a local version of Theorem 3.4.

Theorem 3.8
Consider the infinite horizon discounted optimal control problem (OCP(β)) *with discount factor* $\beta \in (0,1)$ *and assume that the system* (2.1) *is locally strictly dissipative at* $(x_l^\beta, u_l^\beta) \in \mathbb{X}_\mathcal{N} \subset \mathbb{X}$. *Consider a subset* $\mathbb{X}_{inv} \subset \mathbb{X}_\mathcal{N}$ *such that all optimal solutions* $x_{\boldsymbol{u}^\star}(k, x_0)$ *with* $x_0 \in \mathbb{X}_{inv}$ *satisfying* $x_{\boldsymbol{u}^\star}(k, x_0) \in \mathbb{X}_{inv}$ *for all* $k \geq 0$ *and suppose that the assumptions of Theorem 3.4 hold for all* $x \in \mathbb{X}_{inv}$.

Then, the optimal control problem has the turnpike property on $\mathbb{X}_{inv}$ *in the following sense:*

For each $\varepsilon > 0$ *and each bounded set* $\mathbb{X}_b \subset \mathbb{X}_{inv}$ *there exists a constant* $P > 0$ *such that for each* $M \in \mathbb{N}$ *there is a* $\delta > 0$, *such that for all* $x_0 \in \mathbb{X}_b$, $u \in \mathbb{U}^\infty(x_0)$ *with* $J_\beta^\infty(x_0, \boldsymbol{u}) \leq V_\beta^\infty(x_0) + \delta$ *and* $x_{\boldsymbol{u}}(k, x_0) \in \mathbb{X}_{inv}$ *for all* $k \in \{0, \dots, M\}$, *the set*

$$\mathcal{Q}(x, \boldsymbol{u}, \varepsilon, M, \beta) := \{k \in \{0, \dots, M\} \mid \|x_{\boldsymbol{u}}(k, x_0) - x_l^\beta\| \geq \varepsilon\}$$

has at most P *elements.*

Proof. The proof proceeds completely identical to the proof of Theorem 3.4, using the fact that all inequalities used therein remain valid as long as the considered solutions stay in $\mathbb{X}_{\text{inv}}$, which is guaranteed by the invariance of $\mathbb{X}_{\text{inv}}$. We note that Lemma 3.7 is needed for establishing the lower bound on $\widetilde{V}_\beta^\infty$ required from a practical Lyapunov function. □

Remark 3.9
Instead of assuming the existence of the invariant set $\mathbb{X}_{inv}$ we could also assume inequality (3.11) *to hold for all $x_0 \in \mathbb{X}_{\mathcal{N}}$. Then, by standard Lyapunov function arguments, the largest sublevel set of $\widetilde{V}_\beta^\infty$ contained in $\mathbb{X}_{\mathcal{N}}$ is forward invariant for the optimal solutions and can then be used as set $\mathbb{X}_{inv}$. Using the descent condition* (3.6) *we can even ensure that this sublevel set is also forward invariant for all solutions satisfying $J_\beta^\infty(x_0, \boldsymbol{u}) \leq V_\beta^\infty(x_0) + \delta$ provided $\delta > 0$ is sufficiently small. Hence, for this choice of $\mathbb{X}_{inv}$ the assumption that $x_{\boldsymbol{u}}(k, x_0) \in \mathbb{X}_{inv}$ for all $k \in \{0, \dots, M\}$ in Theorem 3.8 would be automatically satisfied if δ is not too large.*

3.3.2 The Local Turnpike Property by Enforcing Invariance

Theorem 3.8 shows that near-optimal trajectories exhibit the local turnpike property provided the trajectories start in a neighborhood of x_l^β stay in $\mathbb{X}_{\text{inv}}$. We proceed to show that this condition is "automatically" satisfied for appropriate discount factors. Hence, we enforce the trajectory to stay at the local equilibrium regarding the discount factor β, enabling us to conclude a local turnpike property from local strict dissipativity. To this end, we aim to show that there exists a range of discount factors β for which it is more favorable to stay near the locally dissipative equilibrium than to move to other parts of the state space. Exploiting the stronger (x, u)-dissipativity leads to a property of trajectories that move out of a neighborhood of a local equilibrium x_l^β.

Lemma 3.10
Consider a discounted optimal control problem (OCP(β)) *subject to system* (2.1) *with continuous f. Assume that the system* (2.1) *is locally strictly (x, u)-dissipative at an equilibrium (x_l^β, u_l^β) according to Definition 3.6 and let $\rho > 0$ be such that $\mathcal{B}_\rho(x_l^\beta) \subset \mathbb{X}_{\mathcal{N}}$ holds for the neighborhood $\mathbb{X}_{\mathcal{N}}$ from Definition 3.6.*

Then, there exists $\eta > 0$ such that for each $K \in \mathbb{N}$ and any trajectory $x(\cdot)$ with $x_0 = x(0) \in \mathcal{B}_\eta(x_l^\beta)$ and $x(K) \notin \mathcal{B}_\rho(x_l^\beta)$ there is an $M \in \{0, \dots, K-1\}$ such that $x(0), \dots, x(M) \in \mathcal{B}_\eta(x_l^\beta)$ and either

$$\text{(i) } x(M+1) \in \mathcal{B}_\rho(x_l^\beta) \backslash \mathcal{B}_\eta(x_l^\beta) \quad \text{or} \quad \text{(ii) } \|u(M) - u_l^\beta\| \geq \eta$$

holds.

Proof. The continuity of f implies that there exists $\varepsilon > 0$ such that

$$\|f(x, u) - x_l^\beta\| < \rho$$

for all $(x, u) \in \mathbb{Y}$ with $\|x - x_l^\beta\| < \varepsilon$ and $\|u - u_l^\beta\| < \varepsilon$, and with $\rho > 0$ from the assumption. We let $K_{\min}$ be minimal with $x(K_{\min}) \notin \mathcal{B}_\rho(x_l^\beta)$, set $\eta := \min\{\varepsilon, \rho\}$, and claim that this implies the assertion for $M = K_{\min} - 1$.

We prove this claim by contradiction. To this end, we assume that for $M = K_{\min} - 1$, neither assertion (i) nor assertion (ii) holds. This implies on the one hand that $\|x(M) - x_l^\beta\| < \eta$, since $x(M) \in \mathcal{B}_\rho(x_l^\beta)$ by minimality of $K_{\min}$ and (i) is not fulfilled. On the other hand, it implies $\|u(M) - u_l^\beta\| < \eta$, because (ii) does not hold.

Since $\eta \leq \varepsilon$, the continuity of f implies

$$\|x(K_{\min}) - x_l^\beta\| = \|f(x(M), u(M)) - x_l^\beta\| < \rho.$$

This means that $x(K_{\min}) \in \mathcal{B}_\rho(x_l^\beta)$, which is a contradiction to the choice of $K_{\min}$. Consequently, either assertion (i) or assertion (ii) must hold for $M = K_{\min} - 1$. □

Remark

Lemma 3.10 describes the trajectory behavior locally independent of a cost function. Hence, whenever a trajectory "jumps" out of a neighborhood, there can only be the reasons from the lemma. Further, since the proof is based on continuity arguments, we use strict dissipativity to define the neighborhoods appropriately for the following investigation.

The next lemma shows that the behavior characterized in Lemma 3.10 induces a lower bound for the rotated discounted cost function $\widetilde{J}_\infty$ from the modified discounted problem (3.2) along trajectories that start in a neighborhood of x_l^β and leave this neighborhood. We note that even if merely local strict dissipativity holds, the modified stage cost $\widetilde{\ell}_\beta$ from (3.10) is well-defined since λ is defined for all $x \in \mathbb{X}$. However, the inequality $\widetilde{\ell}_\beta(x, u) \geq \alpha_\beta(\|(x - x_l^\beta, u - u_l^\beta)\|)$ and, more generally, positivity of $\widetilde{\ell}_\beta$ are only guaranteed for $x \in \mathbb{X}_\mathcal{N}$.

Lemma 3.11

Let the assumptions of Lemma 3.10 hold. In addition, assume that the storage function λ from Definition 3.6 is bounded and the stage cost ℓ is bounded from below.

Then, there exists $\beta^\star \in (0, 1)$ with the following property: For any $\beta \in (0, \beta^\star)$ and any $K \in \mathbb{N}$ there is $\sigma(\beta, K) > 0$ such that for any trajectory $x(\cdot)$ with $x_0 = x(0) \in \mathcal{B}_\eta(x_l^\beta)$ and $x(P) \notin \mathcal{B}_\rho(x_l^\beta)$ for some $P \in \{1, \dots, K\}$ the inequality

$$\widetilde{J}_\beta^\infty(x_0, \boldsymbol{u}) \geq \sigma(\beta, K) \tag{3.12}$$

holds.

Proof. First, observe that boundedness from below of ℓ and boundedness of λ imply boundedness from below of $\widetilde{\ell}_\beta$. Define $\widetilde{\ell}_{\min} := \inf_{(x,u)\in\mathbb{Y}} \widetilde{\ell}_\beta(x, u)$. Since $\widetilde{\ell}_\beta(x^\beta, u^\beta) = 0$ holds, it follows that $\widetilde{\ell}_{\min} \leq 0$. Moreover, local dissipativity implies that $\widetilde{\ell}_\beta(x, u) \geq 0$ for all $x \in \mathbb{X}_\mathcal{N}$ and all $u \in \mathbb{U}$ with $f(x, u) \in \mathbb{X}$. We note that it is important for the

remainder of the proof that this inequality holds for all these $u \in \mathbb{U}$ and not only when $f(x,u) \in \mathbb{X}_{\mathcal{N}}$.

Since the trajectory under consideration satisfies the assumptions of Lemma 3.10 with $K = P$, there exists $M \in \{0,\dots,P\}$ such that either assertion (i) or assertion (ii) of this lemma holds. Within the strict (x,u)-dissipativity, in case (i), we obtain that

$$\widetilde{\ell}(x(M),u(M)) \geq \alpha_\beta(\|x(M) - x_l^\beta\|) \geq \alpha_\beta(\eta)$$

and in case (ii), we obtain

$$\widetilde{\ell}_\beta(x(M),u(M)) \geq \alpha_\beta(\|u(M) - u_l^\beta\|) \geq \alpha_\beta(\eta).$$

Hence, we get the same inequality in both cases, and we abbreviate $\delta := \alpha_\beta(\eta) > 0$. Moreover, Lemma 3.10 yields $x(0),\dots,x(M) \in \mathcal{B}_\eta(x_l^\beta) \subset \mathbb{X}_{\mathcal{N}}$, which implies $\widetilde{\ell}_\beta(x_{\mathbf{u}}(k,x_0),u(k)) \geq 0$ for all $k = 0,\dots,M-1$, and the lower bound on $\widetilde{\ell}_\beta$ implies $\widetilde{\ell}_\beta(x_{\mathbf{u}}(k,x_0),u(k)) \geq \widetilde{\ell}_{\min}$ for all $k \geq M+1$. Together this yields

$$\begin{aligned}
&\widetilde{J}_\beta^\infty(x_0,u) = \sum_{k=0}^{\infty} \beta^k \widetilde{\ell}_\beta(x_{\mathbf{u}}(k,x_0),u(k)) \\
&= \sum_{k=0}^{M-1} \beta^k \underbrace{\widetilde{\ell}_\beta(x_{\mathbf{u}}(k,x_0),u(k))}_{\geq 0} + \beta^M \underbrace{\widetilde{\ell}_\beta(x_{\mathbf{u}}(M,x_0),u(M))}_{\geq \delta} + \sum_{k=M+1}^{\infty} \beta^k \underbrace{\widetilde{\ell}_\beta(x_{\mathbf{u}}(k,x_0),u(k))}_{\geq \widetilde{\ell}_{\min}} \\
&\geq \beta^M \delta + \frac{\beta^{M+1}}{1-\beta}\widetilde{\ell}_{\min} = \frac{\beta^M}{1-\beta}\left(\left(\widetilde{\ell}_{\min} - \delta\right)\beta + \delta\right).
\end{aligned}$$

We now claim that the assertion holds for $\sigma = \frac{\beta^K \delta}{2(1-\beta)} \leq \frac{\beta^M \delta}{2(1-\beta)}$. To this end, it is sufficient to show the existence of $\beta^\star$ with

$$\frac{\beta^M}{1-\beta}\left(\left(\widetilde{\ell}_{\min} - \delta\right)\beta + \delta\right) \geq \frac{\beta^M \delta}{2(1-\beta)}$$

for all $\beta \in (0,\beta^\star)$. This can be reformulated to

$$\frac{\beta^M}{1-\beta}\left(\left(\widetilde{\ell}_{\min} - \delta\right)\beta + \frac{\delta}{2}\right) \geq 0 \quad \Leftrightarrow \quad \left(\widetilde{\ell}_{\min} - \delta\right)\beta + \frac{\delta}{2} \geq 0,$$

since $\widetilde{\ell}_{\min} - \delta < 0$. This inequality holds for all $\beta \in (0,\beta^\star)$ if $\beta^\star = \delta/(2(\delta - \widetilde{\ell}_{\min}))$. □

Remark 3.12
The choice of the factor $\frac{1}{2}$ for σ in the proof of Lemma 3.11 is arbitrary. We can also use a more general fraction $\frac{1}{k+1}$ with $k \in \mathbb{N}$. Then, with the same calculation as above, we get that $\beta^\star = \dfrac{k}{k+1}\dfrac{\delta}{\delta - \widetilde{\ell}_{\min}}$.

Based on the estimate from Lemma 3.11, we can now conclude that near-optimal solutions starting near x_l^β stay in $\mathbb{X}_\mathcal{N}$ for a certain amount of time.

Lemma 3.13
Consider a discounted optimal control problem (OCP(β)) *subject to system* (2.1) *with f continuous and stage cost ℓ bounded from below. Assume the system is locally strictly (x,u)-dissipative at an equilibrium (x_l^β, u_l^β) according to Definition 3.6 with bounded storage function λ. Assume furthermore that there is $\gamma \in \mathcal{K}_\infty$ and $\hat{\beta} \in (0,1]$ such that $\widetilde{V}_\beta^\infty(x_0) \leq \gamma(\|x_0 - x_l^\beta\|)$ for all $x_0 \in \mathbb{X}_\mathcal{N}$ and all $\beta \in (0, \hat{\beta}]$.*

Then, there exists $\beta_2 \in (0,1)$ with the following property: For any $\beta \in (0, \beta_2)$ and any $K \in \mathbb{N}$ there exists a neighborhood $\mathcal{B}_{\varepsilon(\beta,K)}(x_l^\beta)$ and a threshold value $\theta(\beta,K) > 0$ such that all trajectories with $x_0 \in \mathcal{B}_{\varepsilon(\beta,K)}(x_l^\beta)$, $\boldsymbol{u} \in \mathbb{U}^\infty(x_0)$, and $J_\beta^\infty(x_0, \boldsymbol{u}) < V_\beta^\infty(x_0) + \theta(\beta,K)$ satisfy $x_{\boldsymbol{u}}(k, x_0) \in \mathbb{X}_\mathcal{N}$ for all $k \in \{0, \dots, K\}$.

Proof. We choose β_2 as the minimum of $\beta^\star$ from Lemma 3.11 and $\hat{\beta}$. We further use $\sigma(\beta,K) > 0$ from Lemma 3.11 to set $\varepsilon(\beta,K) := \gamma^{-1}(\sigma(\beta,K)/2)$ and $\theta(\beta,K) := \sigma(\beta,K)/2$. Now consider a trajectory meeting the assumptions and observe that since J_β^∞ and $\widetilde{J}_\beta^\infty$ differ only by a term that is independent of $\mathbf{u}$, the assumption $J_\beta^\infty(x_0, \mathbf{u}) \leq V_\beta^\infty(x_0) + \theta(\beta,K)$ together with the assumption on x_0 implies

$$\widetilde{J}_\beta^\infty(x_0, \mathbf{u}) < \widetilde{V}_\beta^\infty(x_0) + \theta(\beta,K) < \gamma(\varepsilon(\beta,K)) + \theta(\beta,K).$$

The definition of θ and ε then implies

$$\widetilde{J}_\beta^\infty(x_0, \mathbf{u}) < \sigma(\beta,K)/2 + \sigma(\beta,K)/2 = \sigma(\beta,K).$$

Since by Lemma 3.11 any trajectory leaving $\mathbb{X}_\mathcal{N}$ (and thus also $\mathcal{B}_\rho(x_l^\beta)$) up to time K has a rotated value satisfying

$$\widetilde{J}_\beta^\infty(x_0, u) \geq \sigma(\beta,K),$$

the trajectory under consideration cannot leave $\mathbb{X}_\mathcal{N}$ for $k \in \{0, \dots, K\}$. □

We note that $\widetilde{V}_\beta^\infty(x_0) \leq \gamma(\|x_0 - x_l^\beta\|)$ can be ensured if we can locally steer the system to x^β fast enough and $\widetilde{\ell}$ is continuous. For a more detailed discussion, we refer again to Remark 3.5 (ii). Further, as in the proof of Theorem 3.4 we obtain a lower $\mathcal{K}_\infty$-bound on $\widetilde{V}_\beta^\infty$ for $x_0 \in \mathbb{X}_\mathcal{N}$ by local strict dissipativity.

Using the previous lemmas, we can now prove our main theorem on the existence of a local turnpike property for discounted optimal control problems on the infinite horizon.

Theorem 3.14
Consider a discounted optimal control problem (OCP(β)) *subject to system* (2.1) *with* f *continuous and stage cost* ℓ *bounded from below. Assume that the system* (2.1) *is locally strictly* (x,u)*-dissipative at an equilibrium* (x_l^β, u_l^β) *according to Definition 3.6 with bounded storage function* λ*. Assume furthermore that there is* $\gamma \in \mathcal{K}_\infty$ *and* $\hat{\beta} \in (0,1]$ *such that* $\widetilde{V}_\beta^\infty(x_0) \leq \gamma(\|x_0 - x_l^\beta\|)$ *for all* $x_0 \in \mathbb{X}_\mathcal{N}$ *and all* $\beta \in (0,\hat{\beta})$*, and that there is an interval* $[\beta_1, \beta^\star]$ *of discount rates with* $\beta_1 < \hat{\beta}$ *and* $\beta^\star$ *from Lemma 3.11, such that for each* $\beta \in (\beta_1, \beta^\star)$ *the assumptions of Theorem 3.4 hold for all* $x \in \mathbb{X}_\mathcal{N}$*.*

Then, there is $\beta_2 \in (0,1)$ *such that for all* $\beta \in (\beta_1, \beta_2)$*, there exists a neighborhood* $\mathcal{N}$ *of* x_l^β *on which the system exhibits a local turnpike property in the following sense:*

For each $\varepsilon > 0$ *there exist a constant* $P > 0$ *such that for each* $M \in \mathbb{N}$ *there is a* $\delta > 0$*, such that for all* $x_0 \in \mathcal{N}$ *and all* $\boldsymbol{u} \in \mathbb{U}^\infty(x_0)$ *satisfying* $J_\beta^\infty(x_0, \boldsymbol{u}) \leq V_\beta^\infty(x_0) + \delta$*, the set*

$$\mathcal{Q}(x, \boldsymbol{u}, \varepsilon, M, \beta) := \{k \in \{0, \dots, M\} \mid \|x_{\boldsymbol{u}}(k, x_0) - x^\beta\| \geq \varepsilon\}$$

has at most P *elements.*

Particularly, if $J_\beta^\infty(x_0, \boldsymbol{u}) = V_\beta^\infty(x_0)$*, i.e., if the trajectory is optimal, then for each* $\varepsilon > 0$*, the set*

$$\mathcal{Q}(x, \boldsymbol{u}, \varepsilon, \infty, \beta) := \bigcup_{M \in \mathbb{N}} \mathcal{Q}(x, \boldsymbol{u}, \varepsilon, M, \beta)$$

has at most P *elements, implying the convergence* $x_{\boldsymbol{u}}(k, x_0) \to x^\beta$ *as* $k \to \infty$*.*

Proof. We use β_2 from Lemma 3.13. The idea of the proof is to construct for each $\beta \in (\beta_1, \beta_2)$ a neighborhood $\mathcal{N}$ of x_l^β and a $\delta > 0$ such that all trajectories starting in $x_0 \in \mathcal{N}$ and satisfying $J_\beta^\infty(x_0, \mathbf{u}) \leq V_\beta^\infty(x_0) + \delta$ stay in $\mathcal{N}$ for all future times. Then, the turnpike property follows from Theorem 3.8 applied with $\mathbb{X}_{\text{inv}} = \mathcal{N}$.

We fix $\beta \in (\beta_1, \beta_2)$, and consider the neighborhood $\mathcal{B}_{\varepsilon(\beta,1)}(x_l^\beta)$ and the threshold value $\theta(\beta, 1)$ from Lemma 3.13 for $K = 1$. We choose $\mathcal{N}$ as the largest sublevel set of $\widetilde{V}_\beta^\infty$ that is contained in $\mathcal{B}_{\varepsilon(\beta,1)}(x_l^\beta)$ and denote the level by $\eta > 0$, i.e.,

$$\mathcal{N} = \{x \in \mathbb{X}_\mathcal{N} \,|\, \widetilde{V}_\beta^\infty(x) < \eta\}.$$

Further, we abbreviate $\kappa = (1-\beta) - 1/C$, observing that $\kappa < 0$ because of inequality (3.5) (cf. also the proof of Theorem 3.4). Set

$$\delta := \beta^M \min\left\{\theta(\beta, 1), -\frac{\kappa\eta}{2\beta}, \frac{\eta}{2}\right\}.$$

Now let x_0 and $\mathbf{u}$ be as in the assertion, i.e., satisfying $J_\beta^\infty(x_0,\mathbf{u}) \le V_\beta^\infty(x_0)+\delta$, and denote the corresponding trajectory by $x(\cdot)$. Just as in the first part of the proof of Theorem 3.4, we obtain the estimate

$$\widetilde{J}_\beta^\infty(x(k),\mathbf{u}(\cdot+k)) \le \widetilde{V}_\beta^\infty(x(k)) + \frac{\delta}{\beta^k}$$

for all $k \in \mathbb{N}$. By definition of δ this implies

$$\widetilde{J}_\beta^\infty(x(k),\mathbf{u}(\cdot+k)) \le \widetilde{V}_\beta^\infty(x(k)) + \theta(\beta,1) \tag{3.13}$$

for all $k = 0,\dots,M$.

We prove by induction that $x(k) \in \mathcal{N}$ for all $k = 0,\dots,M$.
For $k = 0$, this follows from the choice of x_0.
For $k \to k+1$, we make the induction assumption that $x(k) \in \mathcal{N}$, i.e., $\widetilde{V}_\beta^\infty(x(k)) < \mu$. Then, because of inequality (3.13) and $\mathcal{N} \subseteq \mathcal{B}_{\varepsilon(\beta,1)}(x_l^\beta)$, Lemma 3.13 (applied with initial value $x_0 = x(k)$ and control $\mathbf{u}(\cdot+k)$) implies that $x(k+1) \in \mathbb{X}_\mathcal{N}$. Hence, all the (in)equalities leading to inequality (3.6) in the proof of Theorem 3.4 are valid and, together with the definition of δ, this yields

$$\begin{aligned}\widetilde{V}_\beta^\infty(x(k+1)) - \widetilde{V}_\beta^\infty(x(k)) &\le \frac{\kappa}{\beta}\widetilde{V}_\beta^\infty(x(k)) + \frac{\delta}{\beta^k} \\ &\le \frac{\kappa}{\beta}\widetilde{V}_\beta^\infty(x(k)) + \min\left\{\theta(\beta,1), -\frac{\kappa\eta}{2\beta}, \frac{\eta}{2}\right\}.\end{aligned}$$

If $\widetilde{V}_\beta^\infty(x(k)) \ge \eta/2$, then the second term in the minimum defining δ implies

$$\widetilde{V}_\beta^\infty(x(k+1)) - \widetilde{V}_\beta^\infty(x(k)) \le \frac{\kappa}{\beta}\frac{\eta}{2} - \frac{\kappa\eta}{2\beta} = 0,$$

from which follows $\widetilde{V}_\beta^\infty(x(k+1)) \le \widetilde{V}_\beta^\infty(x(k)) < \eta$ and thus $x(k+1) \in \mathcal{N}$.

If $\widetilde{V}_\beta^\infty(x(k)) < \eta/2$, then the third term in the minimum defining δ implies

$$\widetilde{V}_\beta^\infty(x(k+1)) - \widetilde{V}_\beta^\infty(x(k)) \le \underbrace{\frac{\kappa}{\beta}\widetilde{V}_\beta^\infty(x(k))}_{\le 0} + \frac{\eta}{2} \le \frac{\eta}{2}.$$

Here we have used that $\widetilde{V}_\beta^\infty(x(k)) \ge 0$ which follows since $x(k) \in \mathcal{N}$: If the optimal trajectory starting in $x(k)$ stays in $\mathcal{N}$, then the statement follows from strict dissipativity on $\mathbb{X}_\mathcal{N} \supset \mathcal{N}$ and if the optimal trajectory leaves $\mathcal{N}$ then the statement follows from Lemma 3.11. This implies $\widetilde{V}_\beta^\infty(x(k+1)) \le \widetilde{V}_\beta^\infty(x(k)) + \eta/2 < \eta$, i.e., again $x(k+1) \in \mathcal{N}$. This proves the induction step, hence $x(k) \in \mathcal{N}$ for all $k = 0,\dots,M$.

As discussed at the beginning of the proof, the turnpike property follows from Theorem 3.8 applied with $\mathbb{X}_{\text{inv}} = \mathcal{N}$. □

Remark 3.15
The interval (β_1, β_2) may be empty. This is because

(i) the condition (3.4) needed for proving the turnpike property for trajectories staying near x_l^β may require sufficiently large β to hold.

(ii) a trajectory starting near x_l^β will in general only stay near x_l^β for sufficiently small β.

More precisely, the upper bound in (ii), as identified at the end of the proof of Lemma 3.11, depends on the cost $\widetilde{\ell}$ outside a neighborhood of x_l^β and the cost to leave this neighborhood. In turn, the lower bound in (i) for observing the turnpike property depends on the cost to reach the equilibrium x_l^β from a neighborhood. If this cost is high and, in addition, the cost to leave the neighborhood and the cost outside the neighborhood are low, then we do not expect a local turnpike behavior. Hence, the set of discount rates for which a local turnpike behavior occurs may be empty.

Remark 3.16
The attentive reader may have noted that we apply Lemma 3.13 with $K = 1$ in this proof rather than with $K = M$, which might appear more natural given that we want to make a statement for $\{0, \dots, M\}$. This is because the size of the neighborhood $\mathcal{B}_{\varepsilon(\beta,K)}(x_l^\beta)$ delivered by Lemma 3.13 depends on K. If we applied Lemma 3.13 with $K = M$ to construct the neighborhood $\mathcal{N}$, this neighborhood may shrink to $\{x_l^\beta\}$ as M increases. In contrast, the fact that $\widetilde{V}_\beta^\infty$ is a (practical) Lyapunov function allows us to construct a neighborhood $\mathcal{N}$ that does not depend on M.

3.3.3 Finite Horizon

Since the turnpike property can also be defined for finite horizon optimal control problems as in Proposition 2.16, we aim to investigate the turnpike behavior of discounted optimal control problems on the finite horizon. Hence, we address the question of whether Theorem 3.14 still holds for the discounted optimal control problem with horizon $N \in \mathbb{N}$:

$$\begin{aligned} \min_{\mathbf{u}\in\mathbb{U}^N(x_0)} J_\beta^N(x_0, \mathbf{u}) &= \sum_{k=0}^{N-1} \beta^k \ell(x_{\mathbf{u}}(k, x_0), u(k)) \\ \text{s.t.} \quad x_{\mathbf{u}}(k+1, x_0) &= f(x_{\mathbf{u}}(k, x_0), u(k)), \quad k = 0, \dots, N-1, \\ x_{\mathbf{u}}(0, x_0) &= x_0. \end{aligned} \tag{OCP(β, N))}$$

For this purpose, we use Theorem 4.4 in [49], which shows that under mild conditions on the problem data, the finite horizon turnpike property holds if and only if the

infinite horizon turnpike property holds. Consequently, from Theorem 3.14, we can conclude the local turnpike property on the finite horizon. We provide a variation of Theorem 4.4 from [49] adapted to our local setting.

Theorem 3.17
Consider the discounted optimal control problem on finite horizon (OCP(β, N)) *with bounded stage cost* ℓ *and suppose that the system* (2.1) *is locally strictly* (x, u)*-dissipative at an equilibrium* (x_l^β, u_l^β) *according to Definition 3.6.*

Then, the discounted optimal control problem on finite horizon (OCP(β, N)) *exhibits a local turnpike property if and only if the discounted optimal control problem on the infinite horizon* (OCP(β)) *exhibits a local turnpike property.*

Proof. The argumentation in the proof of Theorem 4.4 in [49] remains valid if we restrict ourselves to the subset $\mathbb{X}_\mathcal{N} \subset \mathbb{X}$: The turnpike property on infinite horizon implies the turnpike property on finite horizon, and vice versa. We require the boundedness of the stage cost ℓ to ensure the uniform convergence of $V_\beta^N \to V_\beta^\infty$ as $N \to \infty$ on bounded subsets of $\mathbb{X}$. Further, the boundedness of the stage cost ℓ implies Assumption 4.3 (ii) in [49], namely that for near-optimal trajectories with optimal value function V_β^N bounded by a constant C it suffices to choose N' large enough such that $\beta^{N'} C \leq \tilde{\varepsilon}$ holds for $\tilde{\varepsilon} > 0$. However, we need to clarify whether Theorem 4.4 in [49] is applicable to our local setting, i.e., applicable to a subset of the admissible set $\mathbb{X}_\mathcal{N} \subset \mathbb{X}$. This is ensured because the proof of [49, Theorem 4.4] only argues with bounded subsets of the set and does not need any property of the whole admissible set. □

We remark here that the assumption of bounded stage cost ℓ, bounded cost function, and bounded optimal value function can be relaxed at the expense of the conditions becoming more technical. For more details, we refer to the discussion below Assumption 4.3 in [49]. However, if the stage cost ℓ is bounded along optimal trajectories, then, due to the exponential decay of β^k, the value of the tail becomes arbitrarily small. In this case, we obtain the convergence of $V_\beta^N \to V_\beta^\infty$. Furthermore, the boundedness of ℓ implies the boundedness of J_β^N and V_β^N, and, thus, Assumption 4.3 (iii) in [49] which indicates how large the horizon is to choose.

To obtain a local discounted turnpike property on a finite horizon N, we now transfer Theorem 3.14 to the finite horizon case by applying Theorem 3.17. This leads to the next theorem.

Theorem 3.18
Consider a discounted optimal control problem on infinite horizon (OCP(β)) *with discount factor* $\beta \in (0, 1)$*, and bounded stage cost* ℓ*. Assume that the system* (2.1)

is locally discounted strictly(x,u)-dissipative at an equilibrium (x^β, u^β) with bounded storage function λ and let $\rho > 0$ be such that $\mathcal{B}_\rho(x_l^\beta) \subset \mathbb{X}_\mathcal{N}(x_l^\beta)$. Assume further that the assumptions of Theorem 3.14 hold.

Then, there is $\beta_2 \in (0,1)$ such that for all $\beta \in (\beta_1, \beta_2)$, there exists a neighborhood $\mathcal{N}$ of x_l^β on which the system exhibits a local turnpike property on finite horizon N in the following sense: For each $\varepsilon > 0$ there exist a constant $P > 0$ such that for each $M \in \mathbb{N}$ there is a $\delta > 0$ such that for all $N \geq M$, $x_0 \in \mathcal{N}$ and all $\boldsymbol{u} \in \mathbb{U}^N(x_0)$ with $J_\beta^N(x_0, \boldsymbol{u}) \leq V_\beta^N(x_0) + \delta$ the set

$$\mathcal{Q}(x_0, \boldsymbol{u}, \varepsilon, M, N, \beta) := \{k \in \{0, \dots, M\} \mid \|x_{\boldsymbol{u}}(k, x_0) - x_l^\beta\| \geq \varepsilon\}$$

has at most P elements.

Proof. The discounted optimal control problem with $\beta \in (0,1)$ on the infinite horizon and the near-optimal trajectories under consideration fulfill the assumptions of Theorem 3.14. Hence, we can conclude a turnpike property on the infinite horizon. Now, we apply Theorem 3.17 to obtain the desired local turnpike property on finite horizon N. □

3.4 Illustrative Examples

We conclude our investigation on discounted optimal control problems with examples illustrating our theoretical results. All numerical solutions were obtained using a dynamic programming algorithm as described in [53]. The first example exhibits a local and a global optimal equilibrium independent of the discount factor β. This example illustrates that we can numerically find the boundaries of the interval $[\beta_1, \beta^\star]$ from Theorem 3.14.

Example 3.19
Consider the dynamics $f(x,u) = x + u$ and the stage cost

$$\ell(x,u) = x^4 - \frac{1}{4}x^3 - \frac{7}{4}x^2.$$

As visualized in Figure 3.2, the stage cost ℓ has a local minimum in $x = \frac{3-\sqrt{905}}{32}$, a maximum in $x = 0$, and a global minimum in $x = \frac{3+\sqrt{905}}{32}$. As discussed in Section 2.1.2, we can calculate the storage function λ by using the optimality conditions for optimal equilibria.

In [45, Section 4], it is shown that computing global storage functions this way is possible for discounted problems. We remark that the procedure also works for the local dissipativity in the case of local convexity, which is given in this example, cf.

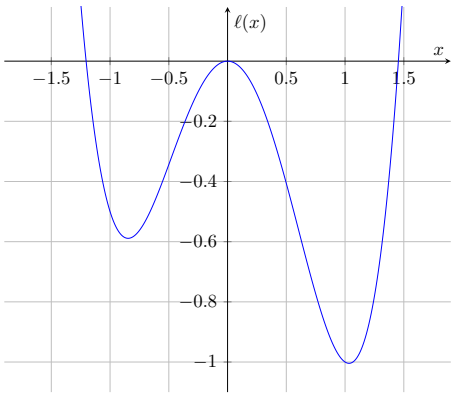

Figure 3.2: Stage cost $\ell(x)$

also the discussion after Example 3.20, below. By a straightforward calculation, we get the local equilibrium

$$(x_l^\beta, u_l^\beta) = \left(\frac{3 - \sqrt{905}}{32}, 0 \right)$$

and the storage function $\lambda \equiv 0$*. Inserting this, we obtain the rotated stage cost*

$$\widetilde{\ell}_\beta(x,u) = x^4 - \frac{1}{4}x^3 - \frac{7}{4}x^2 - \ell(x_l^\beta, 0)$$

and local discounted strict (x,u)*-dissipativity of the system* $f(x,u) = x + u$ *at* x_l^β *for any* $\beta \in (0,1)$*. Thus, the assumptions of Lemma 3.10 and Lemma 3.11 are fulfilled. Hence, following the proof of Lemma 3.11 we can estimate* $\beta_2 \approx 0.67$ *with* $\delta \approx 1$ *and* $\widetilde{\ell}_{\min} \approx -0.42$*. Further, since* $\|\widetilde{\ell}_\beta(x,u)\|$ *is bounded for* x *in a neighborhood* $\mathcal{B}_\varepsilon(x_0)$*,* $\varepsilon > 0$*, Theorem 3.14 can be applied. We set* $\mathbb{U} = [-0.75, 0.75]$ *to illustrate the theoretical results.*

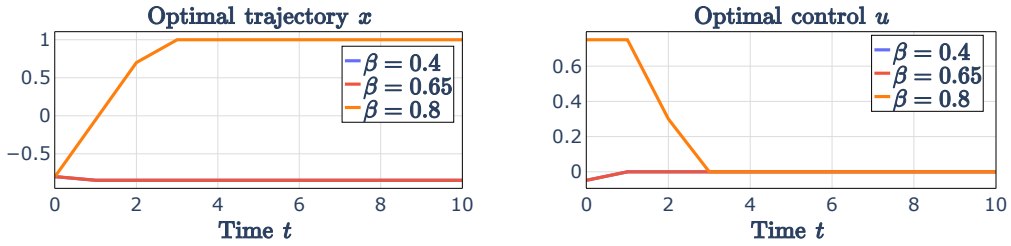

Figure 3.3: Optimal trajectory and control of Example 3.19 with $x_0 = -0.8$

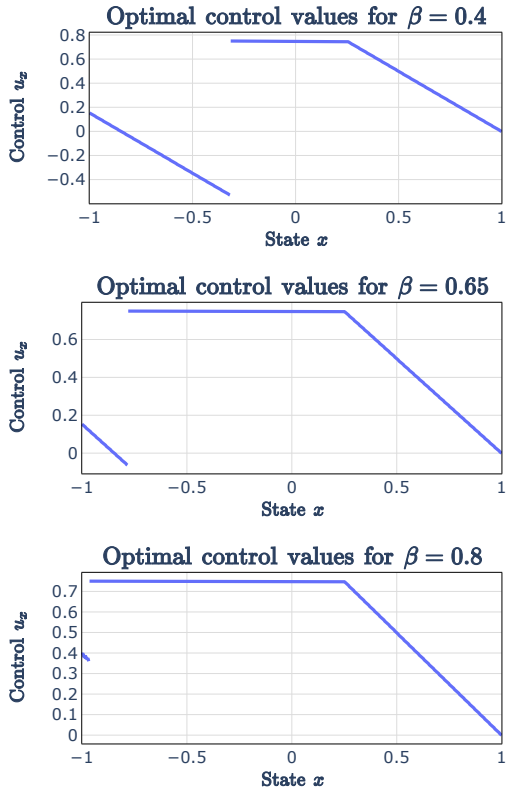

Figure 3.4: Domains of attraction of Example 3.19 with $x_0 = -0.8$

In Figure 3.3, we show the behavior of the trajectory x and the control u for different discount factors β. In Figure 3.4, we can observe the optimal feedback control values u_x and, therefore, the domain of attraction of the equilibria dependent on β. After a maximum of three time instants, the trajectory reaches the global equilibrium for β large enough. In contrast, for $\beta \leq 0.67$, we can observe that it is more favorable to stay in a neighborhood of the local equilibrium x_l^β. We remark that it is sufficient to depict $\beta = 0.8$ as a representative for all $\beta \in (0.67, 1)$ since the trajectory behavior, the control, and the stage cost do not change significantly. In this example, β_1 can be chosen arbitrarily close to 0 because it is always cheaper to approach x^β than to stay elsewhere in the neighborhood of x^β due to the absence of u-dependent terms in $\widetilde{\ell}_\beta$.

Figure 3.5 shows the trajectory behavior for fixed $\beta = 0.7$ and different initial values x_0. As we can see, the initial value determines to which equilibrium the trajectory converges. This underpins the theoretical results of Theorem 3.14 and especially of Lemma 3.11. We note that for a completely controllable system, such a behavior cannot occur in undiscounted problems.

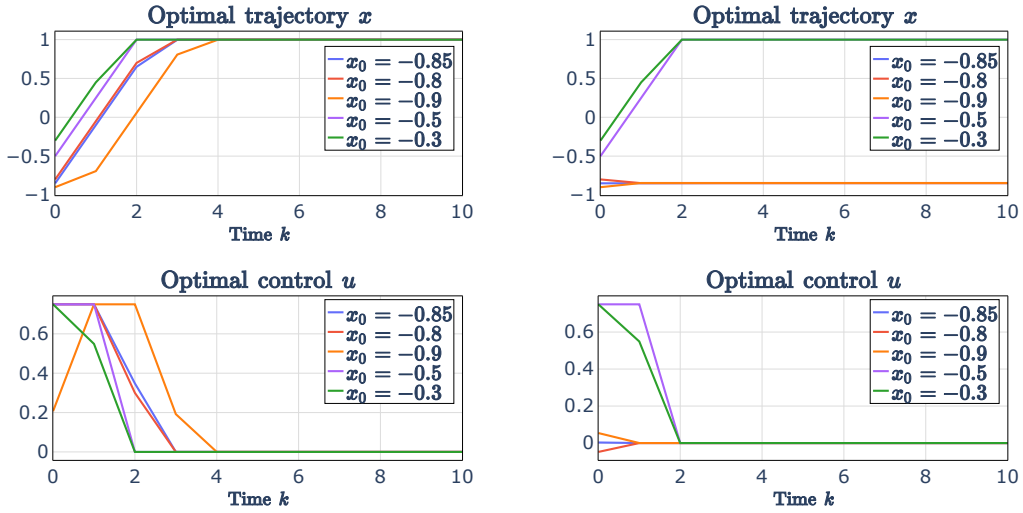

Figure 3.5: Example 3.19 with $\beta = 0.7$ (left) and $\beta = 0.6$ (right) for different initial values x_0

The following example modifies Example 3.19 and illustrates the case that the interval (β_1, β_2) is empty.

Example 3.20

Consider again the system $f(x,u) = x + u$, but now with stage cost

$$\ell(x,u) = x^4 - \frac{1}{4}x^3 - \frac{7}{4}x^2 + \gamma|u|$$

with $\gamma \neq 0$. As the added term $\gamma|u|$ does not influence the conditions of Theorem 3.14, we can again estimate $\beta_2 \approx 0.67$. Further, for $\gamma = 0$, we get the same stage cost as in Example 3.19 above. In contrast to Example 3.19, for γ large enough we can observe that (β_1, β_2) is empty. This fact is illustrated in Figure 3.6 for $\gamma = 10$. We use the same setting for the numerical results as in Example 3.19.

In the graph with $\gamma = 10$, the trajectories no longer converge to the local equilibrium independent of the discount factor β. If we introduce state constraints that restrict the optimal solutions to a neighborhood of the local equilibrium x_l^β, then we only get convergence to x_l^β for $\beta \approx 1$. More precisely, we have numerically determined the threshold of $\beta_1 \approx 0.999$. Without such state constraints, already for $\beta \approx 0.95$, we observe convergence to the optimal equilibrium, which suggests that $\beta_2 \leq 0.95$ and thus (β_1, β_2) is empty.

In order to examine this behavior in more detail, we illustrate the behavior of different values of γ for fixed discount factors β in Figure 3.7. For $\gamma > 1$ and $\beta \lesssim 0.95$, we can observe that the trajectories stay near the initial value and do not

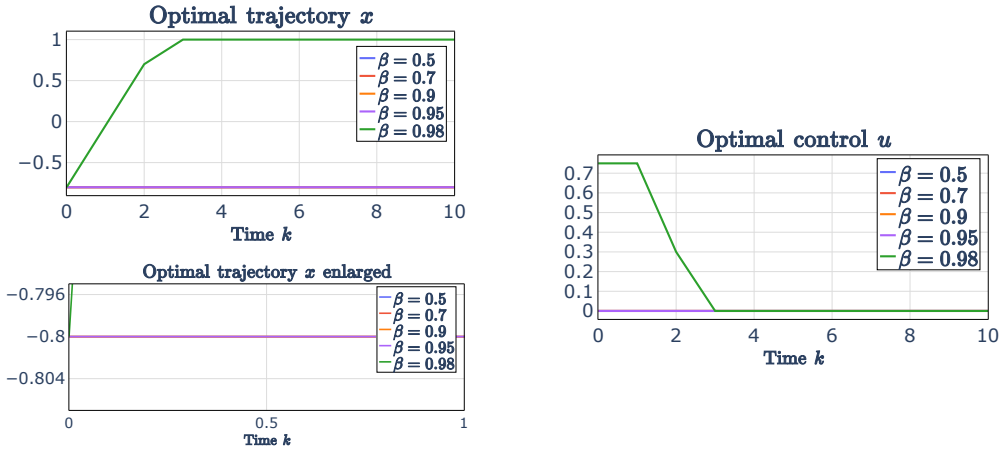

Figure 3.6: Example 3.20 with $\gamma = 10$ for different discount factor β

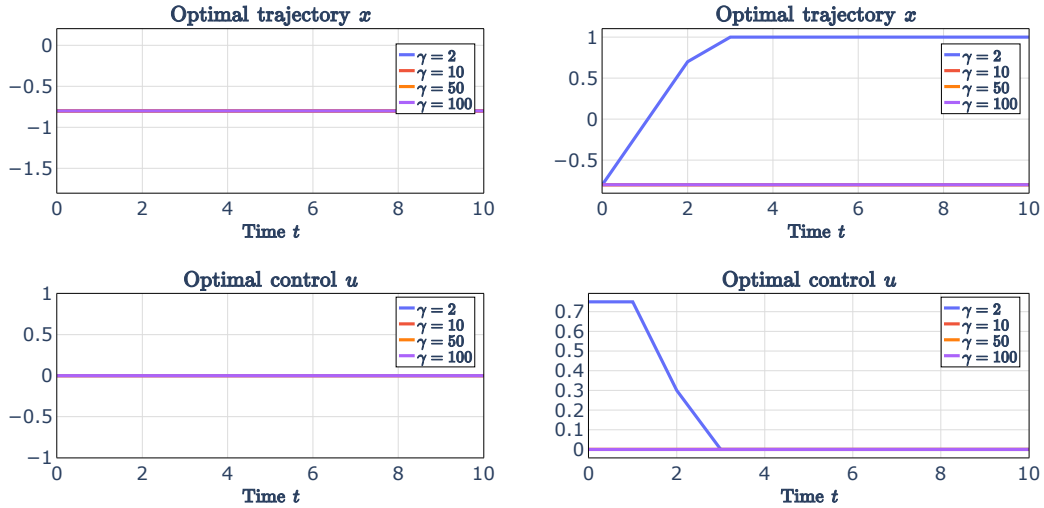

Figure 3.7: Example 3.20 with $\beta = 0.7$ (left) and $\beta = 0.95$ (right) for different γ

move away. Instead, for $\beta \approx 1$, the trajectories converge to the global equilibrium. Thus, we do not get convergence to the local equilibrium anymore.

The two examples above have the particular feature that the dynamics are affine, and the stage cost ℓ is strictly convex in a neighborhood of the optimal equilibria. In this case, similar arguments as used in the proof of Theorem 4.1 in [45] show that local strict dissipativity always holds. More precisely, we can restrict the proof of Theorem 4.1 in [45] to a bounded neighborhood $\mathbb{X}_{\mathcal{N}} \subset \mathbb{X}$ of the local equilibrium

x_l^β, e.g., $\mathcal{B}_\varepsilon(x_l^\beta)$, $\varepsilon > 0$, instead of $\mathbb{X}$, and a local strict convex stage cost function ℓ. Following the proof, for the Jacobian $\mathrm{D}\widetilde{\ell}_\beta(x_l^\beta, u_l^\beta) = 0$ holds in the neighborhood $\mathbb{X}_\mathcal{N}$, which by the local strict convexity of $\widetilde{\ell}_\beta$ implies that (x_l^β, u_l^β) is a strict local minimum. The boundedness of $\mathbb{X}_\mathcal{N}$ implies the existence of $\alpha_\beta \in \mathcal{K}_\infty$ and thus local discounted strict dissipativity. We remark that the calculation of λ is the same as in the global case and yields a linear storage function. In the particular case of Example 3.19, it yields the storage function $\lambda \equiv 0$. In conclusion, local strict dissipativity always holds if the dynamics are affine and the stage cost ℓ is strictly convex near the locally optimal equilibrium.

With this observation, our dissipativity-based analysis provides a complementary approach to the stable manifold-based analysis carried out, e.g., in [56]. Particularly, we can conclude that the model from this reference exhibits two equilibria at which the local turnpike property holds, which explains why the optimal trajectories are correctly reproduced by nonlinear model predictive control as shown in [47, Section 5.1].

Our final example demonstrates that strict convexity of ℓ is unnecessary for obtaining strict dissipativity, thus showing that a dissipativity-based analysis allows for strictly weaker assumptions than strict convexity of ℓ.

Example 3.21
Consider the 1d control system

$$x^+ = f(x,u) = 2x + u$$

with state constraints $\mathbb{X} = [-1,1]$, *control constraints* $\mathbb{U} = [-3,3]$, *and stage cost*

$$\ell(x,u) = -x^2/2 + u^2.$$

The stage cost is obviously strictly concave in x and strictly convex in u. Nevertheless, we can establish discounted strict (x,u)-dissipativity in $(x^e,u^e) = (0,0)$ (in this example even global) for $\beta \geq 3/5$ with $\lambda(x) = -x^2$. This follows from the fact that with $a = 2\beta/\sqrt{1+\beta}$ and $b = \sqrt{1+\beta}$ we have

$$\begin{aligned}\widetilde{\ell}_\beta(x,u) = \ell(x,u) + \lambda(x) - \beta\lambda(f(x,u)) &= -x^2/2 + u^2 - x^2 + \beta(2x+u)^2 \\ &= (4\beta - 3/2)x^2 + 4\beta xu + (1+\beta)u^2 \\ &= (ax+bu)^2 + \left(4\beta - \frac{3}{2} - \frac{4\beta^2}{1+\beta}\right)x^2.\end{aligned}$$

The case of $ax + bu \geq \frac{b}{2}u$ implies $(ax+bu)^2 \geq \frac{b^2}{4}u^2$, and since the term in the large brackets is greater than zero for $\beta \geq 3/5$ the strict (x,u)-dissipativity.

Is $ax + bu < \frac{b}{2}u$, *it follows that* $|x| > \dfrac{b}{2a}u$. *By plugging in, we can estimate*

$$\widetilde{\ell}_\beta(x,u) \geq \left(4\beta - \frac{3}{2} - \frac{4\beta^2}{1+\beta}\right)x^2 = \frac{1}{2}\left(4\beta - \frac{3}{2} - \frac{4\beta^2}{1+\beta}\right)x^2 + \frac{1}{2}\left(4\beta - \frac{3}{2} - \frac{4\beta^2}{1+\beta}\right)x^2$$
$$\geq \frac{1}{2}\left(4\beta - \frac{3}{2} - \frac{4\beta^2}{1+\beta}\right)x^2 + \frac{1}{2}\left(4\beta - \frac{3}{2} - \frac{4\beta^2}{1+\beta}\right)\frac{b^2}{8a^2}u^2,$$

implying the strict (x,u)*-dissipativity for* $\beta \geq 3/5$.

Since the system is completely controllable in finite time, hence exponentially stabilizable, Theorem 3.4 in conjunction with Remark 3.5(ii) implies that for sufficiently large β *turnpike behavior occurs at* $x^e = 0$. *This is confirmed for* $\beta = 0.7$ *in the left graph in Figure 3.8. In contrast, the right graph in Figure 3.8 shows that for* $\beta = 0.6$, *the turnpike behavior for* $x^e = 0$ *does not occur. Instead, the optimal solution converges to the upper bound* $x = 1$ *of the state constraint set. In this example, the numerical computations indicate that* $\beta = 3/5 = 0.6$ *is a relatively precise estimate of the threshold for the occurrence of the turnpike property at* $x^e = 0$. *However, for* β *decreasing from* 0.7 *to* 0.6, *the set of initial values around* $x^e = 0$ *for which the turnpike behavior can be seen shrinks rapidly.*

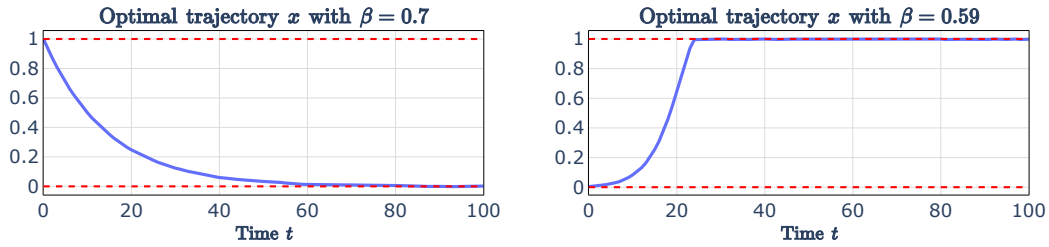

Figure 3.8: Optimal trajectories for Example 3.21 with $\beta = 0.7$ and $x_0 = 1$ (left) and with $\beta = 0.59$ and $x_0 = 0.004$ (right)

4 Multiobjective Strict Dissipativity via the Weighted Sum Approach

Dissipativity, as introduced into systems theory by Willems [93, 94], has turned out to be a highly useful concept for understanding the qualitative behavior of optimally controlled systems. Motivated by the observation of the importance of dissipativity concepts in model predictive control [7, 19, 72, 73] and for the characterization of the turnpike property [51], cf. Section 2.1.2, extending the dissipativity concept to multiobjective problems is a natural idea.

Recent literature has highlighted the difficulty in formulating a model predictive control scheme for multiobjective optimal control problems *without* terminal conditions, see, for instance, [88, Chapter 5] or [57]. One approach to overcome this challenge is scalarizing multiobjective problems and solving single-objective problems instead as done, for example, in [82]. A common scalarization technique is the weighted sum approach introduced and discussed in Section 2.2.1. Hence, by solving single-objective optimal control problems with varying weight vectors $w \in [0,1]^n$, we can compute efficient solutions (under some convexity assumptions). This way, we can apply the theory and properties of MPC based on single-objective optimal control problems without terminal conditions.

As already highlighted, strict dissipativity is a useful concept for deriving properties of the closed-loop, cf. Section 2.1.2, or, e.g., [31], [46, Section 7]. In the context of multiobjective optimal control problems without terminal conditions, we aim to investigate the theoretical question: If the system is strictly dissipative for the $s \geq 2$ stage costs ℓ_i, $i = 1, 2 \ldots, s$, is it also strictly dissipative for the convex-combined sum $\ell_w = \sum_i w_i \ell_i$ with $w_i \in [0,1]$ and $\sum_i w_i = 1$ of these costs?

By addressing this question, we seek to provide a basis for a better understanding of the behavior of economic multiobjective optimal control problems without terminal conditions. Our analysis yields strict dissipativity for convexly combined stage costs under the assumptions derived below.

In order to render our presentation less technical, we give all results and proofs for only two cost functions ℓ_1 and ℓ_2, in which case the weighted sum specializes to

$$\ell = w\ell_1 + (1-w)\ell_2, \quad w \in [0,1].$$

After each main result, we provide a remark explaining how the assumptions and assertions extend to the general setting with $s > 2$ stage costs.

Throughout this chapter, we consider an optimal control problem (OCP_N) with stage cost $\ell_w = w\ell_1 + (1-w)\ell_2$, and we impose a non-empty combined state and input constraint set $\mathbb{Y} \subseteq \mathbb{R}^n \times \mathbb{R}^m$. As in Section 2.1, we define the induced state and input constraint sets $\mathbb{X} := \{x \in \mathbb{R}^n \mid \exists\, u \in \mathbb{R}^m \text{ with } (x,u) \in \mathbb{Y}\}$ and $\mathbb{U} := \{u \in \mathbb{R}^m \mid \exists\, x \in \mathbb{R}^n \text{ with } (x,u) \in \mathbb{Y}\}$.

4.1 Strict Dissipativity of Convex Combined Stage Costs with Linear Dynamics

We will proceed methodically by first examining the case of linear dynamics (2.12). Hence, we consider an optimal control problem (OCP_N) with linear dynamics of the form

$$\begin{aligned} x(k+1) &= f(x(k),u(k)) = Ax(k) + Bu(k), \qquad k = 0,\dots,N, \\ x(0) &= x_0, \end{aligned} \tag{4.1}$$

with $A \in \mathbb{R}^{n\times n}$ and $B \in \mathbb{R}^{m\times n}$. We recall the relation between strict dissipativity and steady-state problems previously presented in Section 2.1.2. Additionally, we take advantage of the fact that, in this case, the storage function can be represented by the corresponding Lagrange multiplier. This insight allows us to establish strict dissipativity for convexly combined strictly dissipative stage costs.

4.1.1 The Linear-Quadratic Case

In the case of linear dynamics, a common choice of stage costs is a quadratic cost function

$$\ell_i(x,u) = x^T Q_i x + u^T R_i u + s_i^T x + v_i^T u, \quad i = 1,2 \tag{4.2}$$

with $Q_i \in \mathbb{R}^{n\times n}$, $R_i \in \mathbb{R}^{m\times m}$, $s_i \in \mathbb{R}^n$ and $v_i \in \mathbb{R}^m$. Here we assume that Q_i and R_i are symmetric, Q_i is positive semidefinite, and R_i is positive definite. These stage costs are called generalized quadratic costs, as they also contain linear terms. In this setting, dissipativity characterizations and storage functions can be explicitly computed using the techniques from [41], which leads to the following theorem.

Theorem 4.1
Consider the optimal control problem (OCP_N) *with linear dynamics* (4.1) *and quadratic costs* ℓ_1 *and* ℓ_2 *of the form* (4.2). *We assume that the constraint set* $\mathbb{Y}$ *is either convex and compact or* $\mathbb{Y} = \mathbb{R}^n \times \mathbb{R}^m$, *i.e., there are no constraints, and that the system* (4.1) *is strictly dissipative for both* ℓ_1 *and* ℓ_2. *In case* $\mathbb{Y}$ *is compact, we assume*

that the global optimal equilibria (x_w^e, u_w^e) *minimizing the steady-state problem* (SSP) *for* $\ell = \ell_w := w\ell_1 + (1-w)\ell_2$ *satisfy* $(x_w^e, u_w^e) \in \operatorname{int} \mathbb{Y}$ *for all* $w \in [0,1]$.

Then, the system (4.1) *is strictly dissipative for* ℓ_w *at* (x_w^e, u_w^e) *for all* $w \in [0,1]$.

Proof. We first observe that $(x_w^e, u_w^e) \in \operatorname{int} \mathbb{Y}$ for $w = 0$ and $w = 1$. Then, by Lemma 4.1 from [41], strict pre-dissipativity for ℓ_i, $i = 1, 2$ holds if and only if there is a symmetric solution P_i of the matrix inequality

$$Q_i + P_i - A^T P_i A > 0. \tag{4.3}$$

In this case, the storage function can be chosen to be of the linear-quadratic form

$$\lambda_i(x) = x^T P_i x + p_i^T x$$

for an appropriate vector $p_i \in \mathbb{R}^n$ (see the discussion after this proof). In case $\mathbb{Y} = \mathbb{R}^n \times \mathbb{R}^m$, the matrix P_i must be positive semi-definite for λ_i to be bounded from below. Then, however, we may choose P_i to be positive definite because when a positive semi-definite matrix P_i satisfies inequality (4.3), then for sufficiently small $\varepsilon > 0$, the positive definite matrix $P_i + \varepsilon I$ also satisfies inequality (4.3).

Thus, the strict dissipativity assumptions on ℓ_1 and ℓ_2 imply that we can find symmetric solutions P_1, P_2 of the matrix inequality (4.3) for $i = 1, 2$, respectively, which we can choose to be positive definite if $\mathbb{Y} = \mathbb{R}^n \times \mathbb{R}^m$. It is then easy to see that $P_w = wP_1 + (1-w)P_2$ solves the inequality (4.3) for $Q_w = wQ_1 + (1-w)Q_2$. Hence, since $(x_w^e, u_w^e) \in \operatorname{int} \mathbb{Y}$, and using [41, Lemma 4.1] strict pre-dissipativity for the cost ℓ_w with storage function $\lambda_w(x) = x^T P_w x + p_w^T x$ (and again with an appropriate vector $p_w \in \mathbb{R}^n$) follows.

If $\mathbb{Y} = \mathbb{R}^n \times \mathbb{R}^m$, P_w is positive definite, and thus boundedness from below of $\lambda_w(x)$ holds (regardless of what p_w is). If $\mathbb{Y}$ is compact, λ_w is bounded from below on $\mathbb{X}$ by its continuity. Thus, in both cases, λ_w is bounded from below on $\mathbb{X}$, which, together with strict pre-dissipativity, implies strict dissipativity. □

Remark 4.2
Theorem 4.1 and its proof immediately generalize to s *cost functions* $\ell_1, \ldots, \ell_s$ *of the form* (4.2)*, since it is easy to check that* $P_w = \sum_i w_i P_i$ *solves* (4.3) *for* $Q_w = \sum_i w_i Q_i$ *if each* P_i *for* $i = 1, \ldots, s$ *solves matrix inequality* (4.3) *for* Q_i.

The construction in the proof implies that the matrix P_w in the quadratic storage function λ_w is a convex-combined sum $P_w = wP_1 + (1-w)P_2$ of the matrices P_1 and P_2 from the single storage functions λ_i, $i = 1, 2$. Moreover, it follows from

Proposition 2.15 that the vector p_w is the Lagrange multiplier $\nu_w = \nu$ of the steady-state problem

$$\begin{aligned} &\min_{(x,u)\in\mathbb{Y}} \ell(x,u) \\ \text{s.t.} \quad &x - f(x,u) = 0, \end{aligned} \tag{SSP}$$

with $\ell = \ell_w$. In contrast to the matrix P_w, the vector p_w can, in general, *not* be chosen as a convex combination $p_w = wp_1 + (1-w)p_2$. Likewise, the optimal equilibrium (x_w^e, u_w^e) is in general not a weighted sum of (x_1^e, u_1^e) and (x_2^e, u_2^e). The following one-dimensional example illustrates this fact.

Example 4.3
Consider the one-dimensional dynamics $x^+ = ax + bu$ with $\mathbb{Y} = \mathbb{R} \times \mathbb{R}$ and the costs of the form

$$\ell_i(x,u) = q_i x^2 + r_i u^2 + s_i x + v_i u$$

with $q_i, r_i, s_i, v_i > 0$, $i = 1, 2$, and $a, b \in \mathbb{R}$. Since $q_i > 0$, the stage costs ℓ_i are both strictly convex functions. Moreover, $P_i = 0$ solves the one-dimensional matrix inequality (4.3) for $Q_i = q_i$ and $A = a$, thus, we do not need a quadratic part in the storage function. We do, however, in general, need a linear part, which we compute as described above via the Lagrange multiplier ν_i of the optimization problem

$$\begin{aligned} &\min_{(x,u)\in\mathbb{Y}} \ell_i(x,u) = q_i x^2 + r_i u^2 + s_i x + v_i u \\ &s.t.\ x = ax + bu. \end{aligned}$$

For this purpose, we define the Lagrange function

$$L_i(x,u,\nu_i) = \ell_i(x,u) + \nu_i(x - ax - bu)$$

and calculate the corresponding derivatives

$$\frac{\partial L_i}{\partial x}(x,u,\nu_i) = 2q_i x + s_i + \nu_i(1-a) \tag{4.4}$$

$$\frac{\partial L_i}{\partial u}(x,u,\nu_i) = 2r_i u + v_i - \nu_i b \tag{4.5}$$

$$\frac{\partial L_i}{\partial \nu_i}(x,u,\nu_i) = x - ax - bu. \tag{4.6}$$

Solving the system (4.4)–(4.6) *provides*

$$\begin{aligned} x_i^e &= \frac{(1-a+b)b(-bs_i-(1-a)v_i)}{(1-a+b)(2q_ib^2+2(1-a)^2r_i)} = \frac{b(-bs_i-(1-a)v_i)}{2(q_ib^2+(1-a)^2r_i)}, \\ u_i^e &= \frac{(1-a)(-bs_i-(1-a)v_i)}{2(q_ib^2+(1-a)^2r_i)} \\ \nu_i &= \frac{1}{1-a+b}\left(\frac{(-bs_i-(1-a)v_i)(r_i(1-a)-bq_i)}{q_ib^2+(1-a)^2r_i}+v_i-s_i\right) \\ &= \frac{q_iv_ib-(1-a)r_is_i}{q_ib^2+(1-a)^2r_i}. \end{aligned} \tag{4.7}$$

According to Proposition 2.13, the scalar optimal control problems are strictly dissipative at (x_i^e, u_i^e) *with storage function* $\lambda_i(x) = \nu_i x$.

Next, we consider the combined stage cost

$$\ell_w(x,u) = w\ell_1(x,u) + (1-w)\ell_2(x,u), \tag{4.8}$$

which is again strictly convex for all $w \in [0,1]$, *since a convex combination of strictly convex functions is again strictly convex. As above, we define the Lagrange function*

$$L(x,u,\nu_w) = \ell_w(x,u) + \nu_w(x-ax-bu),$$

and solve

$$\begin{aligned} \frac{\partial L}{\partial x}(x,u,\nu_w) &= w(2q_1x+s_1)+(1-w)(2q_2x+s_2)+\nu_w(1-a) = 0 \\ \frac{\partial L}{\partial u}(x,u,\nu_w) &= w(2r_1u+v_1)+(1-w)(2r_2u+v_2)-\nu_w b \qquad = 0 \\ \frac{\partial L}{\partial \nu_w}(x,u,\nu_w) &= x-ax-bu \qquad = 0. \end{aligned}$$

The solution is given by

$$\begin{aligned} x_w^e &= \frac{-b(w(bs_1+(1-a)v_1)+(1-w)(bs_2+(1-a)v_2))}{2(w(b^2q_1+(1-a)^2r_1)+(1-w)(b^2q_2+(1-a)^2r_2))} \\ u_w^e &= \frac{-\big((1-a)b(ws_1+(1-w)s_2)+(1-a)^2(wv_1+(1-w)v_2)\big)}{2\left(w(b^2q_1+(1-a)^2r_1)+(1-w)(b^2q_2+(1-a)^2r_2)\right)} \end{aligned}$$

$$\nu_w = \frac{b(wq_1+(1-w)q_2)(wv_1+(1-w)v_2)-(1-a)(wr_1+(1-w)r_2)(ws_1+(1-w)s_2)}{b^2(wq_1+(1-w)q_2)+(1-a)^2(wr_1+(1-w)r_2)}.$$

A simple numerical example using the system $x^+ = 2x+4u$ *with stage costs*

$$\ell_1(x,u) = 0.1x^2+10u^2+6x+7u \quad \textit{and} \quad \ell_2(x,u) = 4x^2+3u^2+3x+8u \tag{4.9}$$

shows that ν_w does indeed not depend linearly on w, cf. Figure 4.1. Hence, this stresses that we can not simply combine the storage functions to deduce the strict dissipativity for convex-combined stage costs.

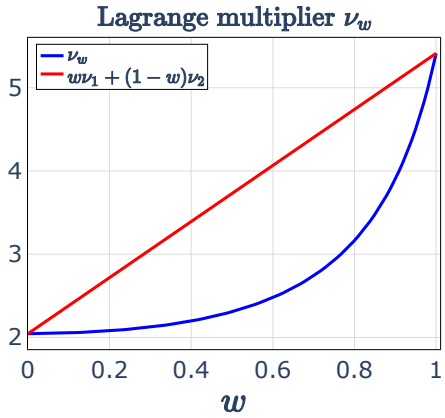

Figure 4.1: Lagrange multiplier ν_w depending on w (blue) and convex combination $w\nu_1 + (1-w)\nu_2$ (red) for costs from (4.9)

In order to find out whether there are cases in which ν_w depends linearly on w, we examine the equation

$$\nu_w - w\nu_1 - (1-w)\nu_2 = 0. \tag{4.10}$$

Upon straightforward calculations, we find that sufficient conditions for this equation to hold for all $w \in [0,1]$ are either $a = 1$ or $q_1 r_2 = q_2 r_1$. This observation demonstrates that equality (4.10) holds only for highly specialized cases when considering arbitrary $w \in (0,1)$. Therefore, even in the simple case of scalar-valued linear dynamics, the coefficients in the storage function for arbitrary w can generally not be determined as a weighted sum of the coefficients for $w = 0$ and $w = 1$.

4.1.2 The Case of Non-Quadratic Costs

We extend our analysis of linear dynamics (2.12) by including non-quadratic costs, assuming that the occurring cost functions are either convex or strictly convex. Then, we can apply Proposition 2.13 to show strict dissipativity for the combined stage costs.

Theorem 4.4
Consider the optimal control problem (OCP_N) with linear dynamics (4.1) and convex

stage costs ℓ_1 and ℓ_2, where at least one of the functions ℓ_1 and ℓ_2 is also strictly convex. Assume that the constraint set $\mathbb{Y}$ is convex and compact and that the Slater condition from Proposition 2.13 is satisfied.

Then, the system (4.1) *is strictly dissipative for the stage cost $\ell_w = w\ell_1 + (1-w)\ell_2$ at the optimal equilibrium (x_w^e, u_w^e) for all $w \in (0,1)$.*

Proof. From the strict convexity of either ℓ_1 or ℓ_2 together with the convexity of the other stage cost, we can deduce the strict convexity of $\ell_w = w\ell_1 + (1-w)\ell_2$ for all $w \in (0,1)$. With this observation, the claim follows from Proposition 2.13. □

Remark 4.5
If the assumptions of Theorem 4.4 hold, and both ℓ_1 and ℓ_2 are strictly convex, we obtain strict dissipativity for all w in the closed-interval $[0,1]$. The theorem generalizes easily to s convex cost functions of which at least one is strictly convex, provided at least one w_i corresponding to a strictly convex ℓ_i is not zero.

4.2 Strict Dissipativity of Convex Combined Stage Costs with Nonlinear Dynamics

We now turn our attention to optimal control problems with nonlinear dynamics. Hence, we can not profit from Proposition 2.13 anymore, and, therefore, we do not know how to determine the storage function properly. Still, considering the KKT conditions will be crucial for our investigation. Before discussing sufficient conditions for a convex combination of strictly dissipative stage costs to remain strictly dissipative, we first present a necessary condition on the mapping $w \mapsto x_w^e$ and a sufficient condition for one weight $w^\star$.

4.2.1 A Necessary Condition

The following theorem examines the relation between the weight and the optimal equilibrium. In the case of strict dissipativity, the mapping is continuous; otherwise, the strict dissipativity no longer holds.

Theorem 4.6
Assume that the system (2.1) *is strictly dissipative for the cost function $\ell_w = w\ell_1 + (1-w)\ell_2$ at the corresponding optimal equilibrium (x_w^e, u_w^e) for all weights $w \in [\underline{w}, \overline{w}] \subseteq [0,1]$ and assume that (x_w^e, u_w^e) are contained in a compact set $\widehat{\mathbb{Y}} \subset \mathbb{Y}$.*

Then, the map

$$w \mapsto x_w^e$$

is continuous on $[\underline{w}, \overline{w}]$.

Proof. It follows directly from the strict dissipativity that

$$\ell_w(x_w^e, u_w^e) < \ell_w(x, u) \tag{4.11}$$

for all equilibria $(x, u) \in \mathbb{Y}$ with $x \neq x_w^e$. We prove the claim by contradiction. Assume that $w \mapsto x_w^e$ is discontinuous at some $w^\star \in [\underline{w}, \overline{w}]$. Then, there is a sequence $w_n \to w^\star$ in $[\underline{w}, \overline{w}]$, such that $(x_{w_n}^e, u_{w_n}^e)$ converges to $(\hat{x}_{w^\star}^e, \hat{u}_{w^\star}^e)$ with $\hat{x}_{w^\star}^e \neq x_{w^\star}^e$. Since $f(x_{w_n}^e, u_{w_n}^e) = x_{w_n}^e$, by continuity of f we have that $f(\hat{x}_{w^\star}^e, \hat{u}_{w^\star}^e) = \hat{x}_{w^\star}^e$, i.e., the limit is an equilibrium. Using the continuity of ℓ_w and inequality (4.11) for $w = w_n$ and $(x, u) = (x_{w^\star}^e, u_{w^\star}^e)$, for this equilibrium it holds that

$$\ell_{w^\star}(\hat{x^e}_{w^\star}, \hat{u}_{w^\star}^e) = \lim_{n\to\infty} \ell_{w_n}(x_{w_n}^e, u_{w_n}^e) \leq \lim_{n\to\infty} \ell_{w_n}(x_{w^\star}^e, u_{w^\star}^e) = \ell_{w^\star}(x_{w^\star}^e, u_{w^\star}^e).$$

This, however, means that inequality (4.11) does not hold at $w = w^\star$, which yields a contradiction. □

Remark 4.7
The reasoning in the proof immediately carries over to higher dimensional $w = (w_1, \ldots, w_s)^T$. Thus, if the system is strictly dissipative for $\ell_w = \sum_i w_i \ell_i$ for w from a subset $\Omega \subset \{w \in [0,1]^s \mid \sum_i w_i = 1\}$, then $w \mapsto x_w^e$ is continuous on Ω.

The theorem, in particular, implies that if the globally optimal equilibria x_w^e change discontinuously with w, then strict dissipativity cannot hold. While the theorem is valid for general nonlinear dynamics, discontinuity of x_w^e can occur even in the case of linear dynamics, as demonstrated in the following example.

Example 4.8
Consider the dynamics $x^+ = x + u$ and the stage costs

$$\ell_1(x, u) = \frac{1}{2}x^4 - \frac{1}{4}x^3 - x^2 + \frac{3}{4}x + u^2 \quad \text{and} \quad \ell_2(x, u) = (x-1)^2 + u^2,$$

see Figure 4.2, with compact constraint set $\mathbb{Y} = [-10, 10]^2$.

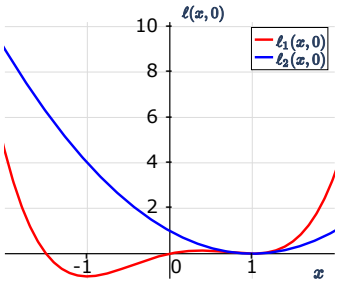

Figure 4.2: Graphs of cost functions $x \mapsto \ell_1(x,0)$ (red) and $x \mapsto \ell_2(x,0)$ (blue)

The stage cost ℓ_1 is bounded from below by the convex function

$$\hat{\ell}_1(x) = (x+1)^2/10 - 1 + u^2.$$

The global minimum $(-1,0)$ of ℓ_1 and $\hat{\ell}_1$ coincides, and it is an equilibrium of the dynamics. Hence, the system is strictly dissipative for stage cost ℓ_1 by Proposition 2.14. The system is strictly dissipative for cost ℓ_2 by Proposition 2.13 because of the convexity of ℓ_2. Since every state $x \in \mathbb{R}$ is an equilibrium of the dynamics and the corresponding equilibrium control $u = 0$ minimizes ℓ_i with respect to u, the globally optimal equilibrium (x_w^e, u_w^e) for cost $w\ell_1(x,0) + (1-w)\ell_2(x,0) + 0^2$ coincides with the global minimum of ℓ_w. This global minimum, however, changes discontinuously at $w^\star = 32/41$, as Figure 4.3 shows.

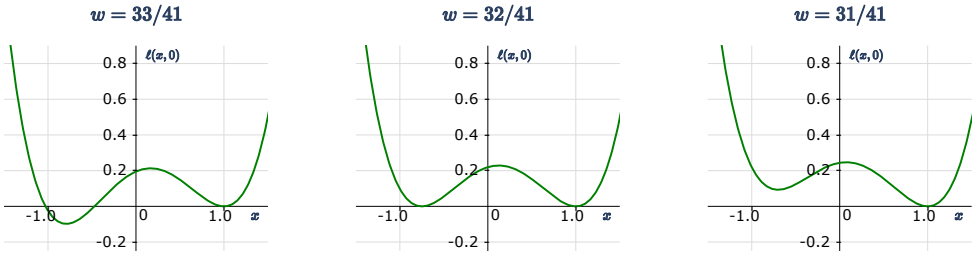

Figure 4.3: Graphs of cost functions $x \mapsto \ell_w(x,0)$ for $w = 33/41,\ 32/41,\ 31/41$ (left to right)

We note that choosing the cost ℓ_1 non-convex is crucial in this example, since for linear dynamics, convex cost ℓ_1 and strictly convex cost ℓ_2, Theorem 4.4 shows strict dissipativity for all ℓ_w, $w \in [0,1)$. Hence, Theorem 4.6 implies continuity of x_w^e on $[0, 1-\varepsilon]$ for all $\varepsilon > 0$ and thus on $[0,1)$.

4.2.2 Sufficient Conditions on the Weight

Previously, we have observed that the optimal equilibria depend continuously on the weight w provided strict dissipativity holds. Especially, Example 4.8 illustrates a case in which the strict dissipativity gets lost. In this section, we investigate the opposite perspective, namely, that strict dissipativity also depends – in a certain sense – continuously on the weight w. More precisely, we establish conditions under which strict dissipativity in $w^\star \in (0,1)$ implies strict dissipativity for small variations of $w^\star$, i.e., for $w \in (w^\star - \varepsilon, w^\star + \varepsilon)$. To this end, we assume that the constraint set $\mathbb{Y}$ is defined in terms of inequality constraints (2.3), i.e.,

$$\mathbb{Y} = \{(x,u) \in \mathbb{R}^n \times \mathbb{R}^m \mid g(x,u) \leq 0\}$$

for a function $g : \mathbb{R}^n \times \mathbb{R}^m \to \mathbb{R}^p$.

Additionally, we recall the connection between strict (x,u)-dissipativity at an equilibrium (x^e, u^e) and the steady-state problem (SSP). We refer to Section 2.1.2 for a detailed discussion of this relation. Moreover, the relevant definitions and results from nonlinear programming can also be found in Section 2.1.2. The following theorem uses these results to establish sufficient conditions under which small changes in the weight w do not affect the strict dissipativity.

Theorem 4.9
Assume that

(i) the functions f, ℓ_1, ℓ_2, g are twice continuously differentiable and $\mathbb{Y}$ is bounded.

(ii) the system (2.1) is strictly (x,u)-dissipative for the cost function $\ell_{w^\star} = w^\star \ell_1 + (1-w^\star)\ell_2$ at the equilibrium $(x^e_{w^\star}, u^e_{w^\star})$ for some $w^\star \in [0,1]$ and the corresponding storage function $\lambda_{w^\star}$ is twice continuously differentiable.

(iii) the equilibrium $(x^e_{w^\star}, u^e_{w^\star})$ is a regular point of the steady-state problem (SSP) and satisfies the strong second order sufficiency conditions for the steady-state problem (SSP), with $\ell = \ell_{w^\star}$ and for $\min_{(x,u)\in\mathbb{Y}} \widetilde{\ell}_{w^\star}$ with $\mathbb{Y}$, respectively, defined as in (2.3), and $\widetilde{\ell}_{w^\star}$ the rotated stage cost.

Then, there exists $\varepsilon > 0$ such that for all $w \in (w^\star - \varepsilon, w^\star + \varepsilon) \cap [0,1]$, there exists an equilibrium (x^e_w, u^e_w) such that the system (2.1) is strictly (x,u)-dissipative for the stage cost $\ell_w = w\ell_1 + (1-w)\ell_2$ at the equilibrium (x^e_w, u^e_w).

This theorem is similar to other theorems in the literature, such as [72, Theorem 5], where small changes in the constraints are considered, and [44, Theorem 8.2], where small changes in the discount factor are considered. As explained in [72, Remark 8], the proof of Theorem 4.9 follows by a slight modification of the proof of [72, Theorem 5]. Nonetheless, for the reader's convenience, we provide the proof of Theorem 8.2 in [44] adapted to the setting of our Theorem 4.9.

Proof. The proof exploits the fact that the strict (x,u)-dissipativity can be reformulated as the equilibrium being the unique minimizer of the steady-state problem (SSP). In particular, we first determine a suitable equilibrium candidate $(x^e(w), u^e(w))$ and a storage function candidate $\lambda_w(x)$, and then show that for $\varepsilon > 0$ small enough $(x^e(w), u^e(w))$ with $w \in (w^\star - \varepsilon, w^\star + \varepsilon) \cap [0,1]$ is the unique minimizer of the corresponding optimization problem.

Let $\ell_w(x,u) = w\ell_1 + (1-w)\ell_2$ with $w \in (w^\star - \varepsilon, w^\star + \varepsilon) \cap [0,1]$ and consider the set of equations

$$\begin{aligned} \nabla_{(x,u)}\ell_w(x,u) + \nu^T \nabla_{(x,u)}(x - f(x,u)) + \eta^T \nabla_{(x,u)} g(x,u) &= 0 \\ x - f(x,u) &= 0 \\ g_i(x,u) + z_i^2 &= 0, \quad i = 1,\dots,p \\ 2\eta_i z_i &= 0, \quad i = 1,\dots,p \end{aligned} \tag{4.12}$$

where $\nu \in \mathbb{R}^n$, $\eta \in \mathbb{R}^p$, and $z \in \mathbb{R}^p$. For each fixed weight w equation (4.12) is a set of $2n + m + 2p$ equations for $2n + m + 2p$ unknowns x, u, ν, η, z. Since the equilibrium $(x^e_{w^\star}, u^e_{w^\star})$ is a regular point by assumption and minimizes the steady-state problem (SSP) it follows that $(x,u,\nu,\eta,z) = (x^e_{w^\star}, u^e_{w^\star}, \nu^e, \eta^e, z^e)$, with $z_i^e := \sqrt{-g_i(x^e_{w^\star}, u^e_{w^\star})}$, is a solution of the equations (4.12). This is due to the fact that for these values, the equations (4.12) correspond to the KKT conditions of problem (SSP). Moreover, the corresponding Jacobian evaluated at the equilibrium is given by

$$J = \begin{pmatrix} H & a^T & b^T & 0 \\ a^T & 0 & 0 & 0 \\ b^T & 0 & 0 & 2\mathrm{diag}(z^e) \\ 0 & 0 & 2\mathrm{diag}(z^e) & 2\mathrm{diag}(\mu^e) \end{pmatrix}$$

where

$$\begin{aligned} H &:= \nabla^2_{(x,u)}\ell_w(x^e_{w^\star}, u^e_{w^\star}) + \sum_{i=1}^n \nu_i^e \nabla^e_{(x,u)} h_i(x^e_{w^\star}, u^e_{w^\star}) + \sum_{i=1}^p \eta_i \nabla^2_{(x,u)} g_i(x^e_{w^\star}, u^e_{w^\star}), \\ a &:= \nabla_{(x,u)} x^e_{w^\star} - f(x^e_{w^\star}, u^e_{w^\star}), \\ b &:= \nabla_{(x,u)} g(x^e_{w^\star}, u^e_{w^\star}). \end{aligned}$$

The Jacobian J is nonsingular since the second order sufficiency conditions for problem (SSP) are satisfied, see [44, Theorem 7.2] and Proposition 2.12. Hence, by using the implicit function theorem we can conclude that for $\varepsilon > 0$ small enough there exists a solution $(x^e(w), u^e(w), \nu^e(w), \eta^e(w), z^e(w))$ to the set of equations (4.12) such that the functions $(x^e(\cdot), u^e(\cdot), \nu^e(\cdot), \eta^e(\cdot), z^e(\cdot))$ are continuously differentiable and

$$(x^e(w^\star), u^e(w^\star), \nu^e(w^\star), \eta^e(w^\star), z^e(w^\star)) = (x^e_{w^\star}, u^e_{w^\star}, \nu^e, \mu^e, z^e)$$

holds. Furthermore, by continuity of $\eta(\cdot)$ and $z(\cdot)$, the fourth equation of (4.12), and assumption (iii), it follows that for $\varepsilon > 0$ small enough the Lagrange multiplier $\eta(\cdot)$ and the active sets $\mathcal{A}(x^e(w), u^e(w))$ and $\mathcal{A}(x^e_{w^\star}, u^e_{w^\star})$ coincide.

By assumption the equilibrium $(x^e_{w^\star}, u^e_{w^\star})$ is a regular point of problem (SSP) and a strict minimizer of $\widetilde{\ell}_{w^\star}$ on the set $\mathbb{Y}$. Hence, it holds that the KKT conditions

$$\nabla_{(x,u)} \widetilde{\ell}_{w^\star}(x^e_{w^\star}, u^e_{w^\star}) + \widetilde{\eta}^T \nabla_{(x,u)} g(x^e_{w^\star}, u^e_{w^\star}) = 0 \tag{4.13}$$

are satisfied for some $\widetilde{\eta} \in \mathbb{R}^p_{\geq 0}$. Further, note the relation

$$\nabla_{(x,u)} \left(\lambda(x^e_{w^\star}) - \lambda(f(x^e_{w^\star}, u^e_{w^\star}))\right) = \nabla_x \lambda(x^e_{w^\star})^T \nabla_{(x,u)} \left(x^e_{w^\star} - f(x^e_{w^\star}, u^e_{w^\star})\right).$$

Thus, by the uniqueness of the Lagrange multipliers ν^e and η^e we can conclude that $\nabla_x \lambda(x^e_{w^\star}) = \nu^e$ and $\widetilde{\eta} = \eta^e$.

In the next step, we define a storage function candidate

$$\lambda(x, w) := \lambda_{w^\star}(x) - \lambda(x^e(w)) + \left(\nu(w)^T - \nabla_x \lambda(x^e(w))^T\right)(x - x^e(w)) \tag{4.14}$$

with $\lambda(x^e(w), w) = 0$. We show for this function that for $\varepsilon > 0$ small enough $(x^e(w), u^e(w))$, $w \in (w^\star - \varepsilon, w^\star + \varepsilon) \cap [0, 1]$ is a (local) minimizer for the problem

$$\min_{(x,u) \in \mathbb{Y}} \widetilde{\ell}_w(x, u). \tag{4.15}$$

For this purpose, as in [44, Proof of Theorem 7.2], we can check that the KKT and the second order sufficiency conditions for this problem are satisfied.

Since $\nabla_x \lambda(x^e_{w^\star}) = \eta^e$, we obtain

$$\begin{aligned}
&\nabla_{(x,u)} \widetilde{\ell}_w(x^e(w), u^e(w)) \\
&= \nabla_{(x,u)} \ell_w(x^e(w), u^e(w)) + \nabla_{(x,u)} \left(\lambda(x^e(w), w) - \lambda(f(x^e(w), u^e(w)), w)\right) \\
&= \nabla_{(x,u)} \ell_w(x^e(w), u^e(w)) + \nabla_x \lambda(x^e(w), w)^T \nabla_{(x,u)} \left(x^e(w) - f(x^e(w), u^e(w))\right) \\
&= \nabla_{(x,u)} \ell_w(x^e(w), u^e(w)) + \nu^{eT} \nabla_{(x,u)} \left(x^e(w) - f(x^e(w), u^e(w))\right).
\end{aligned}$$

From this and $(x^e(w), u^e(w), \nu^e(w), \eta^e(w))$ being a solution of (4.12), we can conclude that $(x^e(w), u^e(w), \nu^e(w), \eta^e(w))$ satisfies equation (4.13). Together with $\eta(w) \geq 0$

and $\eta_i(w) = 0$ for all $i \notin \mathcal{A}(x^e(w), u^e(w))$ the KKT conditions of problem (4.15) are satisfied at $(x^e(w), u^e(w))$. Because of the continuity of $x^e(\cdot)$, $u^e(\cdot)$, and $\nu^e(\cdot)$ the continuity of $\nabla_{(x,u)}\widetilde{\ell}_\cdot(x^e(\cdot), u^e(\cdot))$ follows with

$$\nabla_{(x,u)}\widetilde{\ell}_{w^\star}(x^e(w^\star), u^e(w^\star)) = \nabla_{(x,u)}\widetilde{\ell}_{w^\star}(x^e_{w^\star}, u^e_{w^\star}).$$

The second order sufficiency conditions for problem (4.15) with $\ell_w = \ell_{w^\star}$ hold by the assumptions. Therefore, again by continuity and the fact that $\mathcal{A}(x^e(w), u^e(w)) = \mathcal{A}(x^e_{w^\star}, u^e_{w^\star})$ it follows that the second order sufficiency conditions for problem (4.13) are also satisfied.

Thus, for $\varepsilon > 0$ small enough, $(x^e(w), u^e(w))$, $w \in (w^\star - \varepsilon, w^\star + \varepsilon) \cap [0,1]$, is a strict local minimizer of $\widetilde{\ell}_{w^\star}$. Because of the strict (x,u)-dissipativity of $\ell_{w^\star}$ at $(x^e_{w^\star}, u^e_{w^\star})$, for w sufficiently close to $w^\star$ this equilibrium is the global minimizer of $\widetilde{\ell}_w$ on $\mathbb{Y}$. Hence, by continuity $\varepsilon > 0$ can be chosen small enough such that $(x^e(w), u^e(w))$ is the global minimizer of $\widetilde{\ell}_w$ on $\mathbb{Y}$, i.e., there exists $\alpha \in \mathcal{K}_\infty$ such that $\widetilde{\ell}_w(x,u) \geq \alpha(\|x - x^e(w), u - u^e(w)\|)$ for all $(x,u) \in \mathbb{Y}$. Together with the boundedness from below of λ_w on the compact set $\mathbb{Y}$, this implies the strict (x,u)-dissipativity. □

Remark 4.10
Since the reasoning used in these proofs was already used for multi-dimensional parameters in [72, Theorem 5], the result extends readily to more than two cost functions using a ball $\mathcal{B}_\varepsilon(w^\star)$ instead of the interval $(w^\star - \varepsilon, w^\star + \varepsilon)$.

4.2.3 Sufficient Conditions for all Weights $w \in [0,1]$

While we have considered strict dissipativity for a fixed weight $w^\star$ previously, we now focus on sufficient conditions that ensure strict dissipativity for all $w \in [0,1]$ provided we have strict dissipativity for $w = 0$ and $w = 1$. First, we turn our attention to the rare case in which the optimal equilibrium does not depend on the weight w. Then, we answer our introductory question by imposing appropriate conditions.

Theorem 4.11
Assume that the system (2.1) is strictly dissipative for the cost functions ℓ_1 and ℓ_2 at the same equilibrium x^e.

Then, system (2.1) is strictly dissipative for the cost function $\ell_w = w\ell_1 + (1-w)\ell_2$ for all $w \in [0,1]$.

Proof. For ℓ_1 and ℓ_2 there are storage functions λ_1, λ_2 as well as $\mathcal{K}_\infty$-functions α_1, α_2 such that we have the inequalities

$$\begin{aligned}\lambda_1(f(x,u)) &\leq \lambda_1(x) + \ell_1(x,u) - \ell_1(x^e,u^e) - \alpha_1(\|x - x^e\|),\\ \lambda_2(f(x,u)) &\leq \lambda_2(x) + \ell_2(x,u) - \ell_2(x^e,u^e) - \alpha_2(\|x - x^e\|).\end{aligned}$$

Adding w–times the first equation and $(1-w)$–times the second equation yields

$$\begin{aligned} w\lambda_1(f(x,u)) + (1-w)\lambda_2(f(x,u)) & \\ \leq\ & w\lambda_1(x) + (1-w)\lambda_2(x) + w\ell_1(x,u) + (1-w)\ell_2(x,u) \\ -\ & w\ell_1(x^e,u^e) - (1-w)\ell_2(x^e,u^e) \\ -\ & w\alpha_1(\|x-x^e\|) - (1-\mu)\alpha_2(\|x-x^e\|). \end{aligned}$$

Defining $\lambda_w = w\lambda_1 + (1-w)\lambda_2$ and $\alpha_w = w\alpha_1 + (1-w)\alpha_2$ we, thus, obtain

$$\lambda_w(f(x,u)) \leq \lambda_w(x) + \ell_w(x,u) - \ell_w(x^e,u^e) - \alpha_w(\|x-x^e\|).$$

Since both λ_1 and λ_2 are bounded from below λ_w is also bounded from below. In addition, the combination of two class $\mathcal{K}_\infty$-functions are again $\mathcal{K}_\infty$, see, for instance, [63, Lemma 4.2], and, hence, we can conclude that $\alpha_w \in \mathcal{K}_\infty$ for all $w \in [0,1]$. Putting this together shows the strict dissipativity inequality (2.5) holds for all these weights w. □

Remark 4.12
The proof remains completely identical for more than two cost functions. Hence, the statement holds accordingly in this case.

The situation becomes more challenging when the equilibrium (x_w^e, u_w^e) depends on the weight w, which is usually the case even for simple examples, as in Example 4.8. In the remainder of this section, we present a construction motivated and inspired by the linear quadratic result from Theorem 4.1. Hence, we aim to obtain a storage function for ℓ_w by adding a linear term to the convex combination of the storage functions for ℓ_1 and ℓ_2. It follows from Proposition 2.15 that this linear correction must be such that the gradient of the resulting storage function at (x_w^e, u_w^e) equals the Lagrange multiplier ν_w of the optimal steady-state problem

$$\begin{aligned} \min_{(x,u)\in\mathbb{Y}} \ & w\ell_1(x,u) + (1-w)\ell_2(x,u) \\ \text{s.t. } & x = f(x,u), \end{aligned} \tag{4.16}$$

and also satisfies the necessary optimality conditions (2.10) for $\ell = \ell_w$. The idea and concept were already used in [72, Theorem 5]. We provide the following theorem in two versions. Theorem 4.13 yields only local strict dissipativity (cf. Part (iv) of Definition 2.7), while Theorem 4.18 yields global (i.e., not only local) strict dissipativity, yet under stronger assumptions.

Theorem 4.13
Assume that the system (2.1) *is strictly dissipative for the cost functions ℓ_1 and ℓ_2.*

Suppose that ℓ_1 and ℓ_2 as well as the corresponding storage functions λ_1 and λ_2 are twice continuously differentiable. Furthermore, assume that for each $w \in [0,1]$ the optimal equilibrium satisfies $(x_w^e, u_w^e) \in \operatorname{int} \mathbb{Y}$ and that there exist $m_2(w) > m_1(w) \geq 0$ such that

$$\nabla^2_{(x,u)} \Big(w\widetilde{\ell}_1(x_w^e, u_w^e) + (1-w)\widetilde{\ell}_2(x_w^e, u_w^e) \Big) \geq m_2(w) I \tag{4.17}$$

for the rotated costs $\tilde{\ell}_i$ from (2.5) *and*

$$\nabla^2_{(x,u)} \Big(\tilde{\lambda}_w^T f(x_w^e, u_w^e) \Big) \leq m_1(w) I \tag{4.18}$$

for all $w \in [0,1]$, where

$$\tilde{\lambda}_w = \nu_w - w\nabla_x \lambda_1(x_w^e) - (1-w)\nabla_x \lambda_2(x_w^e) \in \mathbb{R}^n \tag{4.19}$$

and ν_w is the Lagrange multiplier for problem (4.16).

Then, the system (2.1) *is locally strictly dissipative for the cost function ℓ_w for all $w \in [0,1]$ with storage function*

$$\lambda_w(x) = w\lambda_1(x) + (1-w)\lambda_2(x) + \tilde{\lambda}_w^T x. \tag{4.20}$$

Proof. Define

$$\widetilde{\ell}_w(x,u) := \ell_w(x,u) - \ell_w(x_w^e, u_w^e) + \lambda_w(x) - \lambda_w(f(x,u)) \tag{4.21}$$

with λ_w from (4.20). In the following, we show that (x_w^e, u_w^e) is a strict local minimizer of $\widetilde{\ell}_w$, implying local strict dissipativity of the system for the cost function ℓ_w. This will be done by showing that $\nabla_{(x,u)} \widetilde{\ell}_w(x_w^e, u_w^e) = 0$ and $\nabla^2_{(x,u)} \widetilde{\ell}_w(x_w^e, u_w^e) > 0$ for which we adapt the proof of [72, Theorem 5].

First, we define $h(x,u) = x - f(x,u)$ and $\Lambda_w(x,u) = \lambda_w(x) - \lambda_w(f(x,u))$ and note that

$$\begin{aligned}
\nabla_{(x,u)} \Lambda_w(x_w^e, u_w^e) &= \nabla_{(x,u)} \lambda_w(x_w^e) - \nabla_{(x,u)} \lambda_w(f(x_w^e, u_w^e)) \\
&= [I \quad 0]^T \nabla_x \lambda_w(x_w^e) - \nabla_{(x,u)} f(x_w^e, u_w^e) \nabla_x \lambda_w(f(x_w^e, u_w^e)) \\
&= \big([I \quad 0]^T - \nabla_{(x,u)} f(x,u) \big) \nabla_x \lambda_w(x_w^e) \\
&= \nabla_{(x,u)} h(x_w^e, u_w^e) \nabla_x \lambda_w(x_w^e),
\end{aligned}$$

where the second equation follows from the chain rule and the third follows from the equilibrium property of (x_w^e, u_w^e). Further, by using the definitions of λ_w and $\tilde{\lambda}_w$

in equations (4.20) and (4.19), respectively, we obtain the derivative of the storage function

$$\begin{aligned}\nabla_x \lambda_w(x_w^e) &= \nabla_x(w\lambda_1(x_w^e) + (1-w)\lambda_2(x_w^e) + \tilde{\lambda}_w^T x_w^e)\\ &= w\nabla_x\lambda_1(x_w^e) + (1-w)\nabla_x\lambda_2(x_w^e) + \tilde{\lambda}_w\\ &= w\nabla_x\lambda_1(x_w^e) + (1-w)\nabla_x\lambda_2(x_w^e) + \nu_w - w\nabla_x\lambda_1(x_w^e) - (1-w)\nabla_x\lambda_2(x_w^e)\\ &= \nu_w.\end{aligned}$$

Using the two equations above we get that

$$\begin{aligned}\nabla_{(x,u)}\widetilde{\ell}_w(x_w^e, u_w^e) &= \nabla_{(x,u)}\ell_w(x_w^e, u_w^e) + \nabla_{(x,u)}\Lambda_\mu(x_w^e, u_w^e)\\ &= \nabla_{(x,u)}\ell_w(x_w^e, u_w^e) + \nabla_{(x,u)}h(x_w^e, u_w^e)^T\nabla_x\lambda_w(x_w^e)\\ &= \nabla_{(x,u)}\ell_w(x_w^e, u_w^e) + \nabla_{(x,u)}h(x_w^e, u_w^e)^T\nu_w\\ &= 0.\end{aligned}$$

Here, the last equality follows since it corresponds to the KKT conditions of problem (4.16), similar to the proof of Proposition 2.15.

Furthermore, we obtain by rearranging

$$\begin{aligned}&\nabla^2_{(x,u)}\widetilde{\ell}_w(x_w^e, u_w^e) = \nabla^2_{(x,u)}\ell_w(x_w^e, u_w^e) + \nabla^2_{(x,u)}\Lambda_w(x_w^e, u_w^e)\\ &= \nabla^2_{(x,u)}\ell_w(x_w^e, u_w^e) + \nabla^2_{(x,u)}\left(w\lambda_1(x_w^e) + (1-w)\lambda_2(x_w^e) + \tilde{\lambda}_w^T x_w^e\right)\\ &\qquad - \nabla^2_{(x,u)}\left(w\lambda_1(f(x_w^e, u_w^e)) + (1-w)\lambda_2(f(x_w^e, u_w^e)) + \tilde{\lambda}_w^T f(x_w^e, u_w^e)\right)\\ &= \nabla^2_{(x,u)}\left(w\widetilde{\ell}_1(x_w^e, u_w^e) + (1-w)\widetilde{\ell}_2(x_w^e, u_w^e)\right) + \nabla^2_{(x,u)}\tilde{\lambda}_w^T x_w^e - \nabla^2_{(x,u)}\tilde{\lambda}_w^T f(x_w^e, u_w^e)\\ &= \nabla^2_{(x,u)}\left(w\widetilde{\ell}_1(x_w^e, u_w^e) + (1-w)\widetilde{\ell}_2(x_w^e, u_w^e)\right) - \nabla^2_{(x,u)}\tilde{\lambda}_w^T f(x_w^e, u_w^e)\\ &\geq (m_2(w) - m_1(w))I > 0,\end{aligned}$$

which finishes the proof of the theorem. □

Remark 4.14

The assumption $(x_w^e, u_w^e) \in \operatorname{int}\mathbb{Y}$ *in Theorem 4.13 can be omitted if we assume that the second order sufficiency conditions hold for the steady-state problem* (4.16)*. Then, we have to use similar assumptions as in Theorem 4.9 and the corresponding proof of [72, Theorem 5].*

Remark 4.15

The assertion and proof of Theorem 4.13 can be extended to s *cost functions* $\ell_1, \dots, \ell_s$ *if all convex combinations with two functions* $(w\tilde{\ell}_1 + (1-w)\tilde{\ell}_2$*,* $w\nabla_x\lambda_1 + (1-w)\nabla_x\lambda_2$*,* $w\lambda_1 + (1-w)\lambda_2$*, etc.) in the assumptions and in the proof are replaced by the respective convex combinations of* s *cost functions* $\sum_i w_i\tilde{\ell}_i$*,* $\sum_i w_i\nabla_x\lambda_i$*, etc.*

Remark 4.16
It follows from Proposition 2.15 that if a storage function of the form "convex combination of λ_1 and λ_2 plus linear correction" *exists for a given value of w, then the correction term must be of the form* (4.19)*. However, as the following example shows, this construction may fail to produce a valid storage function.*

Example 4.17
Consider the nonlinear system

$$x^+ = f(x,u) = 2x - x^2 + u + u^2 + u^3$$

with stage costs

$$\ell_1(x,u) = 2x^2 + 0.0001u^2 \quad \text{and} \quad \ell_2(x,u) = 2x^2 + 0.9999u^2 + 2u.$$

Strict dissipativity holds locally for both stage costs with storage function and optimal equilibrium

$$\lambda_1(x) = 0, \quad (x_1^e, u_1^e) = (0,0)$$

for ℓ_1 and

$$\lambda_2(x) = 2.198609x, \quad (x_2^e, u_2^e) = (0.2618259, -0.2357480)$$

for ℓ_2 (all values are rounded to 7 digits). For ℓ_1, this is obvious since the function is strictly convex. Hence, strict dissipativity holds even globally, while for ℓ_2, we check that the rotated cost $\tilde{\ell}_2$ has a positive definite second derivative in (x_2^e, u_2^e).

We compute the Lagrange multiplier of the steady-state problem (4.16) *for $w = 0.5$ as $\nu_{0.5} = 1.111667$. The corresponding optimal equilibrium is*

$$(x_{0.5}^e, u_{0.5}^e) = (0.1786289, -0.1709482).$$

This means that if a linear storage function $\lambda_{0.5}$ exists, then it must be of the form $\lambda_{0.5} = 1.111667x$, which is the storage function constructed in equation (4.20) *given that λ_1 and λ_2 are linear. Further, we compute the second derivative*

$$\begin{aligned}\frac{\partial^2}{\partial u^2}\widetilde{\ell}_{0.5}(x_{0.5}^e, u_{0.5}^e) &= \frac{\partial^2}{\partial u^2}\left(2(x_{0.5}^e)^2 + 0.5(u_{0.5}^e)^2 + u_{0.5}^e + \nu_{0.5}x - \nu_{0.5}f(x_{0.5}^e, u_{0.5}^e)\right)\\ &= -0.306538,\end{aligned}$$

implying that there is no $m_2(w) > 0$ such that condition (4.17) *can hold. In particular, $\widetilde{\ell}_{0.5}$ is not convex in $(x_{0.5}^e, u_{0.5}^e)$, which would be a necessary condition for local strict dissipativity.*

We now proceed to a non-local version of Theorem 4.13, which is achieved by extending the convexity assumptions from Theorem 4.13 to all $(x, u) \in \mathbb{Y}$.

Theorem 4.18
Assume that the system (2.1) *is strictly dissipative for both stage costs* ℓ_1 *and* ℓ_2. *Suppose that* ℓ_1 *and* ℓ_2 *as well as the corresponding storage functions* λ_1 *and* λ_2 *are twice continuously differentiable. Furthermore, assume that for each* $w \in [0,1]$ *the optimal equilibrium satisfies* $(x_w^e, u_w^e) \in \operatorname{int} \mathbb{Y}$ *and that there exist* $m_2(x,u,w) > m_1(x,u,w) \geq 0$ *such that*

$$\nabla^2_{(x,u)} \Big(w\widetilde{\ell}_1(x,u) + (1-w)\widetilde{\ell}_2(x,u) \Big) \geq m_2(x,u,w) I \tag{4.22}$$

and

$$\nabla^2_{(x,u)} \Big(\tilde{\lambda}_w^T f(x,u) \Big) \leq m_1(x,u,w) I \tag{4.23}$$

for all $(x,u) \in \mathbb{Y}$, $w \in [0,1]$, *where*

$$\tilde{\lambda}_w = \nu_w - w\nabla_x \lambda_1(x_w^e) - (1-w)\nabla_x \lambda_2(x_w^e) \in \mathbb{R}^n \tag{4.24}$$

and ν_w *is the Lagrange multiplier for the steady-state problem*(4.16).

Then, the system (2.1) *is strictly dissipative for the stage cost* ℓ_w *for all* $w \in [0,1]$ *with storage function*

$$\lambda_w(x) = w\lambda_1(x) + (1-w)\lambda_2(x) + \tilde{\lambda}_w^T x. \tag{4.25}$$

Proof. To show that (x_w^e, u_w^e) is a minimizer, we proceed exactly as in the proof of Theorem 4.13. In order to conclude that (x_w^e, u_w^e) is the strict minimizer, we show that the function $\widetilde{\ell}_w$ is strictly convex by considering the second derivative for all $(x,u) \in \mathbb{Y}$. With the same computation as in the proof of Theorem 4.13 for the second derivative but now for all (x,u) instead of only for (x_w^e, u_w^e), we obtain

$$\begin{aligned} \nabla^2_{(x,u)} \widetilde{\ell}_w(x,u) &= \nabla^2_{(x,u)} \Big(w\widetilde{\ell}_1(x,u) + (1-w)\widetilde{\ell}_2(x,u) \Big) - \nabla^2_{(x,u)} \tilde{\lambda}_w^T f(x,u) \\ &\geq (m_2(x,u,w) - m_1(x,u,w)) I > 0, \end{aligned}$$

for all $(x,u) \in \mathbb{Y}$ and $w \in [0,1]$. Hence, $\widetilde{\ell}_w$ is strictly convex and continuous and together with $\widetilde{\ell}_w(x_w^e, u_w^e) = 0$ positive definite. Thus, we can conclude, that $\widetilde{\ell}_w$ is radially unbounded, see [8], and therefore, see [63, Lemma 4.3], that there exists a $\mathcal{K}_\infty$-function α such that $\widetilde{\ell}_w(x,u) \geq \alpha(\|x - x_w^e\|)$. □

We note that Remark 4.15 applies accordingly to Theorem 4.18.

Remark 4.19
We can relax inequality (4.22) *by assuming that both* $\widetilde{\ell}_1$ *and* $\widetilde{\ell}_2$ *are lower bounded by functions* $\bar{\ell}_1$ *and* $\bar{\ell}_2$ *such that* $\widetilde{\ell}_i(x_w^e, u_w^e) = \bar{\ell}_i(x_w^e, u_w^e)$ *for all* $w \in [0,1]$. *Then, inequality* (4.22) *only needs to hold with* $\bar{\ell}_i$ *in place of* $\widetilde{\ell}_i$, *i.e., we require that* $\nabla_{(x,u)}\bar{\ell}_w(x_w^e, u_w^e) = \nabla_{(x,u)}\widetilde{\ell}_w(x_w^e, u_w^e) = 0$ *and* $\nabla^2_{(x,u)}\bar{\ell}(x_w^e, u_w^e) > 0$. *Together with the fact that* $\bar{\ell}_w$ *is a lower bound for* $\widetilde{\ell}_w$ *and* $\widetilde{\ell}_i(x_w^e, u_w^e) = \bar{\ell}_i(x_w^e, u_w^e)$ *for all* $w \in [0,1]$, *this yields the desired result.*

Next, we illustrate Theorem 4.18 with an example inspired by an economic example originally introduced in [14] and adapted to our setting.

Example 4.20
Consider the nonlinear system

$$x^+ = x^3 - 2x^2 + u,$$

and the two stage costs

$$\begin{aligned}\ell_1(x,u) &= -\ln(5x^{0.34} + u),\\ \ell_2(x,u) &= -\ln(3x^{0.2} + u).\end{aligned}$$

Further, we impose state and control constraint sets $\mathbb{X} = [0,10]$ *and* $\mathbb{U} = [0.1,5]$. *For each stage cost* ℓ_i, *we determine the optimal equilibrium each given by (rounded to 7 digits)*

$$(x_1^e, u_1^e) = (1.7482008, 2.5177510) \quad \textit{and} \quad (x_2^e, u_2^e) = (1.6224804, 2.6162791).$$

The stage costs ℓ_i *are strictly dissipative at their corresponding equilibrium* (x_i^e, u_i^e) *with storage functions*

$$\lambda_1(x) = -0.1167745x \quad \textit{and} \quad \lambda_2(x) = -0.1688854x$$

and rotated stage costs

$$\begin{aligned}\widetilde{\ell}_1(x,u) &= -\ln(5x^{0.34} + u) - 2.14751051 - 0.1167745x + 0.1167745(x^3 - 2x^2 + u),\\ \widetilde{\ell}_2(x,u) &= -\ln(3x^{0.2} + u) - 1.7785341 - 0.1688854x + 0.1688854(x^3 - 2x^2 + u).\end{aligned}$$

It is easy to see that all occurring functions are twice continuously differentiable and, thus, we can check numerically the first conditions of Theorem 4.18. For each $w \in [0,1]$ *the optimal equilibrium lies in the interior of* $\mathbb{Y}$, *i.e.* $(x_w^e, u_w^e) \in \operatorname{int}(\mathbb{X} \times \mathbb{U})$. *Moreover, we can set* $m_2(x,u,w) = 0.0013$ *by using the minimum of all calculated*

second derivatives of $w\widetilde{\ell}_1 + (1-w)\widetilde{\ell}_2$ *with* $w \in [0,1]$*. Next, we have to check the condition on the correction term. To this end, we calculate the Lagrange multiplier of the steady-state problem* (4.16) *as well as the first derivatives of the storage functions* $\nabla_x \lambda_1(x_w^e)$ *and* $\nabla_x \lambda_2(x_w^e)$*. Doing so, we can estimate* $m_1(x,u,w) = 0.0005$*. Therefore, we can conclude, that* $w\ell_1 + (1-w)\ell_2$ *is strictly dissipative at the corresponding equilibrium* (x_w^e, u_w^e) *for all* $w \in [0,1]$ *with storage function*

$$\lambda_w(x) = w\lambda_1(x) + (1-w)\lambda_2(x) + \tilde{\lambda}_w^T x,$$

with $\tilde{\lambda}_w \in (-0.0002, 0)$*.*

Finally, we note that the previous results are not restricted to the weighted sum approach.

Remark 4.21
The requirement $\sum_i w_i = 1$ *was not necessary for the validity of the previous results. Assuming the weights to satisfy* $w_i \geq 0$ *for all* i *and* $w_i > 0$ *for at least one* i *would suffice. Nevertheless, since this thesis is motivated by multiobjective problems that the weighted sum approach can solve, all our results were formulated with convex combinations, i.e., assuming that* $\sum_i w_i = 1$*.*

Indeed, ensuring that all stage costs are strictly dissipative in application examples may be challenging. That is why we impose a multiobjective model predictive control scheme assuming the presence of terminal conditions in the next chapter.

5 Analysis of Multiobjective Model Predictive Control Schemes

In many practical applications, it is desirable to consider several cost criteria instead of a single criterion, as highlighted in [61, 68, 85]. For example, in chemical process control, it may be desirable to stabilize a chemical process at a particular set point while simultaneously maximizing the yield. Another application example is autonomous driving: Besides following a given path, ensuring driving comfort or maintaining a certain driving speed are also of interest. As these several criteria might be conflicting, addressing multiobjective optimal control problems is a natural idea. While we have considered the problem's properties and especially discussed strict dissipativity in the previous chapters, we now focus on examining MPC algorithms for solving such problems in this chapter.

We combine the single-objective "standard" MPC algorithm, see [46], and multiobjective optimization, see [23, 24, 71]. Whereas other approaches, see for instance [36,82], reduce the multiobjective problem to a single-objective optimal control problem, we solve the whole multiobjective optimization problem in each MPC step and choose then an efficient solution. This selection will give us an additional degree of freedom, which we discuss in Section 6.1. Building upon and extending the results from [54, 88, 96], we relax the assumptions in this chapter. Unlike in Chapter 4 we now require strict dissipativity only for one stage cost. This relaxation broadens the problem class, as proving strict dissipativity for all cost criteria in practice can be challenging. Based on these relaxed assumptions, we introduce a multiobjective model predictive control scheme with an additional constraint on the strict dissipative cost function. We show a performance bound for this objective function and prove the asymptotic stability of the closed–loop. Requiring in the algorithm the additional constraint for all objectives leads to performance estimates for *all* objective functions. Finally, we illustrate our theoretical findings with numerical simulations. To this end, we use the introductory example of a chemical reactor.

5.1 Multiobjective Model Predictive Control Algorithms

We begin with analyzing multiobjective model predictive control schemes by introducing the problem class of multiobjective optimal control problems (MO OCPs) with terminal conditions. To guarantee feasibility and the trajectory convergence to a desired equilibrium, we impose Assumption 5.1, which requires strict dissipativity and a compatibility condition of at least one cost criterion. Further, we introduce two multiobjective model predictive control algorithms with Algorithm 2 being a relaxed version of Algorithm 3.

5.1.1 Problem Class

As in Section 2.2, we consider multiobjective optimal control problems for a horizon $N \in \mathbb{N}$, $N \geq 2$. Now, we define the cost functional $J_1^N : \mathbb{X} \times \mathbb{U}^N \to \mathbb{R}$ by

$$J_1^N(x_0, \mathbf{u}) := \sum_{k=0}^{N-1} \ell_1(x_{\mathbf{u}}(k, x_0), u(k)) + F_1(x_{\mathbf{u}}(N, x_0)), \tag{5.1}$$

including a continuous terminal cost $F_1 : \mathbb{X}_0 \to \mathbb{R}_{\geq 0}$, with $\mathbb{X}_0$ the terminal constraint set. For $i \in \{2, \dots, s\}$, $s \geq 2$, we define continuous stage costs $\ell_i : \mathbb{X} \times \mathbb{U} \to \mathbb{R}$ and the corresponding cost functionals $J_i^N : \mathbb{X} \times \mathbb{U}^N \to \mathbb{R}$ by

$$J_i^N(x_0, \mathbf{u}) := \sum_{k=0}^{N-1} \ell_i(x_{\mathbf{u}}(k, x_0), u(k)) \tag{5.2}$$

for $N \in \mathbb{N}$ with $N \geq 2$. We note that we do not require any terminal costs for $i \in \{2, \dots, s\}$, which allows for significantly more problems compared to the design in [54, 88].

Since we aim to minimize all cost functionals $J_1^N, \dots, J_s^N$ at the same time for a given initial value x_0 with respect to $\mathbf{u}$ and along a solution of system (2.1), we consider multiobjective optimal control problems with terminal conditions

$$\begin{aligned} \min_{\mathbf{u} \in \mathbb{U}^N(x_0)} \; & J^N(x_0, \mathbf{u}) := \big(J_1^N(x_0, \mathbf{u}), \dots, J_s^N(x_0, \mathbf{u})\big) \\ \text{s.t.} \quad & x_{\mathbf{u}}(k+1, x_0) = f(x_{\mathbf{u}}(k, x_0), u(k)), \quad k = 0, \dots, N-1, \\ & x_{\mathbf{u}}(0, x_0) = x_0, \\ & x_{\mathbf{u}}(N, x_0) \in \mathbb{X}_0. \end{aligned} \tag{MO OCPt}$$

In the following, we only consider multiobjective optimal control problems with terminal conditions of the form (MO OCPt) with $s \geq 2$ and $N \geq 2$. Unless otherwise mentioned, the abbreviation multiobjective optimal control problem (MO OCPt)

always includes the terminal conditions. The terminal constraint $x_{\mathbf{u}}(N, x_0) \in \mathbb{X}_0$ can generally not be satisfied for all initial values $x_0 \in \mathbb{X}$, such that we recall the definition of the feasible set $\mathbb{X}_N$ from (2.2) noting that $\mathbb{U}^N(x_0) \neq \emptyset$ if and only if $x_0 \in \mathbb{X}_N$. Thus, we need to ensure that $x_{\mathbf{u}}(N, x_0) \in \mathbb{X}_0$ and that $J_1^N(x_0, \mathbf{u})$ is well-defined for $x_0 \in \mathbb{X}_N$ and $\mathbf{u} \in \mathbb{U}^N(x_0)$. Throughout this chapter, we use the following assumptions below to ensure feasibility and the convergence of the trajectory. Especially, item (iv) of the assumption ensures $\mathbb{X}_0 \subseteq \mathbb{X}_N$ for all $N \geq 2$ and thus $\mathbb{X}_N \neq \emptyset$. We show within the theoretical results in the subsequent sections why we need the terminal conditions to guarantee the convergence of the trajectory towards the considered equilibrium and, thus, the performance results.

Assumption 5.1

Consider a multiobjective optimal control problem (MO OCPt) *and assume that*

(i) there exists an equilibrium $(x^e, u^e) \in \mathbb{X} \times \mathbb{U}$ *such that* $f(x^e, u^e) = x^e$.

(ii) the system (2.1) *is strictly* (x, u)*-dissipative for the stage cost* ℓ_1 *at the equilibrium* (x^e, u^e)*, i.e., there is a storage function* $\lambda_1 : \mathbb{X} \to \mathbb{R}$ *bounded from below with* $\lambda_1(x^e) = 0$ *and a function* $\alpha_{\ell,1} \in \mathcal{K}_\infty$ *such that* $\forall (x, u) \in \mathbb{X} \times \mathbb{U}$ *the inequality*

$$\ell_1(x, u) - \ell_1(x^e, u^e) + \lambda_1(x) - \lambda_1(f(x, u)) \geq \alpha_{\ell,1}(\|x - x^e, u - u^e\|) \tag{5.3}$$

holds.

(iii) all stage costs ℓ_i*,* $i = 1, \ldots, s$*, are continuous.*

(iv) $x^e \in \mathbb{X}_0$ *and there exists a local feedback* $\kappa : \mathbb{X}_0 \to \mathbb{U}$ *satisfying*

a) $f(x, \kappa(x)) \in \mathbb{X}_0$ *for all* $x \in \mathbb{X}_0$.

b) $\forall x \in \mathbb{X}_0$*:* $F_1(f(x, \kappa(x))) + \ell_1(x, \kappa(x)) \leq F_1(x) + \ell_1(x^e, u^e)$.

(v) the sets $\mathcal{J}_{\mathcal{E}}^N(x_0)$ *are externally stable (see Definition 2.30) for* $\mathcal{J}^N(x_0)$ *for each* $x_0 \in \mathbb{X}_N$*, with* $\mathbb{X}_N$ *from* (2.2).

We only consider the equilibrium (x^e, u^e) and assume that the optimal control problem is strictly dissipative for the first stage cost ℓ_1 at this equilibrium (x^e, u^e). We note that item (iv b) is usually referred to as compatibility of the terminal cost F_1. Assumption 5.1 states that we require strict dissipativity for the multiobjective optimal control problem only for the first stage cost. In contrast, for the remaining $s - 1$ stage costs, we do not impose any conditions nor the existence of terminal costs. Stabilizing or positive definite stage costs are a special case of stage costs for which strict dissipativity holds with $\lambda \equiv 0$. We introduce two multiobjective model predictive control algorithms for which, under Assumption 5.1 above, we provide performance estimates and show stability properties of the closed-loop.

5.1.2 Two Multiobjective Model Predictive Control Algorithms

This section introduces two multiobjective model predictive control (MO MPC) schemes that rely on solving multiobjective optimal control problems of the type (MO OCPt). In the multiobjective case, however, there is more than one efficient solution, see Section 2.2, and therefore we have to adapt the single-objective or "standard" MPC algorithm, e.g., see [46], to our setting. To this end, we build on the algorithm and the results in [54, 88], which we recall at the appropriate places for completeness. However, in contrast to these references by Assumption 5.1, we can allow for more general problems of the type (MO OCPt) than in [54] since we get rid of the restrictive assumption of the existence of stabilizing stage and terminal costs in all objective functions. In particular, the existence of terminal costs that are jointly compatible with all the stage costs is no longer required.

Algorithm 2 MO MPC with terminal conditions and constraints on J_1

Input: MPC horizon N, number of time steps $K \in \mathbb{N} \cup \{\infty\}$, initial value $x_0 \in \mathbb{X}_N$ and κ from Assumption 5.1 (iv).

for $k = 0, \ldots, K$:

(0) If $k = 0$, set $x(0) = x_0$ and choose an efficient solution $\mathbf{u}^\star_{x(0)} \in \mathbb{U}^N_{\mathcal{E}}(x(0))$ of (MO OCPt). Go to (2).

(1) If $k \geq 1$, choose an efficient solution $\mathbf{u}^\star_{x(k)}$ of (MO OCPt) with $x_0 = x(k)$ so that the inequality

$$J_1^N(x(k), \mathbf{u}^\star_{x(k)}) \leq J_1^N(x(k), \mathbf{u}_{x(k)}) \tag{5.4}$$

holds.

(2) For $x := x_{u^\star_{x(k)}}(N, x(k))$ set

$$\mathbf{u}_{x(k+1)} := \left(u^\star_{x(k)}(1), \ldots, u^\star_{x(k)}(N-1), \kappa(x)\right).$$

(3) Apply the feedback $\mu^N(k, x(k)) := u^\star_{x(k)}(0)$, i.e., evaluate $x(k+1) = f(x(k), \mu^N(k, x(k)))$, set $k = k+1$ and go to (1).

Output: MPC closed-loop trajectory $x_\mu(k, x_0) := x(k)$, $k \in \{0, \ldots, K\}$.

First, we introduce an algorithm that gives a relaxed variant of Algorithm 2 in [54], in which the additional constraint on the efficient solution (5.4) is only imposed for the first cost criterion J_1^N, instead of for all cost criteria J_i^N, $i = 1, \ldots, s$, as in [54]. We denote by $\mathbf{u}^\star_{x(k)} \in \mathbb{U}^N_{\mathcal{E}}(x(k))$ an efficient solution corresponding to the initial

value $x(k)$. We discuss possibilities to compute the efficient solutions in Section 6.1.

In step (2), the importance of the terminal conditions becomes evident: by using the local feedback κ as part of the comparison control sequence in step (2), we enforce the trajectory's convergence through the first objective function, which also includes terminal costs.

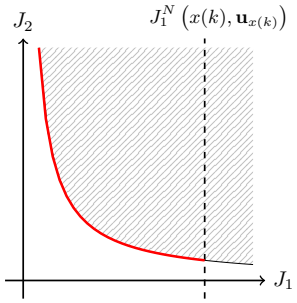

Figure 5.1: Visualization of step (1) of Algorithm 2

In Figure 5.1, we have visualized the bound on the efficient solution in inequality (5.4). The dashed line represents the bound resulting from $\mathbf{u}_{x(k)}$, and the red line is the set of nondominated points of (MO OCPt) satisfying this bound. We like to stress that we do not constrain the other objectives that may appear in the multiobjective optimal control problem. Illustratively, we only cut off the nondominated set in the direction of the first objective, i.e., towards the objective function that has the strictly dissipative stage cost.

However, to establish performance estimates for *all* objective functions, we need the additional constraint on the efficient solution for *all* objectives. To achieve this, we draw on Algorithm 2 in [54], which includes these constraints as additional inequalities in step (2). We interpret these inequalities as descent conditions in each objective.

Algorithm 3 MO MPC with terminal conditions and constraints on $J_1, \ldots, J_s$

Input: MPC Horizon N, number of time steps $K \in \mathbb{N} \cup \{\infty\}$, initial value $x_0 \in \mathbb{X}_N$ and κ from Assumption 5.1 (iv).

for $k = 0, \ldots, K$:

(0) If $k = 0$, set $x(0) = x_0$ and choose an efficient solution $\mathbf{u}^\star_{x(0)} \in \mathbb{U}^N_{\mathcal{E}}(x(0))$ of (MO OCPt). Go to (2).

(1) If $k \geq 1$, choose an efficient solution $\mathbf{u}^\star_{x(k)}$ of (MO OCPt) with $x_0 = x(k)$ so that the inequalities

$$J_i^N(x(k), \mathbf{u}^\star_{x(k)}) \leq J_i^N(x(k), \mathbf{u}_{x(k)}), \quad i = 1, \ldots, s. \tag{5.5}$$

hold.

(2) For $x := x_{u^\star_{x(k)}}(N, x(k))$ set

$$\mathbf{u}_{x(k+1)} := \left(u^\star_{x(k)}(1), \ldots, u^\star_{x(k)}(N-1), \kappa(x)\right).$$

(3) Apply the feedback $\mu^N(k, x(k)) := u^\star_{x(k)}(0)$, i.e., evaluate $x(k+1) = f(x(k), \mu^N(k, x(k)))$, set $k = k + 1$ and go to (1).

Output: MPC closed-loop trajectory $x_\mu(k, x_0) := x(k)$, $k \in \{0, \ldots, K\}$.

Figure 5.2 visualizes the bounds of step (1) in Algorithm 3. The dashed lines represent the bounds (5.5), and the red line is the set of nondominated points satisfying these inequalities. Thus, all cost criteria J_i^N are now bounded by the comparison control sequence.

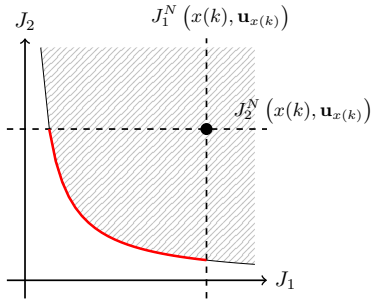

Figure 5.2: Visualization of step (1) of Algorithm 3

We remark that for the subsequent theoretical results, it is not essential which nondominated point on the red part of the nondominated set in Figure 5.1 or Figure 5.2, depending on the algorithm, we choose in step (1). The performance bounds hold for any feasible choice of $\mathbf{u}^\star_{x(k)}$ and only rely on the choice of $\mathbf{u}^\star_{x(0)}$ in step (0). However, this does not mean the choices for $k \geq 1$ do not affect the MPC closed-loop solutions. We thus investigate the development of the nondominated sets and the effect of different selection rules for the efficient point via numerical simulations in Section 6.1. Before we do this, we show in the subsequent sections that this MO MPC algorithm has certain desirable theoretical properties: feasibility, convergence, and performance bounds.

5.2 Performance and Stability Results

In the case of multiobjective model predictive control, we are interested in system theoretic properties, such as feasibility and stability, just as in the single-objective case. We can ensure feasibility and trajectory convergence due to Assumption 5.1. Further, we give conditions that ensure the asymptotic stability of the closed-loop solution. Because of the optimization-based nature of the multiobjective model predictive control method, we also state performance estimates for all objectives. More precisely, we can obtain averaged and non-averaged performance estimates for all considered objective functions by assuming strict dissipativity and the existence of a compatible terminal cost for one of the competing objective functions only. In particular, we show all the desirable properties of an MPC algorithm in this section.

5.2.1 Performance Results for the First Cost Function

We show the feasibility of Algorithm 2 and the convergence of the closed-loop trajectory. By imposing additional conditions on the first cost criterion J_1^N, we can give performance bounds of the feedback μ^N defined in Algorithm 2. We use the techniques and results from [54, 88] to accomplish this. To this end, we first show a performance estimate for the so-called rotated cost function $\widetilde{J}_1^N$ and conclude the trajectory convergence as well as the main performance theorem of this section.

We recall the standard definitions of rotated stage costs, rotated terminal costs, and rotated functionals for using these as auxiliary costs.

Definition 5.2 (Rotated costs)
For $x \in \mathbb{X}$ and $u \in \mathbb{U}$ we define the left side of inequality (5.3) *as the rotated stage cost*

$$\widetilde{\ell}_1(x,u) := \ell_1(x,u) - \ell_1(x^e,u^e) + \lambda_1(x) - \lambda_1(f(x,u)) \tag{5.6}$$

with equilibrium x^e and storage cost λ_1 from Assumption 5.1, and rotated terminal cost

$$\widetilde{F}_1(x) := F_1(x) + \lambda_1(x). \tag{5.7}$$

The corresponding cost functional is given by

$$\widetilde{J}_1^N(x_0, \boldsymbol{u}) := \sum_{k=0}^{N-1} \widetilde{\ell}_1(x_{\boldsymbol{u}}(k, x_0), u(k)) + \widetilde{F}_1(x_{\boldsymbol{u}}(N, x_0)). \tag{5.8}$$

We remark that under Assumption 5.1, for all $x \in \mathbb{X}$, $u \in \mathbb{U}$ the rotated stage cost $\widetilde{\ell}_1$ is bounded from below by $\alpha_{\ell,1}$ from Assumption 5.1(ii) and, thus, the rotated stage costs are positive definite, i.e., $\widetilde{\ell}_1(x, u) \geq 0$.

Next, we use the above definitions to derive relations between rotated and original costs. For the equilibrium (x^e, u^e) the equalities $\widetilde{\ell}_1(x^e, u^e) = 0$ and $\widetilde{F}_1(x^e) = 0$ hold. Further, for $x_0 \in \mathbb{X}_N$ and all admissible control sequences $\mathbf{u} \in \mathbb{U}^N(x_0)$ the relation

$$\begin{aligned}
\widetilde{J}_1^N(x_0, \mathbf{u}) &= \sum_{k=0}^{N-1} \widetilde{\ell}_1(x_{\mathbf{u}}(k, x_0), u(k)) + \widetilde{F}_1(x_{\mathbf{u}}(N, x_0)) \\
&= \sum_{k=0}^{N-1} \ell_1(x_{\mathbf{u}}(k, x_0), u(k)) - \ell_1(x^e, u^e) + \lambda_1 x_{\mathbf{u}}(k, x_0) - \lambda_1(x_{\mathbf{u}}(k+1, x_0)) \\
&\qquad + F_1(x_{\mathbf{u}}(N, x_0)) - \lambda_1(x_{\mathbf{u}}(N, x_0)) \\
&= \sum_{k=0}^{N-1} \ell_1(x_{\mathbf{u}}(k, x_0), u(k)) - \ell_1(x^e, u^e) + F_1(x_{\mathbf{u}}(N, x_0)) + \lambda_1(x_0) \\
&= J_1^N(x_0, \mathbf{u}) - N\ell_1(x^e, u^e) + \lambda_1(x_0)
\end{aligned} \tag{5.9}$$

holds. Moreover, we have that

$$\begin{aligned}
\widetilde{F}_1(f(x, \kappa(x))) &= F_1(f(x, \kappa(x))) + \lambda_1(f(x, \kappa(x))) \\
&\leq F_1(x) + \ell_1(x^e, u^e) - \ell_1(x, \kappa(x)) + \lambda_1(f(x, \kappa(x))) \\
&= F_1(x) + \lambda_1(x) - \big(\ell_1(x, \kappa(x)) - \ell_1(x^e, u^e) + \lambda_1(x) - \lambda_1(f(x, \kappa(x)))\big)
\end{aligned}$$

and, thus,

$$\widetilde{F}_1(f(x, \kappa(x))) \leq \widetilde{F}_1(x) - \widetilde{\ell}_1(x, \kappa(x)) \leq \widetilde{F}_1(x) - \alpha_{\ell,1}(\|x - x^e\|) \tag{5.10}$$

holds for all $x \in \mathbb{X}_N$ and κ from Assumption 5.1 (iv).

Again, we refer to [88], especially Section 5.1.2, where similar results and proofs are provided. The following lemma relates the cost functions on horizon N and $N-1$.

Lemma 5.3
For $N \in \mathbb{N}_{\geq 2}$, $x_0 \in \mathbb{X}_N$, $k = 0, \ldots, N-1$, and $\boldsymbol{u}^\star \in \mathbb{U}_{\mathcal{E}}^N(x_0)$ the relation

$$\ell_1(x_{\boldsymbol{u}}(k, x_0), u^\star_{x(k)}(0)) = J_1^N(x_{\boldsymbol{u}^\star}(k, x_0), \boldsymbol{u}^\star) - J_1^{N-1}(x_{\boldsymbol{u}^\star}(k+1, x_0), \boldsymbol{u}^\star(\cdot + 1)) \quad (5.11)$$

holds, where we use the notation $\boldsymbol{u}^\star(\cdot + 1) := (u^\star(1), u^\star(2), \ldots, u^\star(N-1))$.

Proof. Let $N \in \mathbb{N}_{\geq 2}$, $x_0 \in \mathbb{X}_N$, $\mathbf{u}^\star \in \mathbb{U}_{\mathcal{E}}^N(x_0)$, and $k = 0, \ldots, N-1$. Then, the relation

$$\begin{aligned}
&J_1^N(x_{\mathbf{u}^\star}(k, x_0), \mathbf{u}^\star) \\
&= \sum_{j=0}^{N-1} \ell_1(x_{\mathbf{u}^\star}(k+j, x_0), u^\star_{x(k)}(j)) + F_1(x_{\mathbf{u}^\star}(N, x_0)) \\
&= \ell_1(x_{\mathbf{u}^\star}(k, x_0), u^\star_{x(k)}(0)) + \sum_{j=1}^{N-1} \ell_1(x_{\mathbf{u}^\star}(k+j, x_0), u^\star_{x(k)}(j)) + F_1(x_{\mathbf{u}^\star}(k+N, x_0)) \\
&= \ell_1(x_{\mathbf{u}^\star}(k, x_0), u^\star_{x(k)}(0)) + \sum_{j=0}^{N-2} \ell_1(x_{\mathbf{u}^\star}(k+1+j, x_0), u^\star_{x(k)}(j+1)) \\
&\qquad\qquad + F_1(x_{\mathbf{u}^\star}(k+N, x_0)) \\
&= \ell_1(x_{\mathbf{u}^\star}(k, x_0), u^\star_{x(k)}(0)) + J_1^{N-1}(x_{\mathbf{u}^\star}(k+1, x_0), \mathbf{u}^\star(\cdot + 1))
\end{aligned}$$

holds by a shifting index argument. □

Using the definitions and relations above, we can state the following performance estimate for the rotated stage cost $\widetilde{\ell}_1$, which we need to conclude the convergence of the closed-loop trajectory.

Lemma 5.4 (Non-averaged rotated performance for $\widetilde{J}_1$)
Consider a multiobjective optimal control problem (MO OCPt)*, let Assumption 5.1 hold, and let $x_0 \in \mathbb{X}_N$.*

Then, the inequality

$$\widetilde{J}_1^\infty(x_0, \mu^N) := \lim_{K \to \infty} \sum_{k=0}^{K-1} \widetilde{\ell}_1(x_\mu(k, x_0), \mu^N(k, x_\mu(k, x_0))) \leq \widetilde{J}_1^N(x_0, \boldsymbol{u}^\star_{x_0})$$

holds with μ^N the MPC feedback defined in Algorithm 2.

Proof. The existence of the efficient solutions in steps (0) and (1) is concluded from Assumption 5.1 (v) – the external stability of $\mathcal{J}_{\mathcal{E}}^N(x)$. Feasibility of $\mathbf{u}_{x(k+1,x_0)}$ in (2)

follows from Assumption 5.1 (iv). Recursive feasibility of $\mathbb{X}_N$, see Theorem 2.1, is an immediate consequence.

Further, for each $K \in \mathbb{N}$ it holds, with $\mathbf{u}^\star_{x(k)}$ denoting the efficient control sequence from Algorithm 2,

$$
\begin{aligned}
&\sum_{k=0}^{K-1} \widetilde{\ell}_1(x_\mu(k,x_0), \mu^N(k, x_\mu(k,x_0))) \\
&= \sum_{k=0}^{K-1} \ell_1(x_\mu(k,x_0), \mu^N(k, x_\mu(k,x_0))) - \ell_1(x^e,u^e) + \lambda_1(x_\mu(k,x_0)) - \lambda_1(x_\mu(k+1,x_0)) \\
&= \sum_{k=0}^{K-1} \Big(J_1^N(x_{\mathbf{u}^\star_{x(k)}}(k,x_0), \mathbf{u}^\star_{x(k)}) - J_1^{N-1}(x_{\mathbf{u}^\star_{x(k)}}(k+1,x_0), \mathbf{u}^\star_{x(k)}(\cdot+1)) \Big) \\
&\qquad - K\ell_1(x^e,u^e) + \lambda_1(x_0) - \lambda_1(x_\mu(K,x_0)).
\end{aligned}
$$

The first equality follows from the definition of $\widetilde{\ell}_1$, and the second equality holds with Lemma 5.3 and the definition of the feedback μ^N. Further, because of step (1) in Algorithm 2 and the strict dissipativity of ℓ_1 we can estimate

$$
\begin{aligned}
&\sum_{k=0}^{K-1} \Big(J_1^N(x_{\mathbf{u}^\star_{x(k)}}(k,x_0), \mathbf{u}^\star_{x(k)}) - J_1^{N-1}(x_{\mathbf{u}^\star_{x(k)}}(k+1,x_0), \mathbf{u}^\star_{x(k)}(\cdot+1)) \Big) \\
&\qquad\qquad -K\ell_1(x^e,u^e) + \lambda_1(x_0) - \lambda_1(x_\mu(K,x_0)) \\
\leq\ &\sum_{k=0}^{K-1} \Big(J_1^N(x_{\mathbf{u}^\star_{x(k)}}(k,x_0), \mathbf{u}^\star_{x(k)}) - J_1^N(x_{\mathbf{u}_{x(k)}}(k+1,x_0), \mathbf{u}_{x(k+1,x_0)}) + \ell_1(x^e,u^e) \Big) \\
&\qquad\qquad -K\ell_1(x^e,u^e) + \lambda_1(x_0) - \lambda_1(x_\mu(K,x_0)) \\
\leq\ & J_1^N(x_0,\mathbf{u}^\star_{x_0}) - J_1^N(x_{\mathbf{u}_{x(K)}}(K,x_0), \mathbf{u}_{x(K,x_0)}) + \lambda_1(x_0) - \lambda_1(x(K,x_0)) \\
=\ & \widetilde{J}_1^N(x_0,\mathbf{u}^\star_{x_0}) - \widetilde{J}_1^N(x_{\mathbf{u}_{x(K)}}(K,x_0), \mathbf{u}_{x(K,x_0)}) \\
\leq\ & \widetilde{J}_1^N(x_0,\mathbf{u}^\star_{x_0}).
\end{aligned}
$$

Finally, letting K tend to infinity and using that $\widetilde{\ell}_1(x,u) \geq 0$, for all $x \in \mathbb{X}$ and $u \in \mathbb{U}$ yields the statement. □

From the lemma above, we can directly conclude the convergence of the closed-loop trajectory to the considered equilibrium, which is also the key ingredient for our following analysis. Corollary 5.5 below is the main auxiliary result for showing our performance estimates.

Corollary 5.5 (Trajectory convergence)
Consider a multiobjective optimal control problem (MO OCPt)*, let Assumption 5.1 hold, and let* $x_0 \in \mathbb{X}_N$.

Then, the closed-loop trajectory $x(\cdot) = x_\mu(\cdot, x_0)$ *driven by the feedback* μ^N *from Algorithm 2 converges to the equilibrium* x^e *and the sequence* $\widetilde{\ell}_1(x(k), \mu^N(k, x(k)))$ *converges to* 0 *as* $k \to \infty$.

Proof. We follow the proof of Corollary 4.9 in [88]:
From Lemma 5.4 it follows that the sum $\sum_{k=0}^{\infty} \widetilde{\ell}_1(x(k), \mu^N(k, x(k)))$ converges and, thus, the sequence satisfies $\widetilde{\ell}_1(x(k), \mu^N(k, x(k))) \to 0$ as $k \to \infty$. Hence, since the optimal control problem with stage cost $\widetilde{\ell}_1$ is strictly dissipative and $\alpha_{\ell,1} \in \mathcal{K}_\infty$, we get

$$0 = \lim_{k\to\infty} \alpha_{\ell,1}(\|x(k) - x^e\|) = \alpha_{\ell,1}\left(\lim_{k\to\infty} \|x(k) - x^e\|\right),$$

which is equivalent to $\lim_{k\to\infty} \|x(k) - x^e\| = 0$. □

We now transfer the estimates for $\widetilde{J}_1^\infty$ to J_1^∞. For this and for the subsequent stability analysis in Section 5.2.3, we need an additional continuity assumption.

Assumption 5.6
There exist $\gamma_{F_1} \in \mathcal{K}_\infty$ *and* $\gamma_{\lambda_1} \in \mathcal{K}_\infty$ *such that the following holds.*

(i) For all $x \in \mathbb{X}_0$ *it holds that*

$$|F_1(x) - F_1(x^e)| \leq \gamma_{F_1}(\|x - x^e\|),$$

and it yields that $F_1(x^e) = 0$.

(ii) For all $x \in \mathbb{X}$ *it holds that*

$$|\lambda_1(x) - \lambda_1(x^e)| \leq \gamma_{\lambda_1}(\|x - x^e\|)$$

with λ_1 *from Assumption 5.1.*

Using part (ii) of this assumption and the results above, we can show an infinite horizon performance result on J_1 similar to the one in [54, 88].

Theorem 5.7 (Performance estimate for J_1)
Consider the multiobjective optimal control problem (MO OCPt)*. Let Assumptions 5.1 and 5.6 (ii) hold and assume* $\ell_1(x^e, u^e) = 0$.
Then, the MPC feedback $\mu^N : \mathbb{N}_0 \times \mathbb{X} \to \mathbb{U}$ *defined in Algorithm 2 renders the set* $\mathbb{X}_N$ *forward invariant and has the infinite-horizon closed-loop performance*

$$J_1^\infty(x_0, \mu^N) := \sum_{k=0}^{\infty} \ell_1(x_\mu(k, x_0), \mu^N(k, x_\mu(k, x_0))) \leq J_1^N(x_0, \boldsymbol{u}_{x_0}^\star) \tag{5.12}$$

in which $\boldsymbol{u}^\star_{x_0}$ denotes the efficient solution of step (0) in Algorithm 2.

Proof. As in the proof of Lemma 5.4, the existence of the efficient solutions in step (0) and (1) in Algorithm 2 is, again, concluded from the external stability of $\mathcal{J}^N_{\mathcal{E}}(x)$. Feasibility of $\mathbf{u}_{x(k+1,x_0)}$ in step (2) follows from Assumption 5.1 (iv). Forward invariance of $\mathbb{X}_N$ is an immediate consequence.

Using the definition of $\widetilde{\ell}_1$, the estimate from the proof of Lemma 5.4, the relation (5.9), and $\ell(x^e, u^e) = 0$, it holds that

$$\begin{aligned}
&\sum_{k=0}^{K-1} \ell_1(x_\mu(k, x_0), \mu^N(k, x_\mu(k, x_0))) \\
= \;& -\lambda_1(x_0) + \sum_{k=0}^{K-1} \widetilde{\ell}_1(x_\mu(k, x_0), \mu^N(k, x_\mu(k, x_0))) + \lambda_1(x_\mu(K, x_0)) \\
\leq \;& -\lambda_1(x_0) + \widetilde{J}^N_1(x_0, \mathbf{u}^\star_{x_0}) + \lambda_1(x_\mu(K, x_0)) \\
= \;& J^N_1(x_0, \mathbf{u}^\star_{x_0}) + \lambda_1(x_\mu(K, x_0)).
\end{aligned}$$

Now, we combine Assumption 5.6 (ii) together with the storage function λ_1 from Assumption 5.1 (ii) with $\lambda_1(x^e) = 0$ and the fact that by Corollary 5.5 we have $x_\mu(K, x_0) \to x^e$ as $K \to \infty$. This implies that $\lambda_1(x_\mu(K, x_0)) \to 0$ as $K \to \infty$ and shows the assertion. □

We argue in the aforementioned proof that we get feasibility because of the external stability. We remark that Lemma 2.33 provides conditions such that external stability can be guaranteed.

Remark 5.8
The proof of Theorem 5.7 also implies the averaged performance estimate

$$\limsup_{K\to\infty} \frac{1}{K} \sum_{k=0}^{K-1} \ell_1(x_\mu(k, x_0), \mu^N(k, x_\mu(k, x_0))) = 0.$$

In case $\ell_1(x^e, u^e) \neq 0$, this inequality holds for the shifted cost $\hat{\ell}_1(x, u) = \ell_1(x, u) - \ell_1(x^e, u^e)$ and, thus, we obtain the averaged performance estimate

$$\begin{aligned}
&\limsup_{K\to\infty} \frac{1}{K} \sum_{k=0}^{K-1} \ell_1(x_\mu(k, x_0), \mu^N(k, x_\mu(k, x_0))) \\
&\quad = \limsup_{K\to\infty} \frac{1}{K} \sum_{k=0}^{K-1} \hat{\ell}_1(x_\mu(k, x_0), \mu^N(k, x_\mu(k, x_0))) + \ell_1(x^e, u^e) \\
&\quad \leq \ell_1(x^e, u^e).
\end{aligned}$$

5.2.2 Averaged Performance Results for J_i^N

Besides the performance of J_1 we are also interested in performance estimates for J_i, $i \in \{2, \dots, s\}$. We still do not assume that the system (2.1) is strictly dissipative for the stage costs ℓ_i, $i \in \{2, \dots, s\}$. Hence, we only use the continuity and the closed-loop trajectory convergence from Corollary 5.5 to derive an averaged performance estimate. Before imposing this estimate, we establish a relation between the first stage cost ℓ_1, and the other costs ℓ_i by giving a bound on the stage cost ℓ_i employing the first rotated stage cost $\widetilde{\ell}_1$ in the next lemma.

Lemma 5.9 (Bound on ℓ_i)
For each $i = 2, \dots, s$ there is $\omega_i \in \mathcal{K}_\infty$ such that $|\ell_i(x,u) - \ell_i(x^e,u^e)| \leq \omega_i(\widetilde{\ell}_1(x,u))$.

Proof. Since ℓ_i is continuous, there is $\tilde{\omega}_i \in \mathcal{K}_\infty$ such that

$$|\ell_i(x,u) - \ell_i(x^e,u^e)| \leq \tilde{\omega}_i(\|x - x^e, u - u^e\|).$$

Since $\widetilde{\ell}_1(x,u) \geq \alpha_{\ell,1}(\|x - x^e, u - u^e\|)$, the assertion follows with $\omega_i = \tilde{\omega}_i \circ \alpha_{\ell,1}^{-1}$. □

By means of Lemma 5.9 and Corollary 5.5 we can show an averaged performance estimate for the objectives J_i, $i \in \{2, \dots, s\}$.

Theorem 5.10 (Averaged performance estimate for J_i)
Consider the multiobjective optimal control problem (MO OCPt). *Let Assumptions 5.1 and 5.6 hold.*
Then, the MPC-feedback $\mu^N : \mathbb{N}_0 \times \mathbb{X} \to \mathbb{U}$ defined in Algorithm 2 has the infinite-horizon averaged closed-loop performance

$$\bar{J}_i^\infty(x_0, \mu^N) := \limsup_{K\to\infty} \frac{1}{K} \sum_{k=0}^{K-1} \ell_i(x_\mu(k, x_0), \mu^N(k, x_\mu(k, x_0))) \leq \ell_i(x^e, u^e)$$

for all objectives $i \in \{2, \dots, s\}$ and $x_0 \in \mathbb{X}_N$.

Proof. The existence of efficient solutions and feasibility is ensured by Lemma 5.4 and Theorem 5.7. Further, from Corollary 5.5 and Lemma 5.9 it follows that there exists $M \in \mathbb{N}_0$ such that for all $k \geq M$ the relation

$$\ell_i(x_{\mathbf{u}^\star_{x(k)}}(k, x_0), \mathbf{u}^\star_{x(k)}(0)) = \ell_i(x^e, u^e) + \varepsilon(k), \quad i \in \{2, \dots, s\}$$

with $\varepsilon(k) \to 0$ as $k \to \infty$, holds. Thus, given any arbitrary $\tilde{\varepsilon} > 0$, there exists $\tilde{k} \in \mathbb{N}_0$, $\tilde{K} \geq M$, such that for $k \geq \tilde{k}$ the error term satisfies $\varepsilon(k) < \tilde{\varepsilon}$.

Then, for each fixed, but arbitrary $K \in \mathbb{N}$ with $K > \tilde{k}$

$$\begin{aligned}
&\frac{1}{K}\sum_{k=0}^{K-1} \ell_i(x_\mu(k,x_0),\mu^N(k,x_\mu(k,x_0))) \\
=&\frac{1}{K}\left(\sum_{k=0}^{\tilde{k}-1} \ell_i(x_{\mathbf{u}^\star_{x(k)}}(k,x_0),\mathbf{u}^\star_{x(k)}(0)) + \sum_{k=\tilde{k}}^{K-1} \ell_i(x_{\mathbf{u}^\star_{x(k)}}(k,x_0),\mathbf{u}^\star_{x(k)}(0))\right) \\
\leq&\frac{C}{K} + \frac{1}{K}\sum_{k=\tilde{k}}^{K-1} \ell_i(x^e,u^e) + \underbrace{\varepsilon(k)}_{\leq\tilde{\varepsilon}} \\
\leq&\frac{C}{K} + \left(1-\frac{\tilde{k}}{K}\right)\ell_i(x^e,u^e) + \left(1-\frac{\tilde{k}}{K}\right)\tilde{\varepsilon},
\end{aligned}$$

where $C := \sum_{k=0}^{\tilde{k}-1} \ell_i(x_{\mathbf{u}^\star_{x(k)}}(k,x_0),\mathbf{u}^\star_{x(k)}(0))$ is independent of K and $\mathbf{u}^\star_{x(k)}$ denotes the control from Algorithm 2. Letting $K \to \infty$, this implies

$$\bar{J}_i^\infty(x_0,\mu^N) \leq \ell_i(x^e,u^e) + \tilde{\varepsilon}$$

and since $\tilde{\varepsilon} > 0$ was arbitrary, this shows the assertion. □

We analyze the closed-loop trajectory behavior before moving on with non-averaged performance estimates for J_i^N, $i \in \{2,\dots,s\}$. In particular, in the next section, we show that the equilibrium is asymptotically stable. This stability result we will also need for our performance result.

5.2.3 Stability

In addition to the performance results, control theoretical properties are also of great interest – especially stability results. Hence, we aim to show that Algorithm 2 has a stability property. We use the strong strict dissipativity assumption on the first stage cost ℓ_1, results, and calculations from the previous sections to formulate the main theorem in this section, which adapts the classical stability result from the single-objective case, see, e.g., Theorem 8.13 in [46].

Theorem 5.11 (Asymptotic Stability)
Consider the multiobjective optimal control problem (MO OCPt)*, which we assume to be strictly dissipative for stage cost ℓ_1 at the equilibrium (x^e,u^e). Let Assumptions 5.1 (iv) and (v) and Assumptions 5.6 (i) and (ii) be satisfied. Let $\gamma_J \in \mathcal{K}_\infty$, $x_0 \in \mathbb{X}_N$, and choose the efficient solutions $\boldsymbol{u}^\star_{x_0}$ in step (0) of Algorithm 2 such that they satisfy the inequality*

$$J_1^N(x_0,\boldsymbol{u}^\star_{x_0}) \leq \gamma_J(\|x_0 - x^e\|) + N\ell_1(x^e,u^e). \tag{5.13}$$

Then, the (optimal) equilibrium x^e is asymptotically stable on $\mathbb{X}_N$ for the MPC closed-loop trajectory defined in Algorithm 2.

Proof. We follow the proof of the single-objective case [46, Theorem 8.13] and show that the modified cost functional $\widetilde{J}_1^N$ is a uniform time-varying Lyapunov function for the closed-loop system for x^e (see Definition 2.21). We conclude, using Theorem 2.22, that the equilibrium x^e is asymptotically stable.

Without loss of generality, we may assume $\ell_1(x^e, u^e) = 0$ because replacing ℓ_1 by $\ell_1 - \ell_1(x^e, u^e)$ does not change the closed-loop solutions and thus not the stability.

In order to simplify the notation, we write x instead of $x(k, x_0)$ and x^+ instead of $x(k+1, x_0)$ for the states on the MPC closed-loop solution. Then, for the control sequences defined in Algorithm 2, it holds that

$$x^+ = f(x, \mathbf{u}_x^{\star,N}(0)), \qquad x_{\mathbf{u}_{x^+}}(N, x^+) = f(x_{\mathbf{u}_{x^+}}(N-1, x^+), \kappa(x_{\mathbf{u}_{x^+}}(N-1, x^+)))$$

and

$$x_{\mathbf{u}_{x^+}(\cdot+1)}(j, x^+) = x_{\mathbf{u}_x^\star}(j+1, x) \qquad \text{for } j = 0, \dots, N-1.$$

Moreover, from Lemma 5.3 we observe the relation

$$\begin{aligned}
&\widetilde{J}_1^N(x, \mathbf{u}_x^\star) \\
&= \sum_{j=0}^{N-2} \widetilde{\ell}_1(x_{\mathbf{u}_x^\star(\cdot+1)}(j, x^+), \mathbf{u}_x^\star(j+1)) + \widetilde{\ell}_1(x, \mathbf{u}_x^\star(0)) + F_1(x_{\mathbf{u}_{x^+}(\cdot+1)}(N-1, x^+)).
\end{aligned}$$

Using these identities and inequality (5.4) it thus follows that

$$\begin{aligned}
& \widetilde{J}_1^N(x^+, \mathbf{u}_{x^+}^\star) \le \widetilde{J}_1^N(x^+, \mathbf{u}_{x^+}) \\
= \;& \sum_{j=0}^{N-1} \widetilde{\ell}_1(x_{\mathbf{u}_{x^+}}(j, x^+), \mathbf{u}_{x^+}(j)) + \widetilde{F}_1(x_{\mathbf{u}_{x^+}}(N, x^+)) \\
= \;& \sum_{j=0}^{N-2} \widetilde{\ell}_1(x_{\mathbf{u}_x^\star(\cdot+1)}(j, x^+), \mathbf{u}_x^\star(j+1)) \\
& + \; \widetilde{\ell}_1(x_{\mathbf{u}_x^\star(\cdot+1)}(N-1, x^+), \kappa(x_{\mathbf{u}_{x^+}^\star(\cdot+1)}(N-1, x^+))) + \widetilde{F}_1(x_{\mathbf{u}_{x^+}}(N, x^+)) \\
= \;& \widetilde{J}_1^N(x, \mathbf{u}_x^\star) - \widetilde{\ell}_1(x, \mathbf{u}_x^\star(0)) + \widetilde{\ell}_1(x_{\mathbf{u}_x^\star(\cdot+1)}(N-1, x^+), \kappa(x_{\mathbf{u}_{x^+}^\star(\cdot+1)}(N-1, x^+))) \\
& + \; \widetilde{F}_1(x_{\mathbf{u}_{x^+}}(N, x^+)) - \widetilde{F}_1(x_{\mathbf{u}_{x^+}^\star(\cdot+1)}(N-1, x^+)) \\
\le \;& \widetilde{J}_1^N(x, \mathbf{u}_x^\star) - \widetilde{\ell}_1(x, u_x^\star(0)).
\end{aligned}$$

In the last step, we used inequality (5.10) with $x = x_{\mathbf{u}_{x^+}^\star(\cdot+1)}(N-1, x^+)$ and $\ell(x^e, u^e) = 0$. We will now check that $V(k, x) := \widetilde{J}_1^N(x, \mathbf{u}_x^\star)$, with $\mathbf{u}_x^\star$ denoting

the control from the k-th step of the MPC algorithm, is a uniform time-varying Lyapunov function according to Definition 2.21 for $f(x, \mu^N(k,x))$. To do this, we show the existence of $\alpha_1, \alpha_2, \alpha_3 \in \mathcal{K}_\infty$, such that the inequalities

(i) $\alpha_1(\|x_0 - x^e\|) \leq \widetilde{J}_1^N(x_0, \mathbf{u}^\star_{x_0}) \leq \alpha_2(\|x_0 - x^e\|)$

(ii) $\widetilde{\ell}_1(x,u) \geq \alpha_3(\|x - x^e\|)$

hold for all $x \in \mathbb{X}$ and $x_0 \in \mathbb{X}_N$. Condition (ii) is satisfied by our strict dissipativity assumption with $\alpha_3 = \alpha_{\ell,1}$. For the inequalities in condition (i), we first need to establish a lower bound for $\widetilde{F}_1$. We recall Assumption 5.1 (iv) with local feedback κ for each $x \in \mathbb{X}_0$ as well as $\alpha_{\ell,1}$ from Assumption 5.1 (ii) is a lower bound on $\widetilde{F}_1$

$$\widetilde{F}_1(f(x,\kappa(x))) \leq \widetilde{F}_1(x) - \widetilde{\ell}_1(x,\kappa(x)) \leq \widetilde{F}_1(x) - \alpha_{\ell,1}(\|x - x^e\|),$$

see inequality (5.10), which is independent of the choice of the control as long as the assumption is fulfilled. By induction along the closed-loop solution for the local feedback κ, we then obtain

$$\widetilde{F}_1(x_\kappa(K,x)) \leq \widetilde{F}_1(x) - \sum_{k=0}^{K-1} \alpha_{\ell,1}(\|x_\kappa(k,x) - x^e\|).$$

By Assumptions 5.6 (i) and (ii) and Corollary 5.5 this implies

$$\widetilde{F}_1(x_\kappa(K,x)) \to \widetilde{F}(x^e) = 0 \quad \text{as} \quad K \to \infty$$

from which, we can conclude

$$\widetilde{F}_1(x) \geq \lim_{K\to\infty} \sum_{k=0}^{K-1} \alpha_{\ell,1}(\|x_\kappa(k,x) - x^e\|) \geq \alpha_{\ell,1}(\|x - x^e\|) \geq 0.$$

From this, the definition of $\widetilde{J}_1^N$ immediately implies

$$\widetilde{J}_1^N(x_0, \mathbf{u}^\star_{x_0}) \geq \widetilde{\ell}_1(x_0, \mu^N) \geq \alpha_{\ell,1}(\|x_0 - x^e\|)$$

and thus the inequality for α_1 with $\alpha_1 = \alpha_{\ell,1}$.

Finally, since $\widetilde{J}_1^N(x^e, u^e) = 0$ and due to Assumption 5.6 (ii), the (in)equalities (5.13) and (5.9), and $\ell(x^e, u^e) = 0$ it follows that $\alpha_2 = \gamma_{\lambda_1} + \gamma_{J_1^N}$. □

Note that stabilizing stage costs are a special case of strictly dissipative stage costs with $\lambda \equiv 0$. Further, observe that in this case, we obtain $\lambda_1 \equiv 0$ and $\ell_1(x^e, u^e) = 0$, and thus $\widetilde{J}_1^N = J_1^N$. This implies that the objective function itself is a Lyapunov function.

Remark 5.12

(i) It is a priori unclear if inequality (5.13) *is fulfillable. We consider near-optimal trajectories in a multiobjective sense and bound their generated first cost function by a $\mathcal{K}_\infty$-function. Further, we consider a terminal cost satisfying Assumption 5.1 (iv). Hence, to guarantee inequality* (5.13)*, we can use the techniques used, e.g., in [46, Proposition 5.14] or [81, Propositions 2.15 or 2.16] for single-objective MPC.*

(ii) If inequality (5.13) *can be satisfied, then it will reduce the degree of freedom in choosing the efficient point in step (0) of Algorithm 2. In particular, enforcing* (5.13) *will typically require putting more emphasis on the cost J_1^N at the expense that the performance of J_i^N for $i \in \{2, \dots, s\}$ may deteriorate.*

(iii) Even though condition (5.13) *can be very restrictive, this inequality is essential to establish an upper bound on the time-varying Lyapunov function $\widetilde{J}_1^N$.*

5.2.4 A Non-averaged Performance Result for J_i^N

In order to derive non-averaged performance estimates for all objectives J_i^N, $i \in \{2, \dots, s\}$, we now use the stability of the closed-loop trajectory and combine it with the idea of obtaining performance estimates for single-objective economic MPC without terminal conditions, see [46]. To this end, we consider the trajectories x driven by the first efficient solution $\mathbf{u}_{x_0}^\star$. We denote these trajectories by $x^\star(\cdot) = x_{\mathbf{u}_{x_0}^\star}(\cdot, x_0)$ and name them efficient trajectories.

First, we show that the endpoints of the efficient trajectories are close to the equilibrium by using the strict dissipativity of the first stage cost ℓ_1. In doing this, we recall that $\alpha_{\ell,1}$ from Assumption 5.1 is a lower bound on the rotated terminal cost $\widetilde{F}_1$, as shown in the proof of Theorem 5.11.

Lemma 5.13
Let Assumptions 5.1 and 5.6 hold, $x_0 \in \mathbb{X}_N$, and consider efficient trajectories $x^\star(j) = x_{\boldsymbol{u}_{x_0}^\star}(j, x_0)$, $j = 0, \dots, N$, for which there is $\gamma_J \in \mathcal{K}_\infty$ such that

$$J_1^{N-j}(x^\star(j), \boldsymbol{u}_{x_0}^\star(j+\cdot)) - (N-j)\ell_1(x^e, u^e) \leq \gamma_J(\|x^\star(j) - x^e\|) \qquad \text{for all } j = 0, \dots, N. \tag{5.14}$$

Then, there are $\rho_1, \rho_2 \in \mathcal{K}_\infty$ such that for all $N \in \mathbb{N}$ the final points on the trajectories satisfy

$$\|x^\star(N) - x^e\| \leq \rho_1(\rho_2(\|x_0 - x^e\|)/N).$$

Proof. From inequality (5.14) and the relation between the first objective and the first rotated objective (5.9) we obtain that

$$\widetilde{J}_1^N(x^\star(j), \mathbf{u}^\star_{x_0}(j+\cdot)) \leq \gamma_J(\|x^\star(j) - x^e\|) + \gamma_{\lambda_1}(\|x^\star(j) - x^e\|) =: \rho_2(\|x^\star(j) - x^e\|)$$

with γ_{λ_1} from Assumption 5.6 and $\lambda(x^e) = 0$. Using this inequality for $j = 0$ implies that there exists a time index $j_0 \in \{0, \dots, N\}$ such that

$$\begin{cases} \widetilde{\ell}_1(x^\star(j_0), \mathbf{u}^\star_{x_0}(j_0)) \leq \rho_2(\|x^\star(j_0) - x^e\|)/N, & \text{if } j_0 < N, \\ \widetilde{F}_1(x^\star(N)) \leq \rho_2(\|x^\star(j_0) - x^e\|)/N, & \text{if } j_0 = N. \end{cases}$$

If $j_0 < N$, then using the lower bound from the dissipativity $\alpha_{\ell,1}$ on $\widetilde{\ell}_1$ and, again, from the inequality above it follows that

$$\widetilde{F}_1(x^\star(N)) \leq \widetilde{J}_1^{N-j_0}(x^\star(j_0), \mathbf{u}^\star_{x_0}(j_0+\cdot)) \leq \rho_2\left(\alpha_{\ell,1}^{-1}(\rho_2(\|x^\star(j_0) - x^e\|)/N)\right).$$

Since, $\alpha_{\ell,1}$ is also a lower bound on $\widetilde{F}_1$, see equation (5.10), we obtain

$$\|x^\star(N) - x^e\| \leq \max\{\alpha_{\ell,1}^{-1}(\rho_2(\|x^\star(j_0) - x^e\|)/N), \alpha_{\ell,1}^{-1} \circ \rho_2 \circ \alpha_{\ell,1}^{-1}(\rho_2(\|x^\star(j_0) - x^e\|)/N)\}.$$

This implies the assertion with $\rho_1(r) = \max\{\alpha_{\ell,1}^{-1}(r), \alpha_{\ell,1}^{-1} \circ \rho_2 \circ \alpha_{\ell,1}^{-1}(r)\}$. □

Next, to establish a performance estimate on J_i, for all $i = 2, \dots, s$, we need the decay condition (5.4) in Algorithm 2 for all $i = 1, \dots, s$. Hence, we consider Algorithm 3 for the following performance analysis. We like to stress that we are still not requiring additional properties of the stage cost ℓ_i for $i \geq 2$. By exploiting that the feedback from Assumption 5.1(iv) steers a state x to the equilibrium x^e, we can avoid additional conditions on the stage costs ℓ_i for $i \geq 2$.

Assumption 5.14
For each $i = 2, \dots, s$ there is $\gamma_i \in \mathcal{K}_\infty$ such that

$$\ell_i(x, \kappa(x)) \leq \ell_i(x^e, u^e) + \gamma_i(\|x - x^e\|)$$

holds for all $x \in \mathbb{X}_0$ and κ from Assumption 5.1(iv).

Finally, we provide performance estimates for all objectives J_i, $i \in \{2, \dots, s\}$. For this, we use the previous results and assumptions and adapt the single-objective case from which we have been inspired. The following estimate is structurally similar to estimates for the closed-loop performance of single-objective economic MPC without terminal conditions, see, e.g., [46, Theorem 8.39].

Theorem 5.15 (Performance estimate for J_i)
Let Assumptions 5.1, 5.6, and 5.14 hold and assume that the efficient solutions generated by Algorithm 3 with μ^N satisfy the inequalities (5.14) *for some $\gamma_J \in \mathcal{K}_\infty$. Then, for all $i = 2, \dots, s$ and for any $C > 0$ there is a function $\delta_i \in \mathcal{L}$ such that*

$$J_i^K(x_0, \mu^N) \leq J_i^N(x_0, \boldsymbol{u}_{x_0}^\star) + (K-N)\ell_i(x^e, u^e) + K\delta_i(N) \tag{5.15}$$

for all $N, K \in \mathbb{N}$ with $K \geq N$ and all $x_0 \in \mathbb{X}_N$ with $\|x_0 - x^e\| \leq C$.

Proof. Consider the control sequences $\mathbf{u}_{x(k)}^\star$ and

$$\mathbf{u}_{x(k+1)} = (u_{x(k)}^\star(1), \dots, u_{x(k)}^\star(N-1), \kappa(x))$$

from Algorithm 3, where $x(k)$ denotes the closed-loop solution generated by the algorithm for $k \in \mathbb{N}$. Then, Lemma 5.13 and Assumption 5.14 imply

$$\begin{aligned}
&J_i^N(x(k+1), \mathbf{u}_{x(k+1)}) \\
&= J_i^N(x(k), \mathbf{u}_{x(k)}^\star) - \ell_i(x(k), u_{x(k)}^\star(0)) + \ell_i(x(k+N), \kappa(x(N))) \\
&\leq J_i^N(x(k), \mathbf{u}_{x(k)}^\star) - \ell_i(x(k), u_{x(k)}^\star(0)) + \ell_i(x^e, u^e) + \gamma_i(\|x(N) - x^e\|) \\
&\leq J_i^N(x(k), \mathbf{u}_{x(k)}^\star) - \ell_i(x(k), \mu^N(k, x(k))) + \ell_i(x^e, u^e) + \gamma_i(\rho_1(\rho_2(\widetilde{C})/N)).
\end{aligned}$$

Here, we used that the asymptotic stability property of the closed-loop trajectory from Theorem 5.11 implies that whenever the initial value is close enough to the equilibrium, it satisfies $\|x_0 - x^e\| \leq C$, then there is $\widetilde{C} > 0$ such that $\|x(k) - x^e\| \leq \widetilde{C}$ for all $k \in \mathbb{N}$. This inequality together with inequalities (5.5) for $i = 2, \dots, s$ implies

$$\begin{aligned}
&J_i^K(x_0, \mu^N) = \sum_{k=0}^{K-1} \ell_i(x(k), \mu^N(k, x(k))) \\
\leq\ & \sum_{k=0}^{K-1} \Big(J_i^N(x(k), \mathbf{u}_{x(k)}^\star) - J_i^N(x(k+1), \mathbf{u}_{x(k+1)}) + \ell_i(x^e, u^e) + \gamma_i(\rho_1(\rho_2(\widetilde{C})/N)) \Big) \\
\leq\ & \sum_{k=0}^{K-1} \Big(J_i^N(x(k), \mathbf{u}_{x(k)}^\star) - J_i^N(x(k+1), \mathbf{u}_{x(k+1)}^\star) + \ell_i(x^e, u^e) + \gamma_i(\rho_1(\rho_2(\widetilde{C})/N)) \Big) \\
=\ & J_i^N(x_0, \mathbf{u}_{x_0}^\star) - J_i^N(x(K), \mathbf{u}_{x(K)}^\star) + K\ell_i(x^e, u^e) + K\gamma_i(\rho_1(\rho_2(\widetilde{C})/N)).
\end{aligned}$$

Now, again, the asymptotic stability and the boundedness of $\|x_0 - x^e\|$ imply the existence of a function $\chi \in \mathcal{L}$ such that $\|x(k) - x^e\| \leq \chi(k)$. From this, together with relation (5.9) and inequality (5.14), we can conclude that $\widetilde{J}_1^N(x(k), \mathbf{u}_{x(k)}^\star) \leq \gamma_J(\chi(k))$ and the individual (nonnegative) terms of this sum also satisfy

$$\widetilde{\ell}_1(x_{\mathbf{u}_{x(k)}^\star}(j, x(k)), \mathbf{u}_{x(k)}^\star(j)) \leq \gamma_J(\chi(k)) \quad \text{for all } j = 0, \dots, N-1.$$

By Lemma 5.9 this yields

$$\ell_i(x_{\mathbf{u}^\star_{x(k)}}(j, x(k)), \mathbf{u}^\star_{x(k)}(j)) \geq \ell_i(x^e, u^e) - \omega_i(\gamma_J(\chi(k))),$$

and we can estimate that

$$J_i^N(x(K), \mathbf{u}^\star_{x(K)}) \geq N\ell_i(x^e, u^e) - N\omega_i(\gamma_J(\chi(K))) \geq N\ell_i(x^e, u^e) - K\omega_i(\gamma_J(\chi(N))),$$

where we used $K \geq N$ and the monotonicity of $\chi \in \mathcal{L}$ in the last step. This yields the assertion with

$$\delta_i(N) = \rho_1(\rho_2(\widetilde{C})/N) + \omega_i(\gamma_J(\chi(N))).$$

□

Again, the upper bounds for all objectives J_i, $i \in \{2, \ldots, s\}$, in inequality (5.15) mainly depend on the first chosen efficient solution $\mathbf{u}^\star_{x_0}$. The following remark discusses why these estimates are useful even though the upper bounds depend on K.

Remark 5.16
The fact that the error term $K\delta(N)$ grows linearly with K might make the estimate useless at first glance. However, unless we are in the exceptional case that $\ell_i(x^e, u^e) = 0$, the term $J_i^N(x_0, \mathbf{u}^\star_{x_0}) + (K - N)\ell_i(x^e, u^e)$ also grows affine linearly with K. Hence, for all sufficiently large K, the relative error is proportional to $\delta(N)$ and thus decreases to 0 as $N \to \infty$. Hence, in terms of the relative error, the estimate gives a highly useful estimate.

We can observe the desired behavior in numerical examples, especially in Figure 5.13. However, finding appropriate $\mathcal{L}$–functions depending on the horizon N is not easy and obvious, see Example 5.18 and the discussion therein.

5.3 Illustrative Examples

We conclude this chapter with an application example to illustrate the theoretical results of the previous sections. Therefore, we introduce the example of an isothermal continuous stirred-tank reactor, see [95,96]. We begin our consideration by introducing the example with only two cost criteria to explain the results as simply as possible. Then, we add a third objective to emphasize that our algorithms and theory are not limited to the bi-objective case. In the remainder of this section, we distinguish between the efficient solutions chosen in the different steps of Algorithm 2 and 3. We use the following denominations for the efficient solutions in the algorithms:

- The efficient solution $\mathbf{u}^\star_{x_0}$ chosen in step (0), i.e., in the first step, we call *the first efficient solution.*

- The efficient solutions $\mathbf{u}^\star_{x(k)}$ chosen in step (1), i.e., from time step $k = 2$ onwards, we name *the subsequent efficient solutions.*

Further, since the performance estimates only depend on the first efficient solution, we always choose the subsequent efficient solutions in the same way by using the global criterion method. This method is also known as the compromise programming approach, see, for instance, [71], to find efficient solutions of the multiobjective optimization problems in the subsequent iterations as proposed in a multiobjective MPC context in [95, 96]. More precisely, the subsequent efficient solution $\mathbf{u}^\star_{x(k)}$ is chosen in each iteration such that

$$\mathbf{u}^\star_{x(k)} \in \arg\min \left\{ \left(\sum_{i=1}^{s} |J_i^N(x(k), \mathbf{u}) - z_i^\star|^2 \right)^{\frac{1}{2}} \,\middle|\, \mathbf{u} \in \mathbb{U}^N(x_0), \right. \\ \left. J_1^N(x(k), \mathbf{u}^\star_{x(k)}) \leq J_1^N(x(k), \mathbf{u}_{x(k)}) \right\}, \quad (5.16)$$

where

$$z_i^\star = \min \left\{ J_i^N(x(k), \mathbf{u}) \,\middle|\, \mathbf{u} \in \mathbb{U}^N(x_0),\ J_1^N(x(k), \mathbf{u}^\star_{x(k)}) \leq J_1^N(x(k), \mathbf{u}_{x(k)}) \right\},$$

for all $i = 1, \ldots, s$, is set as the so-called ideal point of the restricted problem, cf. [96]; i.e., $\mathbf{u}^\star_{x(k)}$ is defined as the pre-image of the nondominated point that has the smallest Euclidean distance to the ideal point. Whenever applying Algorithm 3 instead of Algorithm 2, then $J_1^N(x(k), \mathbf{u}^\star_{x(k)}) \leq J_1^N(x(k), \mathbf{u}_{x(k)})$ is replaced by $J_i^N(x(k), \mathbf{u}^\star_{x(k)}) \leq J_i^N(x(k), \mathbf{u}_{x(k)})$ for all $i = 1, \ldots, s$ in the above optimization problems.

Moreover, here, we only discuss the numerical results in view of the theoretical results. For implementation details such as used algorithms for solving multiobjective optimization problems, we refer to Section 6.4.

The following example is based on the examples in [19, 95].

Example 5.17 (Reactor Part 1)
We consider a single first-order, irreversible chemical reaction in an isothermal continuous stirred-tank reactor (CSTR). The material balances and the system data are provided in [19] and given in discrete time by

$$\begin{aligned} c_A(k+1) &= c_A(k) + \frac{1}{2}\left(\frac{u(k)}{V}(c_{A_f} - c_A(k)) - k_r c_A(k) \right), \\ c_B(k+1) &= c_B(k) + \frac{1}{2}\left(\frac{u(k)}{V}(c_{B_f} - c_B(k)) + k_r c_B(k) \right), \\ c(0) &= c_0 = (0.4, 0.2), \end{aligned}$$

where $c_A(k) \geq 0$ and $c_B(k) \geq 0$, $k \in \mathbb{N}$, describe the molar concentrations, of A and B respectively, the control $0 \leq u(k) \leq 20$(L/min) is the flow through the reactor at time k, and $k_r = 1.2$ is the rate constant. The feed concentrations of A and B are given by $c_{A_f} = 1$ mol/L, and $c_{B_f} = 0$ mol/L respectively. The volume of the reactor is given by $V = 10$ L. Solving the equation $(c_A^e, c_B^e) = f(c_A^e, c_B^e, u^e)$ delivers the equilibrium under consideration $(c_A^e, c_B^e, u^e) = (\frac{1}{2}, \frac{1}{2}, 12)$. Further, the stage costs – a tracking type cost forcing the solutions to a desired equilibrium and an economic stage cost maximizing the yield (by minimizing the negative yield) of the reaction – are introduced in [95]. We abbreviate the states by $c = (c_A, c_B)$, and we consider two stage costs given by

$$\begin{aligned}\ell_1(c,u) &= \frac{1}{2}(c_A - \frac{1}{2})^2 + \frac{1}{2}(c_B - \frac{1}{2})^2 + \frac{1}{2}(u-12)^2,\\ \ell_2(c,u) &= -2uc_B + \frac{1}{2}u,\end{aligned}$$

where the second stage cost consists of the price of B and a separation cost. These second costs, therefore, represent the (negative) economic yield of the reaction. Moreover, we set the terminal cost to zero, i.e., $F_i \equiv 0$ for $i = 1, 2$ and the terminal constraint set as the equilibrium point, i.e., $\mathbb{X}_0 = \{(c^e, u^e)\}$. Thus, the overall bi-objective optimal control problem is given by

$$\begin{aligned}\min_{\boldsymbol{u}\in\mathbb{U}^N(c_0)} J^N(c_0,\boldsymbol{u}) &= \left(\sum_{k=0}^{N-1}\ell_1(c(k,c_0),u(k)), \sum_{k=0}^{N-1}\ell_2(c(k,c_0),u(k))\right),\\ s.t.\quad c_A(k+1) &= c_A(k) + \frac{1}{2}\left(\frac{u(k)}{V}(c_{A_f} - c_A(k)) - k_r c_A(k)\right),\\ c_B(k+1) &= c_B(k) + \frac{1}{2}\left(\frac{u(k)}{V}(c_{B_f} - c_B(k)) + k_r c_B(k)\right),\\ c(0) &= c_0 = (0.4, 0.2)\\ c(N,c_0) &\in \mathbb{X}_0 = \{(c^e,u^e)\}\\ \mathbb{X} &= [0,20]\times[0,20], \quad \mathbb{U} = [0,20].\end{aligned} \tag{5.17}$$

This way, Assumption 5.1 is fulfilled since stabilizing stage costs always render the optimal control problem strictly dissipative, and by setting $\kappa = u^e$, there exists a local feedback with the desired properties. Since the terminal cost and the storage function, due to stabilizing stage cost, are equal to zero, Assumption 5.6 is also satisfied. By imposing box constraints $\mathbb{X}$ and $\mathbb{U}$ we can conclude by Lemma 2.33 the external stability of $\mathcal{J}_{\mathcal{E}}^N(c_0)$ and, thus, the trajectory convergence as well as the averaged and non-averaged performance of the first cost criterion J_1 by Corollary 5.5 and Theorem 5.7.

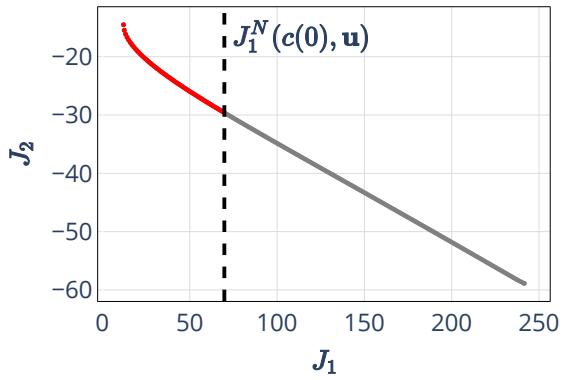

Figure 5.3: Visualization of the nondominated set in step (1)

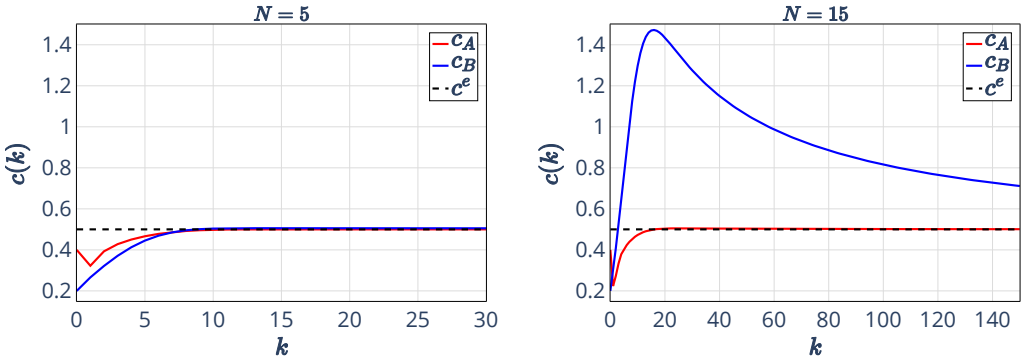

Figure 5.4: Closed-loop trajectory for $N = 5$ (left) and $N = 15$ (right)

In this example, we use

- *Algorithm 2 to substantiate our theoretical results with numerical simulations. Thus, we restrict only the first objective by the constraint in step (1) of the algorithm. The resulting bound on the nondominated set in the second iteration is visualized in Figure 5.3;*

- *as the first efficient solution the efficient solution for* $N = 5$ *with* $J^5(x_0, \mathbf{u}^\star_{c_0}) = (54.034, 9.500)$*, and with* $J^{15}(c_0, \mathbf{u}^\star_{c_0}) = (408.459, -478.459)$ *for* $N = 15$*;*

We note that, for this example, the optimization problems contained as subproblems in MOMPC algorithms are non-convex. Hence, we have no theoretical guarantees that the numerical optimization reached a globally optimal solution. However, the

numerical results strongly suggest that globally optimal solutions were found in all our numerical simulations.

The behavior of the closed-loop trajectory is visualized in Figure 5.4 for MPC-horizons $N = 5$ and $N = 15$. We observe that the trajectories converge to the equilibrium c^e independently of the choice of MPC-horizon and the initial value. Despite this, the MPC-horizon N influences the convergence rate. On the left side, for $N = 5$, the c_B-trajectory converges faster to the equilibrium point $c^e = \frac{1}{2}$ than for $N = 15$. We remark that this is a typical behavior of MPC with equilibrium terminal constraints, see [46, Discussion after Ex. 7.23]. In addition, the components of the trajectory show different transient behavior.

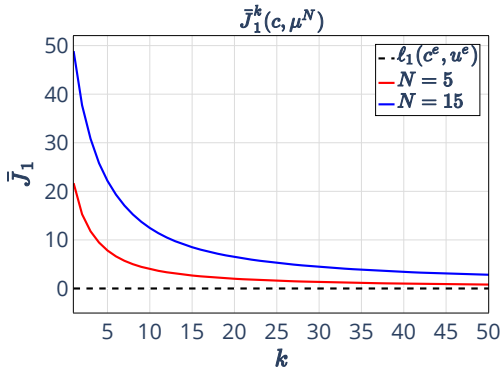

Figure 5.5: $\bar{J}_1^k$ for $N = 5$ and $N = 15$

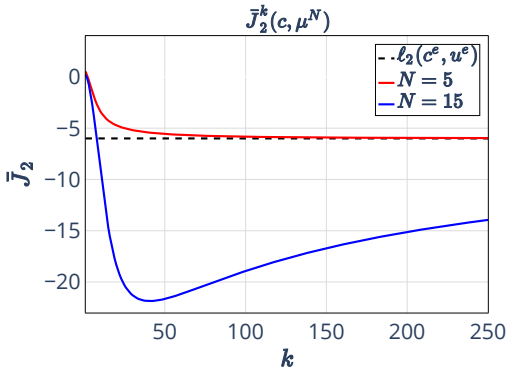

Figure 5.6: $\bar{J}_2^k$ for $N = 5$ and $N = 15$

In contrast, the bound of the averaged performance of J_1 is independent of N, the initial value, and the choice of the efficient solutions in each iteration. According to Remark 5.8 the bound is given by $\ell_1(c^e, u^e) = 0$. This bound and the averaged costs $\bar{J}_1^k$ in dependence of the time step k are visualized in Figure 5.5 for MPC-horizons $N = 5$ and $N = 15$. Additionally, the averaged cost of the cost criterion J_2 is visualized in Figure 5.6 with bound $\ell_2(c^e, u^e) = -6$, according to Theorem 5.10, for MPC-horizon $N = 5$ and $N = 15$. For both cost criteria, the averaged cost $\bar{J}_i^k$, $i = 1, 2$, converges for $k \to \infty$, whereas for $N = 5$, the convergence is significantly faster. Moreover, the second averaged cost $\bar{J}_2^k$ requires considerably more time to converge, highlighting the conflict between the two cost criteria.

Since the upper bound on $J_1^\infty(c_0, \mu^N)$ from Theorem 5.7 depends on the first efficient solution $\boldsymbol{u}_{c_0}^\star$ in Algorithm 2, we have visualized the performance result for different choices of this efficient solution. In Figure 5.7 on the left side, the first nondominated set $\mathcal{J}_\mathcal{E}^N(c_0)$ is shown with the different choices of the first efficient

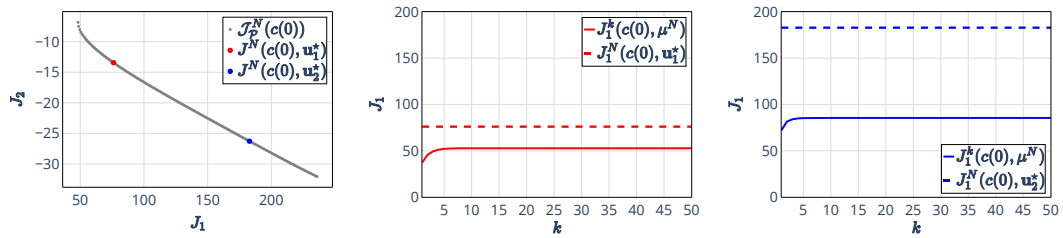

Figure 5.7: Choice of the efficient solution and the corresponding costs J_1

solution. The red point corresponds to the efficient solution such that $J^5(c_0, \boldsymbol{u}_{c_0}^\star) = (76.064, -13.435)$ *and the blue point corresponds to* $J^5(c_0, \boldsymbol{u}_{c_0}^\star) = (182.852, -26.267)$. *Further, the performance of the first cost criterion* J_1 *for* $N = 5$ *is visualized in dependence of the time step* k *and the choice of the first efficient solution (the red line corresponds to the red efficient solution and the blue line respectively to the blue one). The dashed lines mark the upper bounds derived by the values of the first objective function for the chosen first efficient solution* $J_1^N(c_0, \boldsymbol{u}_{c_0}^\star)$. *Hence, we remark that the choice of the first efficient solution has a big impact on the upper bound and on the performance of* J_1. *We remark that the upper bound is not tight for these choices of the first efficient solution.*

By choosing the efficient solution $\boldsymbol{u}_1^\star$ *(red point), which has a relatively small value in the first cost functional, we get an upper bound of about* 76. *In contrast, the efficient solution* $\boldsymbol{u}_2^\star$ *(blue point) with a small value in the second cost delivers an upper bound of approximately* 182. *Moreover, we observe that for both efficient solutions, the values of the cost functional* J_1 *reach a small neighborhood of their stationary values 53 (red) and 86 (blue), respectively, after less than 10 time steps. Additionally, the theoretical upper bound, which depends on the choice of the first efficient solution and is visualized as a dashed line, is adhered to as expected. Thus, we can confirm the dependence of the performance of* J_1 *on the choice of the first efficient solution.*

The last result shown for Algorithm 2 is the asymptotic stability property of the equilibrium (c^e, u^e). *In contrast to the convergence, the condition for stability depends on the initial value. For this reason, we have to ensure that inequality* (5.13) *is verified for the initial value* $c(0) = c_0 = (c_A(0), c_B(0))$ *and the corresponding first efficient solution* $\boldsymbol{u}_{c_0}^\star$. *With a suitable choice of the first efficient solution, we can ensure the existence of* $\gamma_J \in \mathcal{K}_\infty$ *such that inequality* (5.13) *holds, since* $\ell_1(c, u)$ *is a quadratic function, and the system is exponentially controllable to* c^e.

In Figure 5.8, the Euclidean norm $\|c(k) - c^e\|_2$ *of the closed-loop trajectory is visualized for fixed MPC-horizon* $N = 15$ *in dependence of the time step* k *and for different initial values* $c(0)$. *There, we observe that the closer the initial value is to the equilibrium, the smaller the peak of the norm of the trajectory. The numerical*

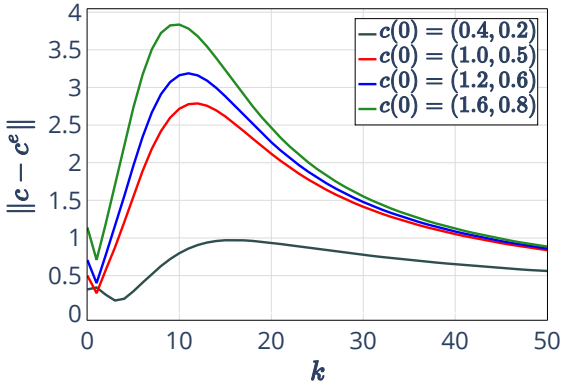

Figure 5.8: $\|c(k) - c^e\|_2$ for different initial values $c(0)$

results indicate that the stability result from Theorem 5.11 holds for this example.

After illustrating results for Algorithm 2, we move on with the reactor example, but now we consider Algorithm 3 and check the stronger assumptions that we will need to apply Theorem 5.15.

Example 5.18 (Reactor Part 2)
We consider again the isothermal reactor described in Example 5.17 with the same constants and constraints. Now, we like to illustrate the performance result for the second cost criterion J_2. Therefore, we consider Algorithm 3 where inequality (5.5) *holds for all cost criteria. Since we have imposed the special case of an endpoint constraint $\mathbb{X}_0 = \{(c^e, u^e)\}$ the endpoint is fixed by $c(N) = (c_A(N), c_B(N)) = (c_A^e, c_B^e)$ and Assumption 5.14 is trivially satisfied for $\kappa = u^e$. Thus, we can conclude the existence of $\delta \in \mathcal{L}$ for which the performance estimate on J_2 according to Theorem 5.15 holds.*

For $N = 5$, numerical test show that for $\delta(5) = 1/5$ the inequality

$$J_2^k(c(0), \mu^5) \leq J_2^N(c(0), \boldsymbol{u}^\star_{c(0)}) + (k-5)\ell_2(c^e, u^e) + \frac{k}{5} =: \mathcal{M}(\boldsymbol{u}^\star_{c_0}, 5, k)$$

holds for $k \geq 5$ large enough. The second cost J_2 and the corresponding bound $\mathcal{M}(\boldsymbol{u}^\star_{c_0}, 5, k)$ are visualized in Figure 5.9. For other MPC-horizons N and other choices of the first efficient solution, finding appropriate values for the $\mathcal{L}-$function δ is not easy. For this reason, we only visualize the bound $\mathcal{M}$ for this special case in Figure 5.9.

In Figure 5.10, the performance of the cost criterion J_2 is visualized for MPC-horizon $N = 5$ and for two different choices of the first efficient solution $\boldsymbol{u}^{\star,N}_{c(0)}$. The

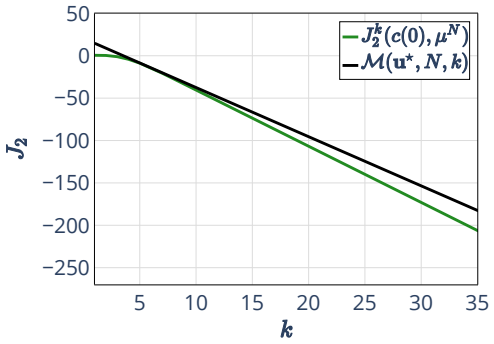

Figure 5.9: $J_2^k(c(0),\mu^N)$ with corresponding bound $\mathcal{M}(\mathbf{u}^\star_{c_0},5,k)$

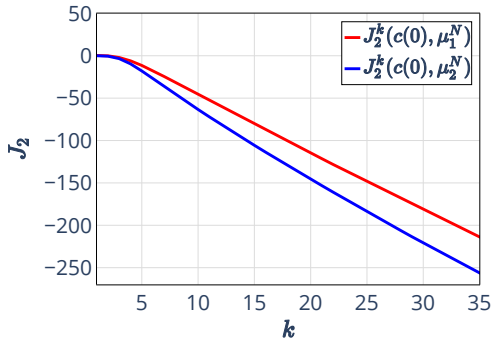

Figure 5.10: $J_2^k(c(0),\mu^N)$ for two different efficient solutions

first efficient solutions are chosen as in Example 5.17 in Figure 5.7 on the left side. Note that the first nondominated set $\mathcal{J}_{\mathcal{E}}^N(c(0))$ is identical for both algorithms. Thus, the efficient solution (and the colors) are the same as in the previous simulations. Again, we remark that the choice of the first efficient solution impacts the performance of the second cost criterion J_2.

With these two examples above, we have substantiated the theoretical results from Section 5.2 using numerical simulations for the isothermal reactor with two cost functions. Now, we turn to illustrate that – as the theoretical results suggest – our approach works for more than two cost criteria. In particular, we would like to emphasize that our theoretical results also apply to a general number of objectives. To this end, we add another cost criterion to the multiobjective optimal control problem (5.17) and present the numerical results in the same manner as in Example 5.17 and 5.18.

Example 5.19 (Reactor with three objectives)
We consider the isothermal reactor from Example 5.17 and the corresponding multiobjective optimal control problem (5.17)*. In order to extend the example, we add a third cost criterion, which aims to minimize the energy effort. Hence, the third cost function is given by*

$$J_3^N(c_0,\boldsymbol{u}) := \sum_{k=0}^{N-1} \ell_3(c(k,c_0),u(k)),\ \textit{with}\ \ell_3(c,u)=u^2,$$

and we now minimize $J^N(c_0,\boldsymbol{u}) = (J_1^N(c_0,\boldsymbol{u}), J_2^N(c_0,\boldsymbol{u}), J_3^N(c_0,\boldsymbol{u}))$.

Stage cost ℓ_3 is a continuous function; thus, Assumption 5.1 is satisfied. Assumptions 5.6 and 5.14 can be shown exactly as in Example 5.17 and 5.18. For

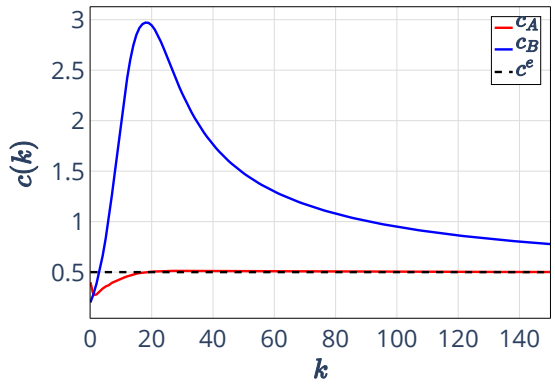

Figure 5.11: Closed-loop trajectory of Example 5.19

our numerical simulations, we consider the MPC-horizon $N = 15$. *As in Example 5.18, we apply Algorithm 3 to illustrate the trajectory convergence, the averaged performance of all cost criteria* J_i, $i = 1, 2, 3$, *and, especially, the non-averaged performance of* J_i *for all* $i \in \{1, 2, 3\}$. *Further, we chose the first efficient solution such that* $J^{15}(c_0, \boldsymbol{u}^\star_{c_0}) = (317.827, -380.092, 1969.311)$.

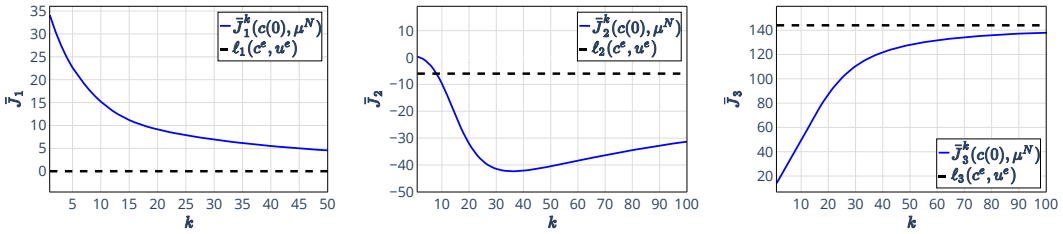

(a) $\bar{J}_1^k(c_0, \mu^N)$ (b) $\bar{J}_2^k(c_0, \mu^N)$ (c) $\bar{J}_3^k(c_0, \mu^N)$

Figure 5.12: Averaged performance of all cost criteria J_i

In Figure 5.11, we observe that the closed-loop trajectory behaves qualitatively as in Figure 5.4, but quantitatively there are differences. Significantly, the peak of the second component c_B *is higher than in Example 5.17. Further, the averaged cost* $\bar{J}_1$ *has a smaller start value, and the amplitude of the second averaged cost* $\bar{J}_2$ *is larger than in the previous example. These phenomena are visualized in Figure 5.12. On the right-hand side in Figure 5.12, the third averaged cost* $\bar{J}_3$ *also converges from below to the theoretical bound* $\ell_3(x^e, u^e) = 144$, *as stated in Theorem 5.10.*

Further, in Figure 5.13 the performances of J_i, $i = 1, 2, 3$, *are shown. Again, the*

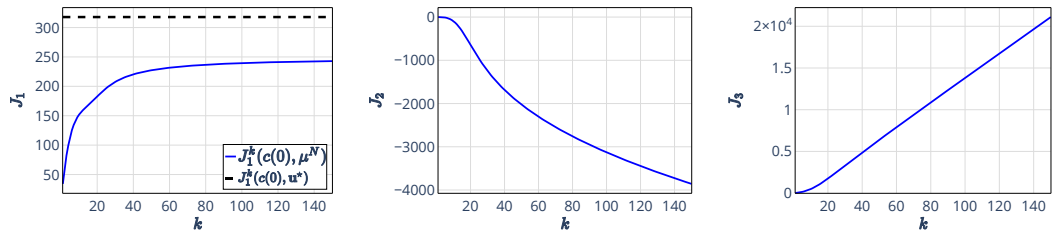

(a) $J_1^k(c_0, \mu^N)$ (b) $J_2^k(c_0, \mu^N)$ (c) $J_3^k(c_0, \mu^N)$

Figure 5.13: Performance of all cost criteria J_i

first cost function J_1 complies with the theoretical bound $J_1^N(c_0, \boldsymbol{u}_{c_0}^\star)$. We can observe that the performance behaves as expected for the second and third cost criteria. The third cost J_3 is strictly increasing since the squared value of the cost in the equilibrium $u^e = 12$ is added in each iteration.

These three examples in this section illustrated our theoretical results numerically, particularly regarding the impact of the choice of the *first* efficient solution $\mathbf{u}_{x(0)}^\star$, chosen in step (0) of our algorithms. In the next chapter, we discuss the impact of the choice of the subsequent efficient solutions on the solution behavior. Although the convergence behavior does not change, the transient behavior does. Analyzing this behavior, we investigate numerically different selection rules.

6 Numerical Simulations – The Impact of Selection Rules on the Solution Behavior

In this chapter, we illustrate our theoretical findings from Section 5 by conducting numerical experiments and simulations and discussing the impact of selection rules. First, we introduce different selection rules for the subsequent efficient solutions and move on to discussing the numerical experiments by application examples. Then, we provide an overview of our implemented program.

6.1 Selection Rules

In Chapter 5, we have shown theoretically and visualized numerically the impact of the choice of the first efficient solution $\mathbf{u}^\star_{x_0}$ on the performance estimates. However, by applying the global criterion method for calculating and selecting the subsequent efficient solutions $\mathbf{u}^\star_{x(k)}$ in the examples of Section 5.3, we have not exploited a degree of freedom – namely, the selection of the subsequent efficient solution $\mathbf{u}^\star_{x(k)}$ in each time step. We recall that we distinguish between the first efficient solution $\mathbf{u}^\star_{x_0}$ chosen in step (0), i.e., in the first iteration, and the subsequent efficient solutions $\mathbf{u}^\star_{x(k)}$ chosen in step (1), i.e., from time step $k = 2$ onwards.

In the following, we introduce rules for choosing the subsequent efficient solutions such that we can further investigate the impact of these selection rules on the solution behavior. In the bi-objective case, generally, an efficient solution with values at the top left of the considered nondominated set will cause the first cost criterion to become smaller and vice versa. Particularly in our setting, where the first cost is always stabilizing, putting a large emphasis on the first cost criterion forces the trajectory to converge faster since this causes a lower cost. To check whether this effect can be seen in practice, we will investigate different selection rules for choosing the subsequent efficient solutions. To this end, we introduce the following selection rules for the subsequent efficient solutions:

- "ideal": The efficient solutions are computed as in (5.16) as pre-images of nondominated points with minimal Euclidean distance to the ideal point $z^\star$

introduced in Example 5.17 with

$$z_i^\star = \min \left\{ J_i^N(x(k), \mathbf{u}) \,\middle|\, \mathbf{u} \in \mathbb{U}^N(x_0),\ J_j^N(x(k), \mathbf{u}^\star_{x(k)}) \leq J_j^N(x(k), \mathbf{u}_{x(k)}) \right\},$$

for all $i = 1, \ldots, s$, where $\mathbf{u}^\star_{x(k)}$ is are the efficient solutions in each time step k in Algorithm 2 or Algorithm 3. Depending on the algorithm, we set $j = 1$ or $j = 1, \ldots, s$, corresponding to the constraints in step (1). This selection rule is illustrated in Figure 6.1 for two objectives.

- "min i" ($i \in \{1, \ldots, s\}$): The efficient solutions are chosen such that J_i^N (with the additional bounds from inequality (5.4) or inequalities (5.5)) is minimal.

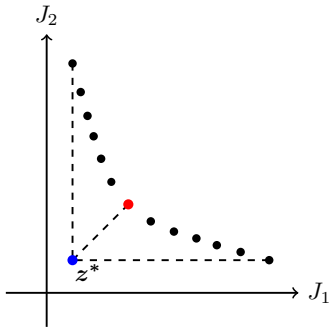

Figure 6.1: Visualization of the selection rule "ideal"

These selection rules are applicable to both Algorithm 2 and Algorithm 3. However, we note that the selection criteria "min i" with $i \in \{1, \ldots, s\}$ theoretically only guarantee to find weakly efficient solutions to the underlying multiobjective optimization problem. These weakly efficient solutions lie at the extremals of the nondominated set. The set of weakly efficient solutions forms a superset of the set of efficient solutions. It also contains those feasible solutions for which just no other feasible solution exists, which strictly improves all objective functions simultaneously. Thus, we must ensure that we only choose and use efficient solutions. In the case of Algorithm 3, the solutions are additionally constrained by the bounds (5.5), which "cut off" these extremal points. Since, according to our numerical experience, this is the situation in all our numerical tests, we can assume that our algorithm yields weakly efficient solutions that are not also efficient.

We begin our investigation with the isothermal reactor from Section 5.3. Using Algorithm 3, we examine the solution behavior by applying different selection rules. We then continue with theoretically discussing a path-following example motivated

by the application. Through numerical simulations, we show that Algorithm 2 is also applicable and that our theoretical results from Section 5.2 are still observable.

6.2 Bi-Objective Examples

To discuss the impact of different selection rules for the subsequent efficient solutions, i.e., those in step (1) of the algorithms, numerically, we consider again the isothermal reactor. Since we want to guarantee the theoretical performance estimates for all cost criteria, we use Algorithm 3. To explain the effects clearly and to visualize the nondominated set easily, we consider bi-objective optimal control problems, and in the case of the reactor, the multiobjective optimal control problem (5.17) from Example 5.17. Second, we consider an example motivated by economic growth to show that the selection rules must not impact the solution behavior.

In order to ensure comparability, we consider the same first efficient solution in all simulations. Closely related to guarantees of the theoretical performance estimates is the development of the nondominated sets during the iterations, which we will discuss in the following example. All approximations of nondominated sets were calculated with the adapted Pascoletti-Serafini optimization [24].

Example 6.1 (Reactor Part 3)
We consider the isothermal reactor from Example 5.17 with the same constants and constraints. For the simulation, we used Algorithm 3 with the different selection rules described in Section 6.1 for choosing the subsequent efficient solution $\boldsymbol{u}^\star_{c(k)}$. *In all simulations we consider the MPC-horizon* $N = 5$ *and use the same first efficient solution* $\boldsymbol{u}^\star_{c(0)}$ *which is chosen as in Example 5.17 such that*

$$J^5(c_0, \boldsymbol{u}^\star_{c_0}) = (54.034, 9.500).$$

Figure 6.2 shows the first nondominated set. Additionally, we marked the point corresponding to the first chosen efficient solution.

Further, in Figure 6.3 on the left side, we visualize the bounds on the nondominated set of Algorithm 3 in time step $k = 2$. *The resulting second nondominated set is enlarged on the right side. The colored points are the efficient solutions chosen according to the selection rules "ideal", "min 1", and "min 2". While in all simulations, the same first efficient solution is chosen, we compare different selection rules for the subsequent efficient solutions, which are, however, identical during the iterations.*

In Figure 6.4, we visualized the nondominated set and the corresponding chosen subsequent efficient solutions in the time step $k = 6$. *We remark that the magnitudes of the cost functionals and, thus, the size and the location of the nondominated sets are*

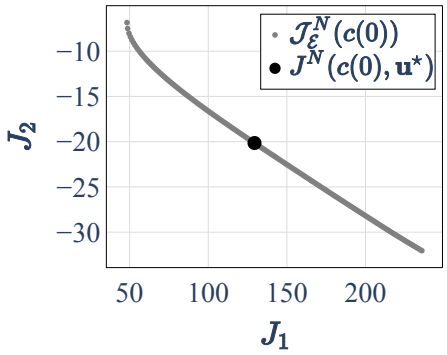

Figure 6.2: First nondominated set with chosen efficient solution

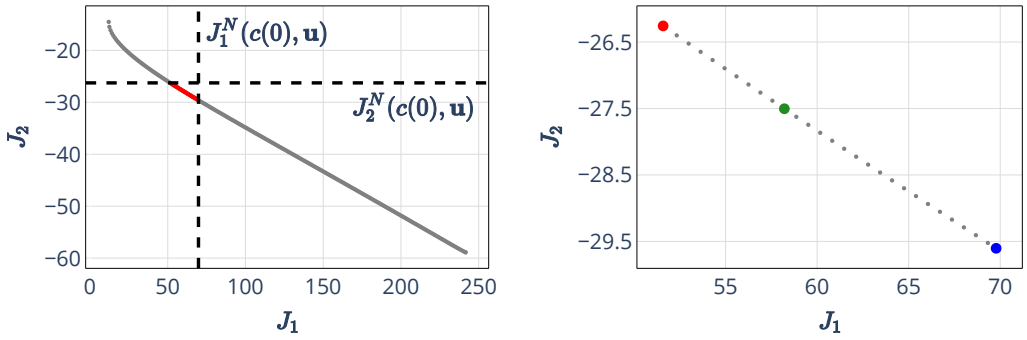

Figure 6.3: Second nondominated set with the chosen efficient solutions

significantly different for the three selection rules. The nondominated set for "min 2" (right) has a range from 7 to 13 and from -58 to -52, and the nondominated set for "min 1" (mid) has a range from 0.5 to 0.8 and from -36 to -34.6 that is substantially smaller. The nondominated set for "ideal" (left) lies between those for "min 1" and "min 2". Hence, for each selection rule, the subsequent efficient solutions are not only chosen according to different rules but also from completely different nondominated sets. This indicates that the choice of efficient solutions should have an impact on convergence rate and performance. Figure 6.5 illustrates the resulting closed-loop trajectories.

On the left-hand side in Figure 6.5, we observe that all selection rules deliver a similar behavior for the first component of the trajectory c_A. In contrast, on the right-hand side, the behavior of the second component c_B depends strongly on the

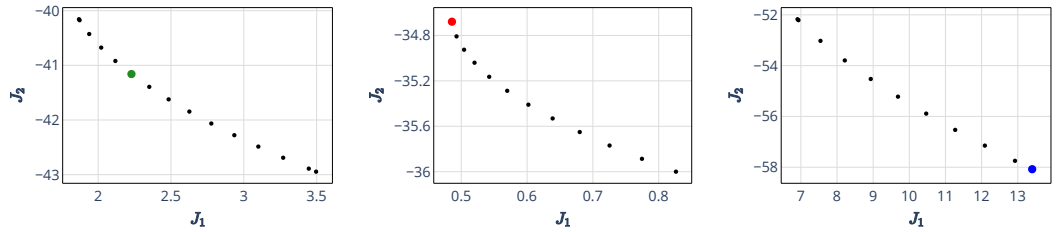

(a) "ideal" (b) "min 1" (c) "min 2"

Figure 6.4: Nondominated set in time step $k = 6$ for the different selection rules

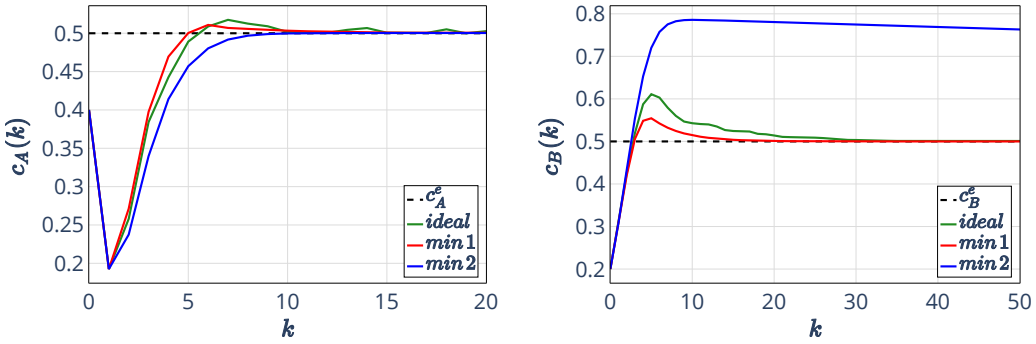

Figure 6.5: Components of the closed-loop trajectory for the different selection rules

selection rule. The rule "min 2" aims to maximize the economic yield. Therefore, the second component of the closed-loop has large values and converges only slowly to the equilibrium. While the trajectory of "min 1" reaches a small neighborhood of the equilibrium within 15 time steps, "min 2" needs about 2000 time steps to get similarly close to the equilibrium.

In Figure 6.6, we visualize the cost criteria J_1^N and J_2^N. Here, we observe that "min 1" results in a significantly smaller J_1 than the other strategies, while J_2 is the largest, whereas "min 2" enforces exactly the opposite. Regarding the cost, the main feature of "ideal" becomes particularly clear. The selection rule "ideal" yields a compromise between both costs, which in this example turns out to be closer to "min 1" than to "min 2".

The results in Example 6.1 show precisely the behavior that we would expect from the different selection rules. Actually, a priori, it was unclear that the quantitative differences were so pronounced. Indeed, as the following example indicates, the effect of the different rules can also be almost negligible.

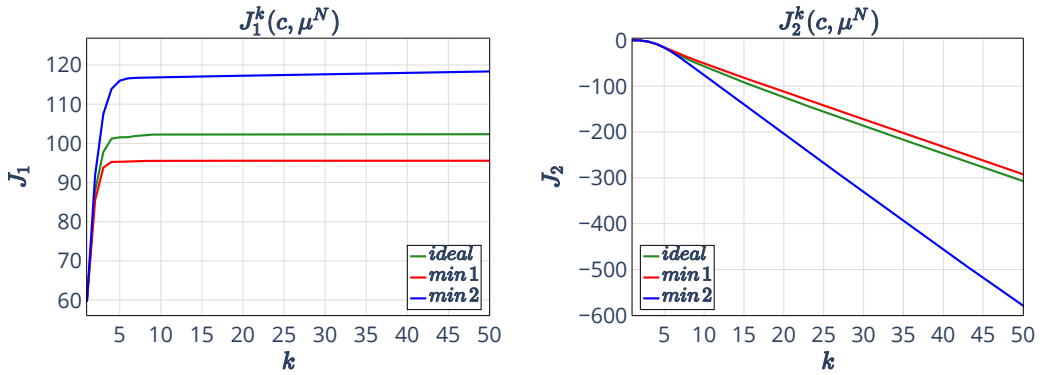

Figure 6.6: Cost criteria J_1 and J_2 for the different selection rules

Example 6.2

We consider an economic growth model introduced in [14]. The system dynamic in discrete time is given by

$$x(k+1) = u(k), \quad k \in \mathbb{N},$$

and the stage cost by

$$\ell_1(x,u) = -\ln(Ax^\alpha - u),$$

with parameters $A = 5$ and $\alpha = 0.34$. We impose state and control constraints $\mathbb{X} = [0,10]$ and $\mathbb{U} = [0.1,5]$. As calculated in [16], the equilibrium at which the system is strictly dissipative is given by $(x^e,u^e) = (x^e,x^e) \approx (2.23,2.23)$. We use the equilibrium to set the endpoint terminal constraint $\mathbb{X}_0 = \{x^e\}$. Next, we introduce the second stage cost

$$\ell_2(x,u) = (x-x^e)^2 + 0.1(u-u^e)^2,$$

which additionally stabilizes the equilibrium. Thus, the multiobjective optimal control problem reads

$$\begin{aligned} \min_{\boldsymbol{u}\in\mathbb{U}^N(x_0)} J^N(x_0,\boldsymbol{u}) &= \left(\sum_{k=0}^{N-1}\ell_1(x(k,x_0),u(k)), \sum_{k=0}^{N-1}\ell_2(x(k,x_0),u(k))\right) \\ s.t. \quad x(k+1) &= u(k), \\ x(0) &= 5, \\ x(N,x_0) \in \mathbb{X}_0 &= \{(2.23,2.23)\}, \\ \mathbb{X} = [0,10],\ \mathbb{U} &= [0.1,5]. \end{aligned} \tag{6.1}$$

Due to the strict dissipativity for the stage cost ℓ_1 at (x^e,u^e), the required Assumptions 5.1 and 5.6 are fulfilled. By introducing endpoint terminal constraints, Assumption 5.14 holds with the same argument as in Example 5.18. Hence, this example fits

in our theoretical setting. Next, to check whether the choice of the subsequent efficient solution in Algorithm 3 impacts the solution behavior, we consider the MPC-horizon $N = 10$ *and the selection rules from Section 6.1. We chose the first efficient solution such that* $J^{10}(x_0, \boldsymbol{u}^\star_{x_0}) = (-15.085, 7.892)$.

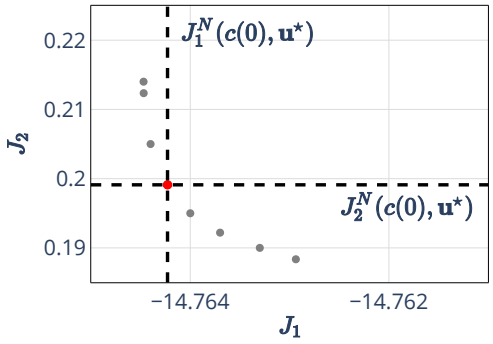

Figure 6.7: Resulting nondominated set

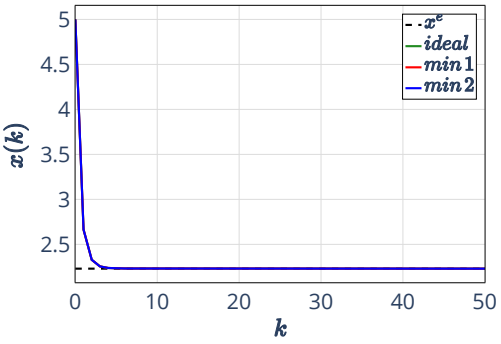

Figure 6.8: Closed-loop trajectories

Figure 6.7 shows the nondominated set in the second time step. Due to the restrictions (5.5)*, only one point is cut out of the nondominated set. Thus, there is no more degree of freedom in choosing the efficient solution, suggesting that the selection rules have no impact on the solution behavior. Indeed, this behavior is confirmed in Figure 6.8, as there are no differences – except for numerical inaccuracies – in the trajectories resulting from the selection rules. The same phenomenon is reflected in the costs. For this example, we, therefore, can conclude that the choice of the subsequent efficient solutions has almost no influence on the trajectory behavior and the cost criteria.*

In summary, the examples show that implementing different selection rules for the subsequent efficient solutions may significantly affect the resulting closed-loop trajectories and costs. These impacts are clearly visible in Example 6.1. In contrast, Example 6.2 shows that this difference may also be negligible.

6.3 The Path-Following Problem

In this section, we extend the illustration of our theoretical results and the impact of selection rules to an additional application example. We consider an autonomous vehicle combined with a path-following problem for which we refer to the work in [28, 29, 34]. More precisely, an autonomous vehicle moves in the $x_1 - x_2-$plane and can be controlled in terms of its speed and steering angle. We pursue multiple goals: driving along a given path (which we interpret as staying on the road), ensuring driving comfort, and maintaining a reference speed. Thus, this multiobjective optimal control problem is motivated and modeled from an application of increasing interest, for instance, we refer to [21, 27, 60, 67] for which we do not claim completeness. Since the objectives are conflicting, we will observe in Section 6.3.2 a significant impact of the selection rules on the solution behavior. We briefly introduce the example theoretically before discussing the numerical simulation results.

6.3.1 Problem Formulation

We draw on a path-following example presented in [28, 29, 34]. The authors of these references do their analysis in a continuous time setting. Hence, we first recall the main ideas and results before adapting the example to our discrete time setting and proposing our multiobjective path-following problem.

We consider an autonomous vehicle moving in the $x_1 - x_2-$plane according to the system

$$\begin{pmatrix} \dot{x}_1 \\ \dot{x}_2 \\ \dot{x}_3 \end{pmatrix} = f(x,u) := \begin{pmatrix} u_1 \cos(x_3) \\ u_1 \sin(x_3) \\ u_1 \tan(u_2) \end{pmatrix}, \quad x(0) = x_0, \tag{6.2}$$

where x_1, x_2 describes the position, x_3 describes the yaw angle, u_1 is the speed, and u_2 is the steering angle of the vehicle. We constrain the speed of the vehicle such that $u_1 \in [0, 6]$ and, thus, driving backwards is impossible. To avoid too strong dislocations, the steering angle is constrained by $\frac{\pi}{5}$ in both directions, i.e., $u_2 \in [-\frac{\pi}{5}, \frac{\pi}{5}]$.

Next, we define the path $\mathcal{P}$ to be followed. The path is an explicitly parameterized curve, see [28, Example 4.3], and is given by

$$\mathcal{P} = \left\{ p(\theta) \in \mathbb{R}^3 \,\middle|\, [\hat{\theta}, 0] \mapsto p(\theta) = \begin{pmatrix} \theta \\ \rho(\theta) \\ \arctan\left(\frac{\partial \rho}{\partial \theta}(\theta)\right) \end{pmatrix} \right\}, \tag{6.3}$$

where $\hat{\theta} = -30$ and

$$\rho(\theta) = -\alpha \log\left(\frac{\gamma}{\beta + |\theta|}\right) \cdot \sin(\omega\theta).$$

The coefficients are given by $\alpha = 6$, $\beta = 5$, $\gamma = 20$, and $\omega = 0.35$. Figure 6.9 visualizes the path in the $x_1 - x_2$-plane. We note that the path is negatively parameterized since $\hat{\theta} < 0$, and $p(0) = 0$ holds. Further, the map p is twice continuously differentiable and bijective. We can conclude that the admissible state space $\mathbb{X}$ is induced by the path and the range of motion of the vehicle and, thus, given by

$$\mathbb{X} = [-30, 0] \times [-3, 6] \times [-2\pi, 2\pi].$$

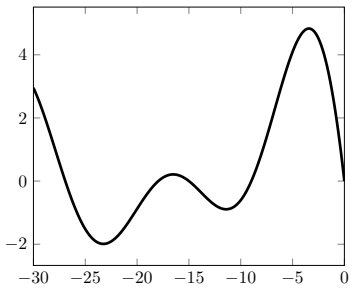

Figure 6.9: Visualization of the path $\mathcal{P}$

Moreover, we impose additional path-following constraints to ensure that the vehicle follows the given path as shown in, for instance, [29]. We consider the linear differential equation

$$\dot{\theta} = g(\theta, v) := -\lambda\theta + v, \quad \theta_0 = \hat{\theta} = -30, \tag{6.4}$$

with $\lambda = -10^{-3}$ and $v \in [0, 6]$. This equation is a timing law with the virtual controller v such that the evolution of the parameter θ can be influenced. As in [29], the timing law is usually not given a priori and must not necessarily be linear, providing us with an additional degree of freedom in the controller design. This way, we can design the controller to depend on the input u and the reference timing $t \mapsto \theta(t)$. We define the state and control as $y = (x, \theta)$, $w = (u, v)$ respectively, and the admissible state and control set expand to $\mathbb{X} = [-30, 0] \times [-3, 6] \times [-2\pi, 2\pi] \times [-30, 0]$ and $\mathbb{U} = [0, 6] \times [-\frac{\pi}{5}, \frac{\pi}{5}] \times [0, 6]$. In the following, we consider the equilibrium

$$(y^e, w^e) = \left(\begin{pmatrix} 0 \\ 0 \\ x_3^e \\ 0 \end{pmatrix}, \begin{pmatrix} 0 \\ u_2|_{\theta=0} \\ 0 \end{pmatrix} \right),$$

with $x_3^e = p_3(0) = \arctan\left(\frac{\partial \rho}{\partial \theta}(0)\right)$, and

$$u_2|_{\theta=0} = \arctan\left(\left(1 + \left(\frac{\partial \rho}{\partial \theta}(0)\right)^2\right)^{-3/2} \frac{\partial^2 \rho}{\partial \theta^2}(0)\right),$$

since the reference speed is $u_1^e = 0$ and the second input u_2 does not vanish at the end of the path, see [34, Section 4].

Additionally, we introduce a terminal condition. Namely, we set the given path $\mathcal{P}$ as our terminal constraint set $\mathbb{X}_0 = \mathcal{P} \times [-30, 0]$. The conceptual idea of doing so is to project the compatibility condition from Assumption 5.1 (iv) b) onto the virtual state θ. Consequently, we shift the costs of driving the system along the path such that they only depend on θ. We need to ensure the existence of a local feedback $\kappa = (\kappa_u, \kappa_v)$ as required in Assumption 5.1, which guarantees the exact path-following. Before imposing a compatibility condition, we must define our cost function and terminal costs.

The cost function in [29, Section 4] is given by a stabilizing stage cost

$$\ell_1(y, w) = (x - p(\theta))^T Q (x - p(\theta)) + q\theta^2 + (u - u^e)^T R (u - u^e) + (v - v^e)^2,$$

where $Q = 8 \cdot \operatorname{diag}(10^4, 10^5, 10^5)$, $q = \frac{1}{2}$, $R = \operatorname{diag}(10, 10)$, and $w^e = (u^e, v^e)$ denotes the control equilibrium. Moreover, the terminal cost is a penalty term

$$F_1(y) = \frac{c}{2}\theta^2,$$

where $c = 1740$ is a constant chosen such that the terminal cost guarantees that $x(t) - p(\theta(t)) \to 0$ for $t \to \infty$.

We define the path-following single-objective optimal control problem in continuous time

$$\begin{aligned} \min_{\mathbf{w} \in \mathbb{U}^N(y_0)} J_1^N(y_0, \mathbf{w}) = \sum_{k=0}^{N-1} \ell_1(y_{\mathbf{w}}(k, y_0), w(k)) + F_1(y_{\mathbf{w}}(N, y_0)) \\ \text{s.t.} \quad \dot{x} = f(x, u), \\ \dot{\theta} = g(\theta, v), \\ x(0) = x_0, \quad \theta(0) = \theta_0, \\ y \in \mathbb{X}, \quad y_{\mathbf{w}}(N, y_0) \in \mathbb{X}_0 \end{aligned} \tag{PF SO}$$

with the quantities described above. The optimal control problem (PF SO) has the following properties, proven in [34].

Property 6.3

(i) The origin is contained in $\operatorname{int}\mathbb{X}$ *and* $\operatorname{int}\mathbb{U}$*, and the sets* $\mathbb{X}$ *and* $\mathbb{U}$ *are compact.*

(ii) The right-hand side of the control system (6.2) $f : \mathbb{X} \times \mathbb{U} \to \mathbb{R}^3$ *is a continuous and local Lipschitz vector field, and it satisfies* $f(0,0) = 0$*. The same holds for the timing law* g *in equation* (6.4)*.*

(iii) The stage cost ℓ_1 *is continuous and positive definite.*

(iv) The path $\mathcal{P}$ *is regular, twice continuously differentiable, negatively parametrized, and bijective.*

(v) The timing law g *is chosen such that for all* $v \in [0,6]$ *and* $\theta \in [-30,0)$ *it yields that* $g(\theta, v) > 0$*.*

(vi) The terminal cost $F_1(x)$ *is continuously differentiable, positive semidefinite and* $F_1(0) = 0$ *holds, and* $\mathcal{P} \subseteq \mathbb{X}_0$*.*

(vii) For all $x \in \mathbb{X}$ *the controller*

$$w_\varepsilon = (u_\varepsilon, v_\varepsilon)^T = \begin{pmatrix} \dot{\theta}\sqrt{1 + \left(\dfrac{\partial \rho}{\partial \theta}\right)^2} \\ \arctan\left(\left(1 + \left(\dfrac{\partial \rho}{\partial \theta}\right)^2\right)^{-\frac{3}{2}} \cdot \dfrac{\partial^2 \rho}{\partial \theta^2}\right) \\ 0 \end{pmatrix} \in \mathbb{U}$$

fulfills

$$\nabla F_1(y) \cdot \begin{pmatrix} f(x, u_\varepsilon) \\ g(\theta, v_\varepsilon) \end{pmatrix} + \ell_1(y, w_\varepsilon) \leq 0$$

and $(f(x,u_\varepsilon), g(\theta, v_\varepsilon)) \in \mathbb{X}_0$ *for all* $y \in \mathbb{X}_0$*.*

The controller w_ε was determined via a flat parametrization of state and input variables, for a discussion, see [28, Example 4.3], and also derived in [34, Section 4].

Due to Property 6.3 the assumptions A1–A7 in [34], and the assumptions of Theorem 1 in [29] are fulfilled. Hence, we can conclude that [29, Theorem 1] holds, and the vehicle stays on the given path $\mathcal{P}$. More precisely, for the closed-loop system of the path-following problem, the error $e(t) = x(t) - p(\theta(t))$ converges to zero for $t \to \infty$.

We extend the path-following problem (PF SO) to a multiobjective problem by considering two further cost criteria. The first one,

$$\ell_2(y, w) = (u_1 \tan(u_2))^2 ,$$

penalizes the deviation of the derivative of the yaw angle from zero and, thus, aims to avoid abrupt changes in the yaw angle. We interpret this cost criterion as ensuring driving comfort, whereas the third stage cost,

$$\ell_3(y, w) = (u_1 - u_{\text{ref}})^2,$$

enforces the maintaining of a reference speed u_{ref}.

In addition, we discretize system (6.2), (6.4) using the Heun method with $h \geq 0$ resulting in

$$\begin{aligned} y(k+1) = \begin{pmatrix} x(k+1) \\ \theta(k+1) \end{pmatrix} = \begin{pmatrix} x(k) + \frac{h}{2}\left(f(x(k), u(k)) + f(\widetilde{x}(k+1), u(k))\right) \\ \theta(k) + \frac{h}{2}\left(g(\theta(k), v(k)) + g(\widetilde{\theta}(k+1), v(k))\right) \end{pmatrix} =: \tilde{f}(y, w) \\ y(0) = (x_0, -30)^T, \end{aligned} \tag{6.5}$$

where we use the explicit Euler method to calculate

$$\begin{pmatrix} \widetilde{x}_1(k+1) \\ \widetilde{x}_2(k+1) \\ \widetilde{x}_3(k+1) \\ \widetilde{\theta}(k+1) \end{pmatrix} = \begin{pmatrix} x_1(k) + hu_1(k)\cos(x_3(k)) \\ x_2(k) + hu_1(k)\sin(x_3(k)) \\ x_3(k) + hu_1(k)\tan(u_2(k)) \\ (1 - h\lambda)\theta(k) + hv(k) \end{pmatrix}.$$

As we aim to apply our multiobjective model predictive control Algorithms 2, 3 to solve the multiobjective path-following problem, we need to verify whether this problem fits in our setting from Section 5.1. To accomplish this, we validate Assumption 5.1:

(i) The functions $\tilde{f}$, F_1, and ℓ_i, $i = 1, 2, 3$ are continuous.

(ii) The equilibrium is given by (y^e, w^e).

(iii) The system (6.5) is strictly(x, u)-dissipative for the stage cost ℓ_1, because ℓ_1 is stabilizing in y and w.

(iv) The equilibrium (y^e, w^e) lies at the end of the path, i.e., $(y^e, w^e) \in \mathcal{P}$. The controller w_ε is designed such that Property 6.3 (vii) holds. Further, the discrete version of this condition, using the difference quotient with $h = 1$, leads to the compatibility condition in Assumption 5.1 (iv) b).

(v) The set $\mathbb{U}$ is compact and the set $\mathbb{X}$ and $\mathbb{X}_0$ are closed. If we choose the initial state x_0 such that the vehicle can be steered on the path, Lemma 2.33 guarantees external stability.

Finally, we establish the multiobjective path-following problem

$$\begin{aligned} \min_{\mathbf{w}\in\mathbb{U}^N(y_0)} \; & J^N(y_0,\mathbf{w}) := \left(J_1^N(y_0,\mathbf{w}), J_2^N(y_0,\mathbf{w}), J_3^N(y_0,\mathbf{w})\right) \\ \text{s.t.} \quad & y(k+1) = \tilde{f}(y(k), w(k)),\ k \in \mathbb{N}, \\ & x(0) = x_0, \quad \theta(0) = \theta_0, \\ & y(N, y_0) \in \mathbb{X}_0. \end{aligned} \tag{PF MO OCP}$$

We remark here that the assumptions also hold for other discretization methods. In addition, the implementation of our algorithms, see Chapter 6.4, allows us to use discretization methods depending on what turns out to be numerically more stable. Hence, we decided to use the Heun discretization for all our numerical investigation of this path-following example.

6.3.2 Numerical Results

We simulate the multiobjective path-following problem (PF MO OCP) by using the implementation of our algorithms, see Chapter 6.4, to analyze the numerical results. In view of the less restrictive additional constraints, we apply Algorithm 2 and investigate the path-following behavior based on the different selection rules introduced in Section 6.1.

Example 6.4 (Path-Following Version 1)
We consider the path-following problem (PF MO OCP) *with the two cost criteria*

$$\ell_1(y,w) = 10^{-4}\left((x-p(\theta))^T Q(x-p(\theta)) + q\theta^2 + (u-u^e)^T R(u-u^e) + (v-v^e)^2\right),$$

where $Q = 8\cdot\operatorname{diag}(10^4, 10^5, 10^5)$, $q = \frac{1}{2}$, $R = \operatorname{diag}(10,10)$, *and*

$$\ell_2(y,w) = 10\left(u_1\tan(u_2)\right)^2.$$

We scaled the stage costs and, thus, the cost function here to bring the resulting values into the same order of magnitude to make the optimization problem numerically robust.

As discussed in the previous section, the path-following problem fulfills Assumption 5.1 from which we can conclude trajectory convergence as well as performance results. Further, from the section above, we adapt the admissible state set $\mathbb{X}$, *control set* $\mathbb{U}$, *and the terminal constraint set* $\mathbb{X}_0 = \mathcal{P}\times[-30,0]$. *We used the program described in Section 6.4 using the Heun discretization with* $h = 1$ *with MPC-horizon* $N = 15$ *and* $K = 150$ *time steps for the numerical simulations.*

The movement of the vehicle in the $x_1 - x_2$*–plane, the speed, and the steering angle of vehicles with different selection rules are visualized in Figure 6.10. We can observe*

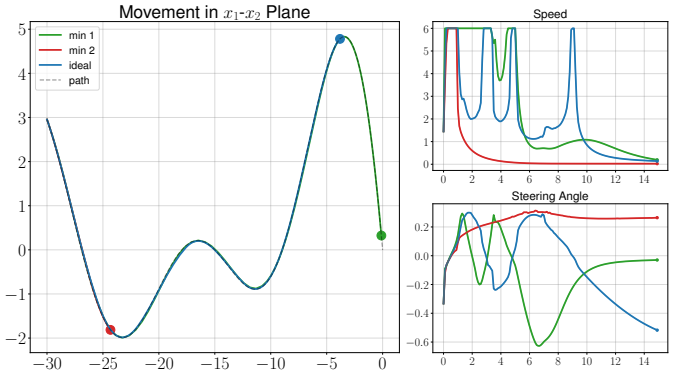

Figure 6.10: Movement, speed and angle of the vehicle for two cost criteria

that the solution behavior is quite different depending on the selection rule. While the qualitative behavior of the movement is very similar, the speed of the movement is very different. In particular, the vehicle that follows the rule "min 2" drives very slowly and barely gets to the first bend, whereas the vehicle that follows the rule "min 1" comes to the end of the path within 150 time steps. We may interpret the vehicle's behavior following "min 2" as maximizing driving comfort by driving along curves very slowly and carefully.

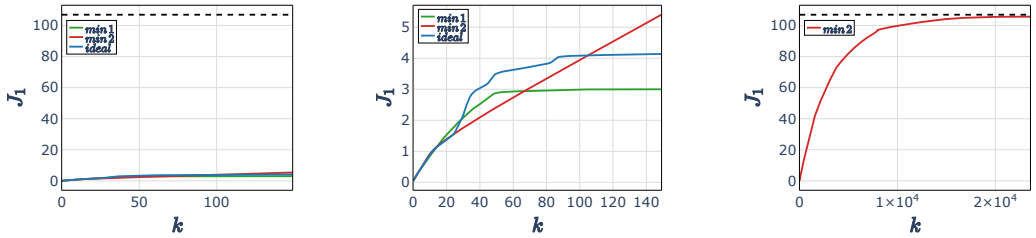

Figure 6.11: Cost function J_1 depending on the time step k

The remarkable difference between the different selection rules is also mirrored in the development of the first cost function depending on the time step k. Figure 6.11 on the left side visualizes the first cost function and the upper bound according to Theorem 5.7. Although the upper bound does not seem to be sharp, the zoomed-in version of the plot in the middle of Figure 6.11 shows that the costs according to "min 2" are increasing. Hence, it is not (numerically) clear if the bound is respected and if the vehicle comes to the end of the path. In order to verify our theoretical results numerically for this special case, we did the same simulation but this time with approximately 23,000 time steps. Then, we can observe in Figure 6.11 on the

right side that the theoretical bound $J_1^N(x_0, \boldsymbol{u}^\star_{x_0})$ is sharp, and in the simulation that the corresponding vehicle comes to the end of the path.

Figure 6.12 illustrates the second cost function J_2^N depending on the time step k. Even though with Algorithm 2, we cannot theoretically guarantee the upper bound shown in Theorem 5.15, the costs seem to converge in the numerical simulations.

The behavior of the second cost criterion is the opposite of the first cost criterion: While the rule "min 2" produces approximately zero costs, the rule "min 1" causes costs of about 500. In contrast, the rule "ideal" selects a compromise solution between "min 1" and "min 2" and, thus, generates moderate for both cost criteria.

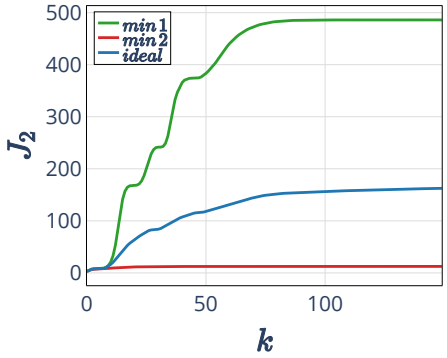

Figure 6.12: Cost function J_2 depending on the time step k

In Example 6.4, we observe that the selection rule "min 2" requires a huge amount of iterations. In order to avoid this, we modify the second stage cost in the next example.

Example 6.5 (Path-following Version 2)
We consider the path-following problem (PF MO OCP) *with the two stage costs described in Example 6.4. In contrast to this example, we modify the second cost criterion by adding a term penalizing the deviation from the reference speed $u_{ref} = 6$ and define the new second stage cost by*

$$\ell_2(y, w) = 10(u_1 \tan(u_2))^2 + 5(u_1 - 6)^2.$$

Indeed, we intend to force the vehicle, driving with the rule "min 2", to move along the path faster. As discussed in Example 6.4, we scale the terms of the stage costs to obtain better numerical robustness. For our simulations, we use the same parameters as in Example 6.4.

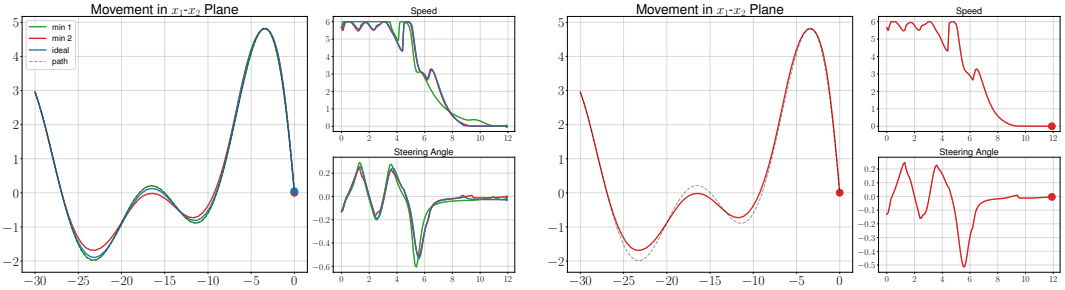

Figure 6.13: Left: Movement for all selection rules, right: Movement for selection rule "min 2"

Then, in Figure 6.13 on the left side, we observe that all vehicles drive along the path at approximately the same speed. However, we also observe that the selection rules "ideal" and "min 2" do not follow the path exactly anymore. This phenomenon is visualized more clearly in Figure 6.13 on the right side for the selection rule "min 2".

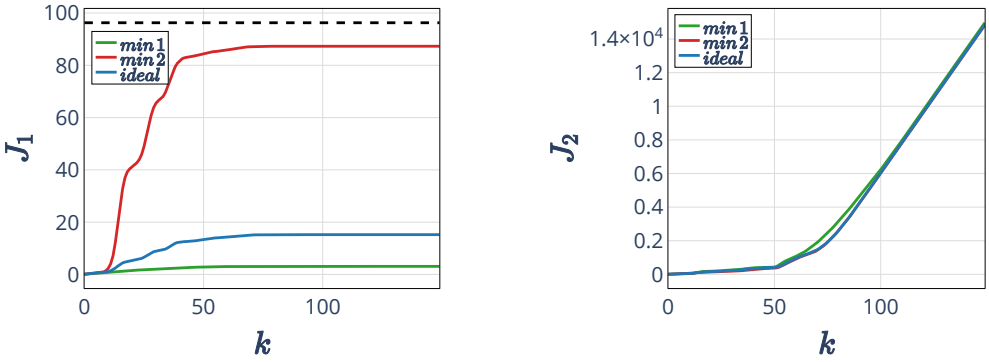

Figure 6.14: Cost function J_1^N and J_2^N depending on the time step k

Further, Figure 6.14 visualizes the two cost criteria J_1^N and J_2^N depending on the time step k. The first cost criterion and the corresponding performance bound from Theorem 5.7 are plotted on the left side. This time, even for the selection rule "min 2", the upper bound is not as sharp as in Example 6.4. On the right side, the second cost criterion behaves approximately the same way for each selection rule, and it seems as if there is a linearly growing performance bound as stated in Theorem 5.15. This allows the assumption that the additional constraints (5.5) for all cost criteria in Algorithm 3 are not necessary to ensure a performance bound on

the cost functions J_i^N, $i \geq 2$.

In the next example, we show that our findings in Section 5.2 are not restricted to only two cost criteria. To achieve this, we investigate a path-following example in which we aim to follow the path, ensure driving comfort, and obtain a reference speed.

Example 6.6 (Path-following Version 3)
We consider the path-following problem (PF MO OCP) *with three cost criteria from Section 6.3.1, namely, path-following*

$$\ell_1(y, w) = 10^{-4} \left((x - p(\theta))^T Q (x - p(\theta)) + q\theta^2 + (u - u^e)^T R (u - u^e) + (v - v^e)^2 \right),$$

ensuring driving comfort

$$\ell_2(y, w) = 10(u_1 \tan(u_2))^2,$$

and obtaining a reference speed

$$\ell_3(y, w) = 5(u_1 - 6)^2.$$

The scaling of the stage costs is again in order to bring the resulting values into the same order of magnitude and, thus, to improve the numerical robustness. We use the

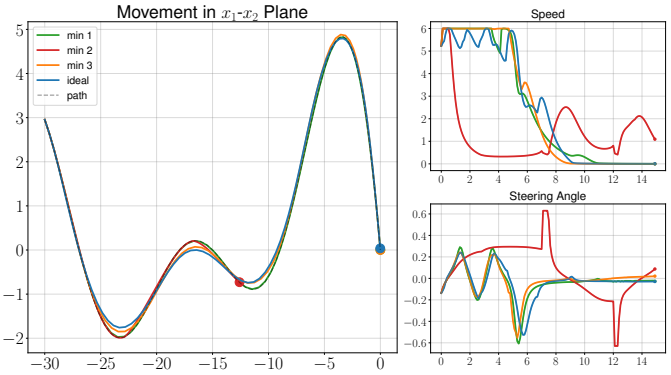

Figure 6.15: Movement, speed and angle of the vehicle for three cost criteria

same admissible state and control sets $\mathbb{X}$ *and* $\mathbb{U}$*, as well as the terminal constraint, set* $\mathbb{X}_0$ *as in Example 6.4, the MPC-horizon is* $N = 15$*, and the number of time steps is given by* $K = 150$.

The results of the simulations with different selection rules are visualized in Figure 6.15. We note a coupling of the phenomena observed in the examples above. While the rule "min 1" follows the path exactly in the given time, the rule "min 2" only follows the path approximately and does not come to the end of the path in the given time. However, the third cost criterion forces this vehicle to drive faster than in Example 6.4. Moreover, the selection rules "min 3" and "ideal" behave comparably, except that the vehicle with the rule "ideal" cuts the curves more. This behavior is likely due to the fact that all three cost criteria are, roughly speaking, equally important.

In Figure 6.16, the behavior of the three cost functions J_i^N, $i = 1, 2, 3$, is visualized. On the left, the first costs of all selection rules respect the performance bound from Theorem 5.7. In contrast, the second and the third cost criterion seem to follow the behavior described in Theorem 5.15. Actually, the second cost function even seems to converge numerically.

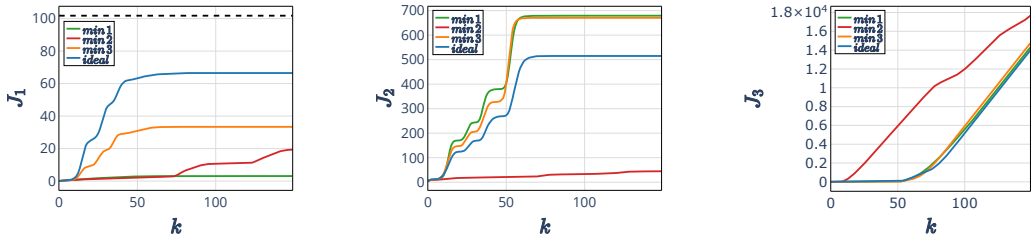

Figure 6.16: Cost function J_1 depending on the time step k

In summary, all the Examples 6.4, 6.5 and 6.6 show the applicability of our Algorithm 2 to multiobjective optimal control problems motivated by and modeled from an application problem. The numerical results also give evidence that the more restrictive Algorithm 3 is not necessary to obtain performance bounds on the cost functions J_i^N, $i \in \{2, \dots, s\}$, as stated in Theorem 5.15.

6.4 Implementation

Based on Mareleen Stieler's program [88, Chapter 7], we implemented the Algorithms 2 and 3 in Python supported by student assistant M.Sc. Jonas Schießl. We already used this implementation to illustrate our theoretical findings in Section 5.3.

Our program supports the optimization with both SciPy (`https://scipy.org`) and CasADi (`https://web.casadi.org`), see [4]. CasADi supports algorithmic differentiation and, thus, can solve large optimization problems efficiently and fast. In

comparison, SciPy can handle non-smooth problems, like the absolute value function as an objective function, better. Due to their respective advantages, we decided to integrate both optimizers in our program such that we can choose one of them depending on the problem. Further, the user can switch between Algorithm 2 and Algorithm 3.

Several methods for solving the multiobjective optimal control problem under consideration are available. We usually use the adapted Pascoletti-Serafini optimization presented in [24] to approximate the whole nondominated set. We used ASMO [1] as the template for our implementation in Python of this method. In the case of convex problems, the weighted sum approach (see [23] or Section 2.2.1) is also available in the code. Our code supports `NSGA II` [17] provided by pymoo (`https://pymoo.org`) [12]. Hence, we are also able to handle highly non-convex problems or problems with a nondominated set consisting of non-contiguous branches. Besides the methods for approximating the whole nondominated set, we can use the global criterion method [71] or a scalarization with fixed weights if we are only interested in one specific efficient solution. We can combine different multiobjective optimization methods depending on what we want to study.

In order to choose the first efficient solution $\mathbf{u}_{x_0}^\star$ graphically and, thus, determine the performance, we provide the possibility to visualize the nondominated set in the first iteration. In the subsequent iteration, we can use scalarization by fixing a weight or still approximate the whole nondominated set. We note that approximating the whole nondominated set in each iteration is computationally expensive and not necessary to ensure our theoretical guarantees. In Section 6.1, we discussed different rules for choosing the subsequent efficient solutions. The implementation of the selection rules ensures that the nondominated set is approximated, and the efficient solution is chosen according to the rule. Alternatively, we can either use the global criterion method or the scalarization method with weights matching the selection rules. Then, only one optimization problem must be solved in each iteration, which saves enormous computational time.

Once a multiobjective optimal control problem is solved with our program, we can directly visualize or store the data of interest. Furthermore, concerning comparing different selections of the subsequent solutions, the code supports loading the first efficient solution $\mathbf{u}_{x_0}^\star$ from saved data and proceeding with this control sequence.

7 Outlook and Future Research

Throughout this thesis, we have investigated different aspects of multiobjective optimal control problems. Besides developing a local turnpike analysis for discounted problems and a formulation for multiobjective strict dissipativity, we examined multiobjective model predictive control algorithms theoretically and numerically. While the local turnpike analysis led to arguments that apply to more problem classes than expected, the question of formulating an appropriate multiobjective dissipativity got unexpected technically. However, these technical studies result in a better understanding of the behavior of optimal control problems with convex-combined stage costs. Moreover, studying the additional degree(s) of freedom in choosing efficient solutions in each time step numerically gave us surprising insights. Especially even with our quite simple selection rules, the impact on the solution behavior was significant, and we were surprised by the unpredicted results, which raised further interesting questions.

To conclude the thesis, we outline some possibilities for future research.

Towards Local Turnpike Properties

In Chapter 3, in Theorem 3.8, we have established that depending on the discount factor, it may be more favorable for the trajectory to stay at a local equilibrium than moving to the cheaper global equilibrium. Roughly spoken, if the prediction is not long enough to detect that the cost in the global equilibrium can offset the "travel cost", the trajectory stays at the local equilibrium. We have expressed the too-short prediction in terms of the discount factor. However, in the non-discounted setting, we can explore the horizon N of the optimal control problem. Based on our findings for discounted problems, we can analyze the trajectory behavior depending on the horizon N in a non-discounted setting. A first investigation has already been published in [64].

Multiobjective Dissipativity using other Scalarization Methods

In our investigation of strict dissipativity for convex combined strict dissipative stage costs, we examined, depending on the weight, the behavior of the optimal equilibrium, and the storage function. We derived assumptions on the problem data depending on

the weight in Theorem 4.13 and Theorem 4.18 to ensure that convex combined strict dissipative stage costs are strictly dissipative. To this end, we used techniques from nonlinear programming. Although the weighted sum approach is commonly used to scalarize multiobjective optimization problems, it is unsuitable for non-convex problems. We expect that it is possible to obtain similar results for other scalarization methods using the approaches presented in Chapter 4. Considering other scalarization methods, we aim to extend our multiobjective strict dissipativity to non-convex problems.

Multiobjective Optimal Control Problems without Terminal Conditions

Closely related to multiobjective strict dissipativity using scalarization methods avoiding terminal conditions is how to get rid of the terminal conditions in Algorithms 2 and 3. Both need the local feedback κ in the terminal constraint set from Assumption 5.1 to construct the comparison control sequence $\mathbf{u}$. In contrast to the methods presented in Chapter 4, in Chapter 5, we only require the strong dissipativity assumption for one objective function. In view of application examples with merely one strictly dissipative staged cost and the absence of terminal conditions, a further investigation on how to construct the comparison control sequence in the Algorithms 2 and 3 is interesting.

Improved Performance Estimates for all Cost Criteria

The path-following problem presented in Sections 6.3.1 and 6.3.2 delivered quite promising numerical results: The less restrictive Algorithm 2 led to numerical performance results behaving similarly to the behavior described in Theorem 5.15 for Algorithm 3. However, whether Theorem 5.15 also holds for Algorithm 2 remains unclear. Further, we have observed in Chapter 6 that the selection rules may impact the solution behavior. Clearly, the trajectory behavior also influences the performance results. Therefore, incorporating the (quite simple) selection rules into our performance estimates can serve as a first step toward improving the performance estimates.

Further Investigation on Selection Rules

Until now, our investigation on selection rules only considers time-invariant rules. We believe exploring the formulation of time-varying selection rules might be interesting. For example, in the path-following problem, the decision maker's preferences may change depending on where the vehicle is on the path. While driving comfort may be a significant factor in curves, acceleration or maintaining a reference speed may

become more crucial on straight sections. Thinking one step further, a learning approach for the selection rules might also be desirable. Allowing the rules to adapt and improve over time could enhance decision-making.

The missing Piece: Multiobjective Optimality on the Infinite Horizon

A well-known fact in single-objective model predictive control is that strict dissipativity implies the turnpike property, and this, in turn, implies that the MPC closed-loop is approximately optimal on the infinite horizon [40]. After deriving a multiobjective dissipativity theory in Chapter 4 the next step is to adapt this result to the multiobjective setting. In fact, it is not clear yet how the error is distributed among the individual objective functions and how the error can be appropriately measured. However, before applying the single-objective MPC results to multiobjective optimal control problems, it is crucial to clarify how an error analysis of an approximated nondominated set can be made. We think that determining the Hausdorff distance between the exact nondominated set and the corresponding approximated nondominated set might be a promising approach.

List of Figures

List of Algorithms

Bibliography

[1] ASMO - a solver for multiobjective optimization. `https://github.com/GEichfelder/ASMO`.

[2] D. Acemoglu. *Introduction to modern economic growth.* Princeton University Press, 2009.

[3] F. Allgöwer and A. Zheng. *Nonlinear model predictive control.* Birkhäuser, 2012.

[4] J. A. E. Andersson, J. Gillis, G. Horn, J. B. Rawlings, and M. Diehl. CasADi – A software framework for nonlinear optimization and optimal control. *Mathematical Programming Computation*, 11(1):1–36, 2019.

[5] I. P. Androulakis. Dynamic Programming: Discounted Problems. In *Encyclopedia of Optimization*, pages 846–850. Springer US, 2008.

[6] D. Angeli, R. Amrit, and J. B. Rawlings. Receding horizon cost optimization for overly constrained nonlinear plants. In *Proceedings of the 48th IEEE Conference on Decision and Control – CDC 2009*, pages 7972–7977, Shanghai, China, 2009.

[7] D. Angeli, R. Amrit, and J. B. Rawlings. On average performance and stability of economic model predictive control. *IEEE Transactions on Automatic Control*, 57(7):1615–1626, 2012.

[8] J. Baker. Strong Convexity Does Not Imply Radial Unboundedness. *The American Mathematical Monthly*, 123(2):185, 2016.

[9] J. Berberich, J. Köhler, M. A. Müller, and F. Allgöwer. Data-driven model predictive control with stability and robustness guarantees. *IEEE Trans. Automat. Control*, 66(4):1702–1717, 2021.

[10] D. Bertsekas. *Reinforcement Learning and Optimal Control.* Athena Scientific, 2019.

[11] D. P. Bertsekas. *Nonlinear Programming.* Athena Scientific, 2nd edition, 1999.

[12] J. Blank and K. Deb. pymoo: Multi-Objective Optimization in Python. *IEEE Access*, 8:89497–89509, 2020.

[13] E. Bradford, L. Imsland, M. Reble, and E. A. del Rio-Chanona. Hybrid Gaussian process modeling applied to economic stochastic model predictive control of batch processes. In *Recent advances in model predictive control—theory, algorithms, and applications*, volume 485 of *Lect. Notes Control Inf. Sci.*, pages 191–218. Springer, Cham, 2021.

[14] W. A. Brock and L. J. Mirman. Optimal economic growth and uncertainty: The discounted case. *Journal of Economic Theory*, 4(3):479–513, 1972.

[15] P. D. Christofides, R. Scattolini, D. M. de la Peña, and J. Liu. Distributed model predictive control: A tutorial review and future research directions. *Computers & Chemical Engineering*, 51:21–41, 2013.

[16] T. Damm, L. Grüne, M. Stieler, and K. Worthmann. An Exponential Turnpike Theorem for Dissipative Discrete Time Optimal Control Problems. *SIAM Journal on Control and Optimization*, 52(3):1935–1957, 2014.

[17] K. Deb, A. Pratap, S. Agarwal, and T. Meyarivan. A fast and elitist multiobjective genetic algorithm: NSGA-II. *IEEE Transactions on Evolutionary Computation*, 6(2):182–197, 2002.

[18] W. D. Dechert and K. Nishimura. A complete characterization of optimal growth paths in an aggregated model with a non-concave production function. *Journal of Economic Theory*, 31:332–354, 1983.

[19] M. Diehl, R. Amrit, and J. B. Rawlings. A Lyapunov function for economic optimizing model predictive control. *IEEE Transactions on Automatic Control*, 56(3):703–707, 2011.

[20] J. Doležal. Existence of optimal solutions in general discrete systems. *Kybernetika*, 11(4):301–312, 1975.

[21] D. Dolgov, S. Thrun, M. Montemerlo, and J. Diebel. Path Planning for Autonomous Vehicles in Unknown Semi-structured Environments. *The International Journal of Robotics Research*, 29(5):485–501, 2010.

[22] R. Dorfman, P. A. Samuelson, and R. M. Solow. *Linear programming and economic analysis*. Dover Publications, 1987.

[23] M. Ehrgott. *Multicriteria Optimization*. Springer-Verlag, 2005.

[24] G. Eichfelder. An Adaptive Scalarization Method in Multiobjective Optimization. *SIAM Journal on Optimization*, 19(4):1694–1718, 2009.

[25] G. Eichfelder. Twenty years of continuous multiobjective optimization in the twenty-first century. *EURO Journal on Computational Optimization*, 9:100014, 2021.

[26] G. Eichfelder, L. Grüne, L. Krügel, and J. Schießl. Relaxed dissipativity assumptions and a simplified algorithm for multiobjective MPC. *Computational Optimization and Applications*, 2022.

[27] A. Faisal, T. Yigitcanlar, M. Kamruzzaman, and G. Currie. Understanding autonomous vehicles: A systematic literature review on capability, impact, planning and policy. *Journal of Transport and Land Use*, 12(1), 2019.

[28] T. Faulwasser. *Optimization-based Solutions to Constrained Trajectory-tracking and Path-following Problems*. PhD thesis, Otto-von-Guericke-Universität Magdeburg, 2012.

[29] T. Faulwasser and R. Findeisen. Constrained Output Path-Following for Nonlinear Systems Using Predictive Control. *IFAC Proceedings Volumes*, 43(14):753–758, 2010.

[30] T. Faulwasser, K. Flaßkamp, S. Ober-Blöbaum, and K. Worthmann. Towards Velocity Turnpikes in Optimal Control of Mechanical Systems. *IFAC-PapersOnLine*, 52(16):490–495, 2019.

[31] T. Faulwasser, L. Grüne, and M. A. Müller. Economic Nonlinear Model Predictive Control. *Foundations and Trends® in Systems and Control*, 5(1):1–98, 2018.

[32] T. Faulwasser and L. Grüne. Turnpike properties in optimal control. In *Numerical Control: Part A*, pages 367–400. Elsevier, 2022.

[33] T. Faulwasser, L. Grüne, J.-P. Humaloja, and M. Schaller. Inferring the adjoint turnpike property from the primal turnpike property. In *2021 60th IEEE Conference on Decision and Control (CDC)*, pages 2578–2583, 2021.

[34] T. Faulwasser, B. Kern, and R. Findeisen. Model predictive path-following for constrained nonlinear systems. In *Proceedings of the 48h IEEE Conference on Decision and Control (CDC)*, pages 8642–8647, 2009.

[35] T. Faulwasser and M. Zanon. Asymptotic Stability of economic NMPC: The importance of adjoints. *IFAC-PapersOnLine*, 51(20):157–168, 2018.

[36] K. Flaßkamp, S. Ober-Blöbaum, and S. Peitz. Symmetry in Optimal Control: A Multiobjective Model Predictive Control Approach. In *Advances in Dynamics, Optimization and Computation*, pages 209–237. Springer International Publishing, 2020.

[37] V. Gaitsgory, L. Grüne, M. Höger, C. M. Kellett, and S. R. Weller. Stabilization of strictly dissipative discrete time systems with discounted optimal control. *Automatica*, 93:311–320, 2018.

[38] V. Gaitsgory, L. Grüne, M. Höger, C. M. Kellett, and S. R. Weller. Stabilization of strictly dissipative discrete time systems with discounted optimal control. *Automatica*, 93:311–320, 2018.

[39] V. Gaitsgory, L. Grüne, and N. Thatcher. Stabilization with discounted optimal control. *Syst. Contr. Lett.*, 82:91–98, 2015.

[40] L. Grüne. Economic receding horizon control without terminal constraints. *Automatica*, 49(3):725–734, 2013.

[41] L. Grüne and R. Guglielmi. Turnpike properties and strict dissipativity for discrete time linear quadratic optimal control problems. *SIAM J. Cont. Optim.*, 56(2):1282–1302, 2018.

[42] L. Grüne, C. M. Kellett, and S. R. Weller. On a discounted notion of strict dissipativity. *IFAC-PapersOnLine*, 49(18):247–252, 2016.

[43] L. Grüne and L. Krügel. Local turnpike analysis using local dissipativity for discrete time discounted optimal control. 2021.

[44] L. Grüne, M. A. Müller, C. M. Kellett, and S. R. Weller. Strict dissipativity for discrete time discounted optimal control problems, September 2019.

[45] L. Grüne, M. A. Müller, C. M. Kellett, and S. R. Weller. Strict dissipativity for discrete time discounted optimal control problems. *Mathematical Control & Related Fields*, 11(4):771, 2021.

[46] L. Grüne and J. Pannek. *Nonlinear Model Predictive Control : Theory and Algorithms. 2nd Edition.* Communications and Control Engineering. Springer, Cham, Switzerland, 2017.

[47] L. Grüne, W. Semmler, and M. Stieler. Using nonlinear model predictive control for dynamic decision problems in economics. *Journal of Economic Dynamics and Control*, 60:112–133, 2015.

[48] L. Grüne and M. Stieler. Asymptotic stability and transient optimality of economic MPC without terminal conditions. *Journal of Process Control*, 24(8):1187–1196, 2014.

[49] L. Grüne, C. Kellett, and S. Weller. On the Relation Between Turnpike Properties for Finite and Infinite Horizon Optimal Control Problems. *Journal of Optimization Theory and Applications*, 173, 2017.

[50] L. Grüne, L. Krügel, and M. A. Müller. Multiobjective strict dissipativity via a weighted sum approach. *Systems & Control Letters*, 170:105396, 2022.

[51] L. Grüne and M. A. Müller. On the relation between strict dissipativity and turnpike properties. *Systems & Control Letters*, 90:45–53, 2016.

[52] L. Grüne and S. Pirkelmann. Closed-loop performance analysis for economic model predictive control of time-varying systems. In *2017 IEEE 56th Annual Conference on Decision and Control (CDC)*, pages 5563–5569, 2017.

[53] L. Grüne and W. Semmler. Using dynamic programming with adaptive grid scheme for optimal control problems in economics. *Journal of Economic Dynamics and Control*, 28(12):2427–2456, 2004.

[54] L. Grüne and M. Stieler. Multiobjective model predictive control for stabilizing cost criteria. *Discrete & Continuous Dynamical Systems - B*, 24(8):3905–3928, 2019.

[55] J. Hahn, R. Schoeffauer, G. Wunder, and O. Stursberg. Using AoI forecasts in communicating and robust distributed model-predictive control. *IEEE Trans. Control Netw. Syst.*, 9(2):742–752, 2022.

[56] J. L. Haunschmied, P. M. Kort, R. F. Hartl, and G. Feichtinger. A DNS–curve in a two state capital accumulation model: a numerical analysis. *Journal of Economic Dynamics & Control*, 27:701–716, 2003.

[57] D. He, Y. Zhang, and S. Yu. Prioritized multi-objective model predictive control without terminal constraints and its applications to nonlinear processes. *Optimal Control Applications and Methods*, 42(4):1030–1044, 2021.

[58] D. J. Hill and P. J. Moylan. Dissipative Dynamical Systems: Basic Input-Output and State Properties. *Journal of the Franklin Institute*, 309(5):327–357, 1980.

[59] C. Hillermeier. *Nonlinear Multiobjective Optimization*. Birkhäuser Basel, 2001.

[60] J. Janai, F. Güney, A. Behl, and A. Geiger. Computer Vision for Autonomous Vehicles: Problems, Datasets and State of the Art. *Foundations and Trends® in Computer Graphics and Vision*, 12(1–3):1–308, 2020.

[61] M. U. Kajgaard, J. Mogensen, A. Wittendorff, A. T. Veress, and B. Biegel. Model predictive control of domestic heat pump. In *Proceedings of the 2013 American Control Conference*, pages 2013–2018. IEEE, 2013.

[62] S. Keerthi and E. Gilbert. An existence theorem for discrete-time infinite-horizon optimal control problems. *IEEE Transactions on Automatic Control*, 30(9):907–909, 1985.

[63] H. K. Khalil. *Nonlinear Systems*. PRENTICE HALL, 2001.

[64] L. Krügel, T. Faulwasser, and L. Grüne. Local Turnpike Properties in Finite Horizon Optimal Control. 2023.

[65] H. W. Kuhn and A. W. Tucker. Nonlinear Programming. *Econometrica, George Banta Pub. Co. for the Econometric Society*, 19:50, 1951.

[66] S. M. LaValle. *Planning Algorithms*. Cambridge University Press, 2006.

[67] J. Levinson, J. Askeland, J. Becker, J. Dolson, D. Held, S. Kammel, J. Z. Kolter, D. Langer, O. Pink, V. Pratt, M. Sokolsky, G. Stanek, D. Stavens, A. Teichman, M. Werling, and S. Thrun. Towards fully autonomous driving: Systems and algorithms. In *2011 IEEE Intelligent Vehicles Symposium (IV)*. IEEE, 2011.

[68] F. Logist, B. Houska, M. Diehl, and J. V. Impe. Fast Pareto set generation for nonlinear optimal control problems with multiple objectives. *Structural and Multidisciplinary Optimization*, 42(4):591–603, 2010.

[69] C. Mark and S. Liu. Recursively feasible data-driven distributionally robust model predictive control with additive disturbances. *IEEE Control Syst. Lett.*, 7:526–531, 2023.

[70] D. Q. Mayne. Model predictive control: Recent developments and future promise. *Automatica*, 50(12):2967–2986, 2014.

[71] K. Miettinen. *Nonlinear Multiobjective Optimization*. Springer US, 1998.

[72] M. A. Müller, D. Angeli, and F. Allgöwer. On Necessity and Robustness of Dissipativity in Economic Model Predictive Control. *IEEE Transactions on Automatic Control*, 60(6):1671–1676, 2015.

[73] M. A. Müller, L. Grüne, and F. Allgöwer. On the role of dissipativity in economic model predictive control. In *Proceedings of the 5th IFAC Conference on Nonlinear Model Predictive Control*, volume 23 of *IFAC PapersOnLine*, pages 110–116, 2015.

[74] M. A. Müller, M. Reble, and F. Allgöwer. Cooperative control of dynamically decoupled systems via distributed model predictive control. *International Journal of Robust and Nonlinear Control*, 22(12):1376–1397, 2012.

[75] J. V. Neumann. A Model of General Economic Equilibrium. In *Readings in the Theory of Growth*, pages 1–9. Palgrave Macmillan UK, 1971.

[76] F. Oldewurtel, A. Parisio, C. N. Jones, M. Morari, D. Gyalistras, M. Gwerder, V. Stauch, B. Lehmann, and K. Wirth. Energy efficient building climate control using Stochastic Model Predictive Control and weather predictions. In *Proceedings of the 2010 American Control Conference*. IEEE, 2010.

[77] R. Postoyan, L. Buşoniu, D. Nešić, and J. Daafouz. Stability of infinite-horizon optimal control with discounted cost. In *Proceedings of the 53rd IEEE Conference on Decision and Control*, pages 3903–3908, 2014.

[78] R. Postoyan, L. Buşoniu, D. Nešić, and J. Daafouz. Stability analysis of discrete-time infinite-horizon optimal control with discounted cost. *IEEE Trans. Automat. Control*, 62(6):2736–2749, 2017.

[79] F. P. Ramsey. A Mathematical Theory of Saving. *The Economic Journal*, 38(152):543, 1928.

[80] J. B. Rawlings. Tutorial overview of model predictive control. *IEEE Control Systems*, 20(3):38–52, 2000.

[81] J. B. Rawlings, D. Q. Mayne, and M. M. Diehl. *Model Predictive Control: Theory, Computation and Design*. Nob Hill Publishing, Madison, Wisconsin, 2017.

[82] P. Sauerteig and K. Worthmann. Towards multiobjective optimization and control of smart grids. *Optimal Control Applications and Methods*, 41(1):128–145, 2019.

[83] Y. Sawaragi. *Theory of multiobjective optimization*. Academic Press, Orlando, 1985.

[84] J. Schießl and L. Krügel. nMPyC - A Python library for solving optimal control problems via MPC. `http://nmpyc.readthedocs.io/`, 2022.

[85] T. Schmitt, T. Rodemann, and J. Adamy. Multi-objective model predictive control for microgrids. *at - Automatisierungstechnik*, 68(8):687–702, 2020.

[86] A. K. Skiba. Optimal growth with a convex-concave production function. *Econometrica*, 46:527–540, 1978.

[87] E. D. Sontag. *Mathematical Control Theory*. Springer New York, 1998.

[88] M. Stieler. *Performance Estimates for Scalar and Multiobjective Model Predictive Control Schemes*. PhD thesis, Universität Bayreuth, Bayreuth, 2018.

[89] C. Szepesvári. *Algorithms for Reinforcement Learning*. Springer International Publishing, 2022.

[90] J. Tarragona, A. de Gracia, and L. F. Cabeza. Bibliometric analysis of smart control applications in thermal energy storage systems. A model predictive control approach. *Journal of Energy Storage*, 32:101704, 2020.

[91] E. Trélat and E. Zuazua. The turnpike property in finite-dimensional nonlinear optimal control. *Journal of Differential Equations*, 258(1):81–114, 2015.

[92] A. van der Schaft. Cyclo-Dissipativity Revisited. *IEEE Transactions on Automatic Control*, 66(6):2920–2924, 2021.

[93] J. C. Willems. Dissipative dynamical systems. I. General theory. *Arch. Rational Mech. Anal.*, 45:321–351, 1972.

[94] J. C. Willems. Dissipative dynamical systems. II. Linear systems with quadratic supply rates. *Arch. Rational Mech. Anal.*, 45:352–393, 1972.

[95] V. M. Zavala. A Multiobjective Optimization Perspective on the Stability of Economic MPC. *IFAC-PapersOnLine*, 48(8):974–980, 2015.

[96] V. M. Zavala and A. Flores-Tlacuahuac. Stability of multiobjective predictive control: A utopia-tracking approach. *Automatica*, 48(10):2627–2632, 2012.

[97] M. N. Zeilinger, D. M. Raimondo, A. Domahidi, M. Morari, and C. N. Jones. On real-time robust model predictive control. *Automatica*, 50(3):683–694, 2014.

Publications

[1] G. Eichfelder, L. Grüne, L. Krügel, and J. Schießl. Relaxed dissipativity assumptions and a simplified algorithm for multiobjective MPC. *Computational Optimization and Applications*, 2022.

[2] L. Grüne and L. Krügel. Local turnpike analysis using local dissipativity for discrete time discounted optimal control. *Applied Mathematics & Optimization*, 84(S2):1585–1606, 2021.

[3] L. Grüne, L. Krügel, and M. A. Müller. Multiobjective strict dissipativity via a weighted sum approach. *Systems & Control Letters*, 170:105396, 2022.

[4] L. Krügel, T. Faulwasser, and L. Grüne. Local Turnpike Properties in Finite Horizon Optimal Control. 2023.

[5] M. Köhler, L. Krügel, L. Grüne, M. A. Müller, and F. Allgöwer. Transient performance of MPC for tracking. *IEEE Control Systems Letters*, 7:2545–2550, 2023.

Eidesstattliche Versicherung

Hiermit versichere ich an Eides statt, dass ich die vorliegende Arbeit selbstständig verfasst und keine anderen als die von mir angegebenen Quellen und Hilfsmittel verwendet habe.

Weiterhin erkläre ich, dass ich die Hilfe von gewerblichen Promotionsberatern bzw. -vermittlern oder ähnlichen Dienstleistern weder bisher in Anspruch genommen habe, noch künftig in Anspruch nehmen werde.

Zusätzlich erkläre ich hiermit, dass ich keinerlei frühere Promotionsversuche unternommen habe.

Bayreuth, den _____

Datum

_____

Lisa Krügel